GUSTAVO HENRIQUE NALON

EXPERIMENTAL EVALUATION OF SELF-SENSING CEMENT-BASED COMPOSITES WITH CARBON NANOFILLERS FOR STRUCTURAL HEALTH MONITORING OF FIRE-DAMAGED STRUCTURES

Dissertation submitted to the Universidade Federal de Viçosa, in partial fulfillment of the requirements of the Civil Engineering Graduate Program, for the degree of *Magister Scientiae*.

Advisor: José Carlos Lopes Ribeiro

Co-advisors: Leonardo Gonçalves Pedroti
Eduardo Nery Duarte de Araújo

VIÇOSA - MINAS GERAIS
2020

Ficha catalográfica elaborada pela Biblioteca Central da Universidade Federal de Viçosa - Campus Viçosa

T
N172e
2020

Nalon, Gustavo Henrique, 1993-
Experimental evaluation of self-sensing cement-based composites with carbon nanofillers for Structural Health Monitoring of fire-damaged structures / Gustavo Henrique Nalon. – Viçosa, MG, 2020.
147f. : il. (algumas color.) ; 29 cm.

Inclui apêndices.
Orientador: José Carlos Lopes Ribeiro.
Dissertação (mestrado) - Universidade Federal de Viçosa.
Inclui bibliografia.

1. Concreto armado. 2. Materiais nanoestruturados. 3. Sensores. 4. Concreto - Efeito da temperatura. 5. Incêndios. I. Universidade Federal de Viçosa. Departamento de Engenharia Civil. Programa de Pós-Graduação em Engenharia Civil. II. Título.

CDD 22 ed. 624.1834

GUSTAVO HENRIQUE NALON

EXPERIMENTAL EVALUATION OF SELF-SENSING CEMENT-BASED COMPOSITES WITH CARBON NANOFILLERS FOR STRUCTURAL HEALTH MONITORING OF FIRE-DAMAGED STRUCTURES

Dissertation submitted to the Universidade Federal de Viçosa, in partial fulfillment of the requirements of the Civil Engineering Graduate Program, for the degree of *Magister Scientiae*.

APPROVED: February 27, 2020.

Assent:

Gustavo Henrique Nalon
Author

José Carlos Lopes Ribeiro
Advisor

ACKNOWLEDGMENTS

I would like to thank God for giving me strength, health, wisdom and peace to accomplish this project.

I express my greatest appreciation to my advisor Prof. Dr. José Carlos Lopes Ribeiro. His exemplary guidance, valuable contribution, friendly advice and huge knowledge have played an important role in this research. Working under his guidance was definitely a great privilege.

I must show my gratitude to Prof. Dr. Rita de Cássia Silva Sant'Anna Alvarenga (*in memorian*), who guided my first steps in Science during my first research opportunity back in 2015. Her love and enthusiasm for research and teaching will always be my inspiration.

I am also very grateful to my co-advisor Prof. Dr. Leonardo Gonçalves Pedroti. His permanent support and motivation enabled this research to be possible.

My sincere thanks also go to Prof. Dr. Eduardo Nery Duarte de Araújo for accepting the invitation to become my co-advisor. Thank you for generously spending your precious time to provide great ideas and important technical support to this work. I have received valuable insights from his knowledge on nanomodified materials.

I would like to thank the other members of my dissertation committee: Prof. Dr. José Maria Franco de Carvalho and Prof. Dr. Diôgo Silva de Oliveira for the constructive comments and valuable suggestions that significantly improved this work.

My thanks are extended to Gustavo Lima and Rodrigo Santos, two friends that I have had the great luck to work with. Their contributions to develop the laboratory tests, acquire materials and equipment and discuss experimental results greatly enriched this work. Words of gratitude also go to my UFV friends João Vitor, Tiago, Fernando, Guilherme, Cíntia, Márcia, Igor, Beatryz, André Oliveira, André Candian, Petrauski, Luís, Ana, Matheus, and Jaqueline. Thanks for the friendship and for being source of support when things got a bit discouraging!

I wish to acknowledge the Nucleus of Microscopy and Microanalysis at the Universidade Federal de Viçosa (UFV), for providing the equipment and technical support for experiments involving electron microscopy.

I also thank the Department of Physics of UFV and the collaboration of Prof. Sukarno Ferreira, Prof. Luciano Moura, Prof. Renê Silva and Prof. Alex Ferreira. They provided valuable comments and technical support for the development of X-ray diffraction, scanning electron microscopy and Raman spectroscopy.

Many thanks to the support provided by the professors and staff of the Civil Engineering Department of UFV. Special thanks to the technicians of the Laboratório de Materiais de Construção: Wellington, José Carlos and Nathália.

I also express my gratitude to the funding source that made this dissertation possible. This study was financed in part by the Coordenação de Aperfeiçoamento de Pessoal de Nível Superior - Brasil (CAPES) - Finance Code 001.

I thank for the carbon nanomaterials donated by Cabot Corporation, Birla Carbon and RESIDROX Chemical Solutions, for the silica fume donated by Pedreira Um Valemix, for the electrodes provided by Kanthal, for the ultrasound probe provided by the Agricultural Biotechnology Research Institute (BIOAGRO) and for the superplasticizer donated by MC Bauchemie.

Finally, I would like to express my gratitude to my parents Sebastião and Rogéria, for the constant support and encouragement. Without their advice and prayers, this work would never have been possible.

ABSTRACT

NALON, Gustavo Henrique, M.Sc., Universidade Federal de Viçosa, February, 2020. **Experimental evaluation of self-sensing cement-based composites with carbon nanofillers for Structural Health Monitoring of fire-damaged structures.** Advisor: José Carlos Lopes Ribeiro. Co-advisors: Leonardo Gonçalves Pedroti and Eduardo Nery Duarte de Araújo.

The deeper understanding of the electrical properties of cement-based materials and the recent knowledge on Nanoscience and Nanotechnology allowed the development of smart pastes, mortars and concretes with intrinsic strain sensing and damage detection properties. Since fire is one of the most severe threats to the structural integrity of concrete elements, the reuse of fire-damaged structures requires an accurate diagnosis of their damage level and residual structural performance. In this work, an experimental evaluation of innovative technologies for Structural Health Monitoring of fire-damaged concrete elements was developed: self-sensing cement-based composites containing multi-walled carbon nanotubes (MWCNT) or carbon-black nanoparticles (CBN). Microstructure, residual mechanical properties and sensing ability of different composites exposed to temperatures of 200 ºC, 400 ºC and 600 ºC were investigated. The effects of rehydration after fire exposure on these parameters were also studied. Composites with an intrinsic ability to measure strain and detect damage after exposure to temperatures up to 600 ºC were developed. They also exhibited an interesting ability of detection of damage recovery due to the post-fire rehydration.

Keywords: Structural Health Monitoring. Nanomodified cementitious materials. Post-fire structural behavior. Self-sensing composites.

RESUMO

NALON, Gustavo Henrique, M.Sc., Universidade Federal de Viçosa, fevereiro de 2020. **Avaliação experimental de compósitos cimentícios sensores com nanofillers de carbono para Monitoramento da Integridade Estrutural de estruturas em situação pós-incêndio.** Orientador: José Carlos Lopes Ribeiro. Coorientadores: Leonardo Gonçalves Pedroti e Eduardo Nery Duarte de Araújo.

O melhor entendimento das propriedades elétricas dos materiais cimentícios e o conhecimento recente em Nanociência e Nanotecnologia possibilitaram o desenvolvimento de pastas, argamassas e concretos inteligentes com propriedades intrínsecas de detecção de danos e medição de deformações. O incêndio consiste em uma das mais severas ameaças à integridade estrutural de elementos de concreto, de modo que a reutilização de estruturas por ele danificadas requer um diagnóstico preciso de seus níveis de dano e da sua performance estrutural residual. Neste trabalho, foi desenvolvida uma avaliação experimental de tecnologias inovadoras para Monitoramento da Integridade Estrutural de elementos de concreto em condição pós-incêndio: compósitos cimentícios auto-sensores produzidos com nanotubos de carbono de paredes múltiplas (MWCNT) ou nanopartículas de negro de fumo (CBN). Foram investigadas a microestrutura, as propriedades mecânicas e a habilidade sensorial pós-incêndio de diferentes tipos de compósitos expostos a temperaturas de 200 ºC, 400 ºC e 600 ºC. Os efeitos da reidratação pós-incêndio nesses parâmetros também foram estudados. Foram desenvolvidos compósitos com as habilidades intrínsecas de medição de deformação e detecção de danos em condição pós-incêndios de até 600 ºC. Eles também demonstraram uma interessante habilidade de detecção da recuperação de dano devido ao processo de reidratação pós-incêndio.

Palavras-chave: Monitoramento da Integridade Estrutural. Materiais cimentícios nanomodificados. Comportamento estrutural pós-incêndio. Compósitos auto-sensores.

LIST OF ABBREVIATIONS AND ACRONYMS

AC - alternating current

CB - carbon black

CBN - carbon-black nanoparticles

CH - calcium hydroxide (portlandite)

CF - carbon fibers

CNC - cellulose nanocrystals

CNF - cellulose nanofibers

CNT - carbon nanotubes

CSH - calcium silicate hydrate

DAQ - data acquisition system

DBP - dibutyl phthalate

DC - direct current

FCR - fractional change in resistivity

GF - gauge factor

GNF - graphite nanofibers

GNP - graphene nanoplateletes

GNS - graphene nanosheets

GO - graphene oxide

GSNS - graphene sulfonate nanosheets

MWCNT - multi-walled carbon nanotubes

NA - nanoalumina

NC - nanoclay

NIO - nano-iron oxide

NM - nanometakaolin

NS - nano-silica

NT - nano-titania

SHM - Structural health monitoring

SP - superplasticizer

SS - stress sensitivity

SWCNT - single-walled carbon nanotubes

TGA – thermogravimetric analysis

LIST OF SYMBOLS

Latin symbols

A - effective area of the voltage pole

C - internal capacitance of the composite

E - static modulus of elasticity

f - compressive strength

f_u - ultimate compressive load

i - electric current

k_j^{res} - residual mechanical property of a specimen j exposed to high temperatures

$k_m^{25^\circ C}$ - average mechanical property of mortars that were not exposed to high temperatures

L - distance between electrodes

R - internal resistance of the composite

R^2 - coefficient of determination

R_0 - initial electrical resistance and resistivity of the composite

R_{cont} - contact resistance in electrodes

R_{comp} - electrical resistance of the composite

R_{ref} - electrical resistance of the reference resistor

U_{comp} - potential difference between the electrodes embedded in the composite

U_{ref} - voltage drop across the reference resistor

t - time

v - voltage source

v_c - network percolation

Greek symbols

ε - compressive strain

Φ_j - relative residual mechanical property factor of a specimen j

ρ - electrical resistivity

σ - compressive stress

τ - time constant

TABLE OF CONTENTS

CHAPTER 1: GENERAL INTRODUCTION

1.1. RESEARCH CONTEXT

Concrete structures are designed to meet many requirements of safety, serviceability, durability, aesthetics and sustainability during their service life. However, many concrete structures are in a state of utter disrepair due to numerous deleterious effects that affect their structural integrity, such as chemical attacks, wetting–drying cycles, freeze-thaw, loads not considered in design, dynamic loading, natural disasters, corrosion in reinforcement, temperature variations, among others [1-3].

Structural health monitoring (SHM) systems have been used for real-time assessment of strains and damage at key locations of civil structures. They play an important role in the optimization of repair, retrofitting and restoration activities of concrete elements [4]. During the past several decades, great SHM achievements have been made through the construction of smart civil structures.

Smart structures can mimic biological systems, since they have the ability to sense, measure, process and diagnose changes in many variables related to the mechanical behavior of the structure [5]. Strain gauges, accelerometers, optical sensors, piezoelectric ceramics, acoustic emission equipment, load cells, high-resolution cameras, corrosion sensors, signal processors, computers, communication networks and other devices have been used for monitoring the in-service structural response of concrete elements.

However, many conventional sensors require extensive maintenance due to their poor durability and limited robustness [6]. Traditional strain gauges also have some drawbacks: limited sensitivity (their gauge factor is usually about 2), low anti-electromagnetic interference and high error for long-term measuring [7, 8]. Some systems are uneconomical because they require the installation of huge quantities of expansive and large transducers [9]. For example, optical systems for structural monitoring are expensive and present complex embedding technology, which limit their popular use [7]. Most SHM instruments have short service life and low compatibility with concrete, leading to decreases in the mechanical properties of the elements within which they were embedded [10]. Moreover, the main restricting factor of traditional SHM architectures is that they are difficult to scale-up to large-scale structures due to management issues [11].

In recent years, an innovative sensing technology for SHM has been developed to solve many of the problems concerned: nanomodified cement-based materials with intrinsic

sensing ability. Extensive international studies have reported the incorporation of functional nanomaterials in mortars and concretes in order to create self-sensing composites able to work as structural elements and systems that monitor strain and damage in smart civil structures. As these multifunctional cement-based materials have structural and sensing abilities, their use reduces or eliminates the need for conventional SHM architectures, which simplifies the design and allows structures to be more compact [12]. In addition, these smart cement-based composites have attracted attention due to their high sensitivity, high robustness, high durability against environmental actions, good embedding approach, low cost, favorable mechanical properties and natural compatibility with concrete structures.

Nanoscience and Nanotechnology provided the understanding and control of matter at the nanoscale. It enabled the improvement of optical, mechanical, chemical, electrical and magnetic properties of materials and the development of multifunctional devices with important engineering applications. Recently, many research groups have focused on the improvement of the performance of cementitious materials through the incorporation of different kinds of nanomaterials: nano-silica (NS), nano-titania (NT), carbon-black nanoparticles (CBN), single-walled carbon nanotubes (SWCNT), multi-walled carbon nanotubes (MWCNT), graphene oxide (GO), graphene nanoplateletes (GNP), graphene nanosheets (GNS), graphene sulfonate nanosheets (GSNS) cellulose nanocrystals (CNC), nanoclay (NC), nanometakaolin (NM), nanoalumina (NA), nano-iron oxide (NIO), cellulose nanofibers (CNF), carbon nanofibers (CF), graphite nanofibers (GNF), among others.

These nanomaterials allowed the development of cement-based composites with higher strength and durability, lower self-weight, lower electrical resistivity or higher ductility. Nano-inclusions have also be applied in cement-matrix composites to develop pastes, mortars and concretes with a self-cleaning, self-heating, self-healing or self-sensing ability. In the case of materials with self-sensing and damage detection properties, a concentration of conductive nanofillers close to the percolation threshold is incorporated into cementitious matrices, in order to decrease the electrical resistivity of the material. Consequently, the internal resistivity and impedance of the composite change when mechanical deformation is applied or damage occurs [3, 6, 13].

Although cementitious materials have high endurance at elevated temperatures, fire can be one of the most severe threats to the structural integrity of concrete elements [14, 15]. The mechanical strength of cementitious materials decreases dramatically when they are exposed to temperatures between 300 ºC and 1000 ºC, due to transformations in their

chemical composition and physical structure, combined with thermal and elastic incompatibilities between their components [16-20].

However, from an ecological and economic perspective, fire-damaged concrete elements can be restored instead of being demolished [21-23]. The reuse of fire-damaged structures requires an accurate diagnosis of their damage level and residual structural performance. Therefore, this dissertation explores the application of Nanoscience and Nanotechnology concepts for the development of innovative technologies for SHM of fire-damaged concrete structures.

1.2. OBJECTIVES

1.2.1. General objective

The general objective of this research was the investigation and evaluation of mechanical and piezoresistive properties of self-sensing cement-based composites with carbon nanofillers for SHM of concrete structures before and after fire exposure.

1.2.2. Specific objectives

The specific objectives of this dissertation can be listed as follows:

a) Evaluation of the microstructure and residual mechanical properties of cement-based materials with CBN or MWCNT exposed to high temperatures.
b) Analysis of the residual sensing ability of smart cement-based composites with CBN or MWCNT exposed to high temperatures.
c) Investigation of the effects of rehydration on the microstructure and mechanical properties of fire-damaged cement-based materials with CBN or MWCNT.
d) Analysis of the influence of rehydration on the sensing ability of fire-damaged smart cement-based composites with CBN or MWCNT.

1.3. JUSTIFICATION

Concrete is widely used as structural material of buildings, bridges, roads, canals, dams and various civil infrastructures. In the last decades, new technologies for assessment of strain and damage of concrete elements have been developed in response to the growing concerns regarding durability and structural performance of concrete structures. This

research deals with one of these emerging technologies: cement-based structural materials that also perform the role of SHM sensors.

Due to their high endurance at elevated temperatures, concrete elements can be rehabilitated and retrofitted after fire. However, a precise investigation of their residual structural behavior must be developed. There is no previous study dealing with the effects of fire on the residual electrical resistivity and piezoresistive response of self-sensing cement-based composites. Then, the most important justification for this research is the development of innovative cement-based self-sensing composites for diagnosis of damage and structural performance of concrete elements exposed to high temperatures. This study aims to make an important contribution to save fire-damaged structural elements before they completely lose their integrity and load-bearing capacity.

Different kinds of nano-scale reinforcement have been recently proposed as an alternative for improving the mechanical strength and durability of cement-based materials at elevated temperatures. Effects of fire-exposure and rehydration reported in the literature for ordinary mortars and concretes cannot be generalized for nanomodified cementitious materials, due to their different composition and properties. Therefore, another important justification for the development of the present study is the experimental evaluation of the mechanical behavior of cement-based materials with different kinds of carbon nanofillers exposed to high temperatures.

Rehydration methods provide recovery of strength, stiffness and durability of fire-damaged cement-based materials, without the need of other special repairs. There is no previous research focused on the investigation of the influence of rehydration on the mechanical or self-sensing properties of fire-damaged mortars containing carbon nanomaterials. Then, another justification for this research is the investigation of effects of rehydration on the microstructure, compressive strength, elastic and dynamic modulus of elasticity, electrical resistivity and piezoresistivity of nanomodified cement-based materials exposed to high temperatures.

1.4. DISSERTATION STRUCTURE

This dissertation has been structured in seven chapters.

In Chapter 1, a background information about cement-based self-sensing composites is presented. It is followed by the objectives, justification and the structure of this dissertation.

In Chapter 2, a set of preliminary studies that create a substantial reference point for the main experimental program is described. It is divided into four sections. A general introduction about the main concepts discussed in the preliminary studies is presented in Section 2.1. In Section 2.2, different kinds of CBN are investigated in order to find a potential candidate for production of the composites of the main trial. In Section 2.3, piezoresistive and mechanical properties of mortars containing different concentrations of one type of CBN are evaluated. Effects of water content on these parameters are also discussed in this section. Finally, methods for microstructural analysis of the composites are tested in Section 2.4.

Chapters 3, 4, 5 and 6 deal with different topics, but have all been structured in four distinct sections: introduction, experimental methods, results and discussion, and conclusions. Chapter 3 presents an experimental investigation of the residual mechanical properties of mortars with carbon nanomaterials exposed to high temperatures. Chapter 4 shows the residual piezoresistive properties of these mortars. Chapter 5 describes an investigation of the effects of rehydration on the mechanical properties of mortars with carbon nanomaterials exposed to high temperatures. Chapter 6 identifies the effects of rehydration on the piezoresistive properties of these mortars.

The main conclusions of this dissertation are summarized in Chapter 7. Suggestions for future research are also indicated.

REFERENCES

[1] W. BALOCH, R. KHUSHNOOD and W. KHALIQ, "Influence of multi-walled carbon nanotubes on the residual performance of concrete exposed to high temperatures," *Construction and Building Materials,* vol. 185, pp. 44-56, 2018.

[2] J. OU and H. LI, "Structural Health Monitoring in mainland China: Review and Future Trends," *Structural Health Monitoring,* vol. 9, no. 3, pp. 219-231, 2010.

[3] B. HAN, S. DING and X. YU, "Intrinsic self-sensing concrete and structures: A review," *Measurement,* vol. 59, pp. 110-128, 2015.

[4] A. MEONI, A. D'ALESSANDRO, N. CAVALAGLI, M. GIOFFRÉ and F. UBERTINI, "Shaking table tests on a masonry building monitored using smart bricks: damage detection and localization," *Earthquake Engineering & Structural Dynamics,* vol. 48, no. 8, pp. 910-928, 2019.

[5] Y. XU and J. HE, Smart civil structures, Boca Raton: CRC Press, 2017.

[6] F. UBERTINI and A. D'ALESSANDRO, "Concrete with self-sensing properties," in *Eco-Efficient Repair and Rehabilitation of Concrete Infrastructures*, Woodhead Publishing, 2018, pp. 501-530.

[7] B. HAN, X. GUAN and J. OU, "Electrode design, measuring method and data acquisition system of carbon fiber cement paste piezoresistive sensors," *Sensors and Actuators A,* vol. 135, pp. 360-369, 2007.

[8] Y. WANG, Y. WANG, B. WAN, B. HAN, G. CAI and Z. LI, "Properties and mechanisms of self-sensing carbon nanofibers/epoxy composites for structural health monitoring," *Composite Structures,* vol. 200, p. 669–678, 2018.

[9] S. DAS and P. SAHA, "A review of some advanced sensors used for health diagnosis of civil engineering structures," *Masurement,* vol. 129, pp. 68-90, 2018.

[10] M. SARWARY, G. YILDIRIM, A. AL-DAHAWI, O. ANIL, K. KHIAVI, K. TOKLU and M. SAHMARAN, "Self-Sensing of Flexural Damage in Large-Scale Steel-Reinforced Mortar Beams," *ACI Materials Journal,* vol. 116, pp. 209-221, 2019.

[11] D. YOO, I. YOU, H. YOUN and S. LEE, "Electrical and piezoresistive properties of cement composites with carbon nanomaterials," *Journal of Composite Materials,* pp. 1-16, 2018.

[12] D. CHUNG, Multifunctional cement-based materials, New York: Marcel Dekker, Inc, 2003.

[13] I. YOU, D. YOO, S. KIM, M. KIM and G. ZI, "Electrical and self-sensing properties of ultra-high-performance fiber-reinforced concrete with carbon nanotubes," *Sensors,* vol. 17, p. 2481, 2017.

[14] H. SUH, H. JEE, J. KIM, R. KITAGAKI, S. OHKI and S. WOOE, "Influences of rehydration conditions on the mechanical and atomic structural recovery characteristics of Portland cement paste exposed to elevated temperatures," *Construction and Building Materials,* vol. 235, p. 117453, 2020.

[15] P. SIKORA, M. ELRAHMAN and D. STEPHAN, "The influence of nanomaterials on the thermal resistance of cement-based composites - A review," *Nanomaterials,* vol. 8, p. 465, 2018.

[16] C. POON, S. AZHAR, M. ANSON and Y. WONG, "Strength and durability recovery of fire-damaged concrete after post-fire-curing," *Cement and Concrete Research,* vol. 31, pp. 1307-1318, 2001.

[17] B. FERNANDES, A. M. GIL, F. L. BOLINA and B. F. TUTIKIAN, "Microstructure of concrete subjected to elevated temperatures: physico-chemical changes and analysis techniques," *IBRACON Structures and Materials Journal,* vol. 10, pp. 838-863, 2017.

[18] J. OLIVEIRA, J. RIBEIRO, L. PEDROTI, C. FARIA, G. NALON and A. OLIVEIRA JÚNIOR, "Durability of Concrete After Fire Through Accelerated Carbonation Tests," *Materials Research,* vol. 22, p. e20190049, 2019.

[19] S. MEMON, S. SHAH, R. KHUSHNOOD and W. BALOCH, "Durability of sustainable concrete subjected to elevated temperature – A Review," *Construction and Building Materials,* vol. 199 , p. 435–455, 2019.

[20] Q. MA, R. GUO, Z. ZHAO, Z. LIN and K. HE, "Mechanical properties of concrete at high temperature - A review," *Construction and Building Materials,* vol. 93, p. 371–383, 2015.

[21] H. CHO, D. LEE, H. JU, H. PARK, H. KIM and K. KIM, "Fire Damage Assessment of Reinforced Concrete Structures Using Fuzzy Theory," *Applied Sciences,* vol. 7, p. 518, 2017.

[22] A. ASEEM, W. BALOCH, R. KHUSHNOOD and A. MUSHTAQ, "Structural health assessment of fire damaged building using non-destructive testing and micro-graphical forensic analysis: A case study," *Case Studies in Construction Materials,* vol. 11, 2019.

[23] T. HA, J. KO, S. LEE, S. KIM, J. JUNG and D. KIM, "A Case Study on the Rehabilitation of a Fire-Damaged Structure," *Applied Sciences,* vol. 6, 2016.

CHAPTER 2: PRELIMINARY STUDIES

2.1. GENERAL INTRODUCTION

Concrete structures are exposed during their service life to hazards that may affect their integrity and structural performance. Structural health systems (SHM) have been used to continuously monitor strains and damage of concrete elements, identify any undesirable structural behavior in the early stages, and prevent the failure of the structures and loss of lives. Nanomodified cement-based composites with intrinsic self-sensing and damage detection properties have been developed to work as structural elements with sensing and health monitoring abilities. These smart cementitious materials are produced with conductive nano-admixtures that improve their electrical conductivity. Then, they can be used as embedded sensors in concrete elements, since mechanical deformation and damage in the cementitious matrix cause changes in the internal electrical resistivity and impedance of the composite [1-4].

The electrical resistivity of cementitious materials is high, ranging from 1×10^4 Ω.cm to 1×10^8 Ω.cm, but can be reduced through the inclusion of different types of conductive nano fillers [5]. For instance, Yoo *et al.* [6] used multi-walled carbon nanotubes, graphite nanofibers, and graphene oxide in mortars; Yildirim *et al.* [7] added carbon fibers and multi-walled carbon nanotubes in concrete beams; Meoni *et al.* [8] evaluated the use of multi-walled carbon nanotubes, carbon nanofibers, and graphene nanoplatelets in masonry bricks; Bai *et al.* [9] added graphene and silica fume in cement matrices; Downey *et al.* [10] added nanotitania in masonry bricks.

The conductivity of cementitious materials changes by several orders of magnitude when the concentration of conductive admixtures reaches a critical value designated as percolation threshold content [2, 3, 11-13]. Then, the percolation threshold represents the amount above which the admixture units form a continuous conduction path [14]. Figure 1 shows the network percolation (v_c) of two types of carbon nanomaterials. Two basic mechanisms originate electrical conduction in self-sensing cement-based composites: ionic conduction and electronic conduction. Below the percolation threshold, the electrical conductivity is dominated by ionic conduction, which is associated with the movement of ions in the water in the material's pores. Above the percolation threshold, the functional fillers form a continuous network through which electrons preferably flow [2, 3, 6]. When the fraction of nanoparticles is above the percolation threshold, a self-sensing behavior can

be observed in cement-based composites. Due to the piezoresistivity phenomenon, the material's electrical resistivity changes reversibly with deformation [15].

Figure 1 – Network percolation (v_c) of different kinds of carbon nanomaterials

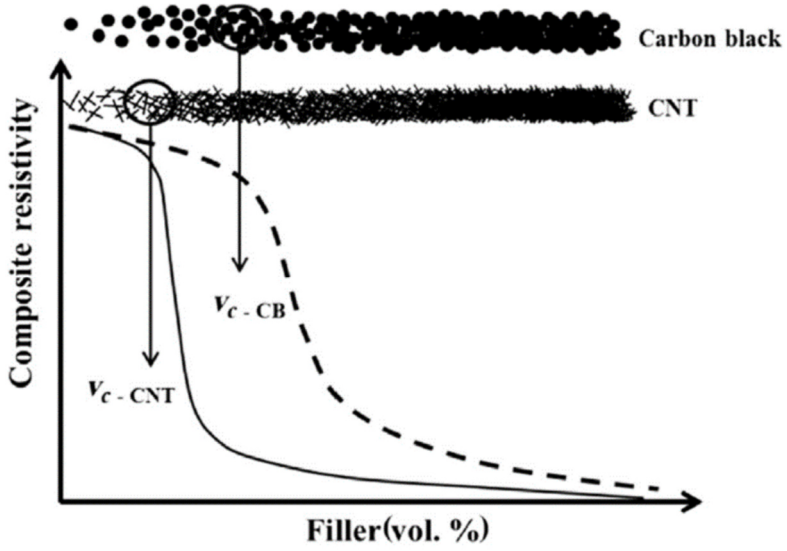

Source: Hwang et al. [12] and Han, Yu and Ou [13]

The direct current (DC) method is the simplest way to determine the electrical resistance of cement-based composites. However, when the DC electrical field is applied, the material polarizes by orienting the dipole moments of the molecules that were randomly oriented in normal conditions [16]. When the ionic conduction is dominant, the DC electrical resistance increases with measurement time due to this polarization effect [2]. One of the ways to mitigate the material's inherent time-based drift is delaying measurements until the drift levels out [8, 17-19]. However, insufficient stabilization before the piezoresistivity analysis or a long-term residual capacitive charging effect can cause slight hysteresis in fractional change in resistance (FCR) versus deformation curves [17].

The polarization effect can also be lessened to an acceptable range by employing alternating current (AC) signals with equal magnitudes of positive and negative peaks [2]. However, AC methods require more expensive electronics and do not typically allow a simultaneous data acquisition from multi-sectioned self-sensing cement-based materials [18, 20]. More recently, Downey et al. [18] proposed a promising biphasic DC measurement approach, in which an alternating square wave voltage signal with a duty cycle of 50% was proposed for enhanced measurement stability, elimination of polarization effects and multi-channel sampling of multi-functional self-sensing structural materials.

Many practical applications of cement-based sensors for SHM have been studied over the last years. For example, Downey et al. [10] proposed smart bricks with NT for strain sensing and crack detection in masonry structures (Figure 2a). Xiao, Li and Ou [21] used cement-based composites with CBN to evaluate strain in different stress zones of a bending concrete beam (Figure 2b). D'Alessandro et al. [22] used smart cement-based sensors with MWCNT for static and dynamic strain monitoring of reinforced concrete beams (Figure 2c). Han et al. [23] developed a self-sensing concrete pavement system with CNT for real-time vehicle flow detection (Figure 2d). Yeh, Chang e Liao [24] and Ubertini and D'Alessandro [3] used cement-based composites for strain measurement and damage detection in reinforced concrete portal frames and concrete beams, respectively (Figure 2e and Figure 2f). Ou [25] embedded smart cement-based composites with CBN into concrete girders of the Chongqing Guangyang Island Bridge (Figure 2e).

Figure 2 – Practical SHM applications of self-sensing cement-based composites

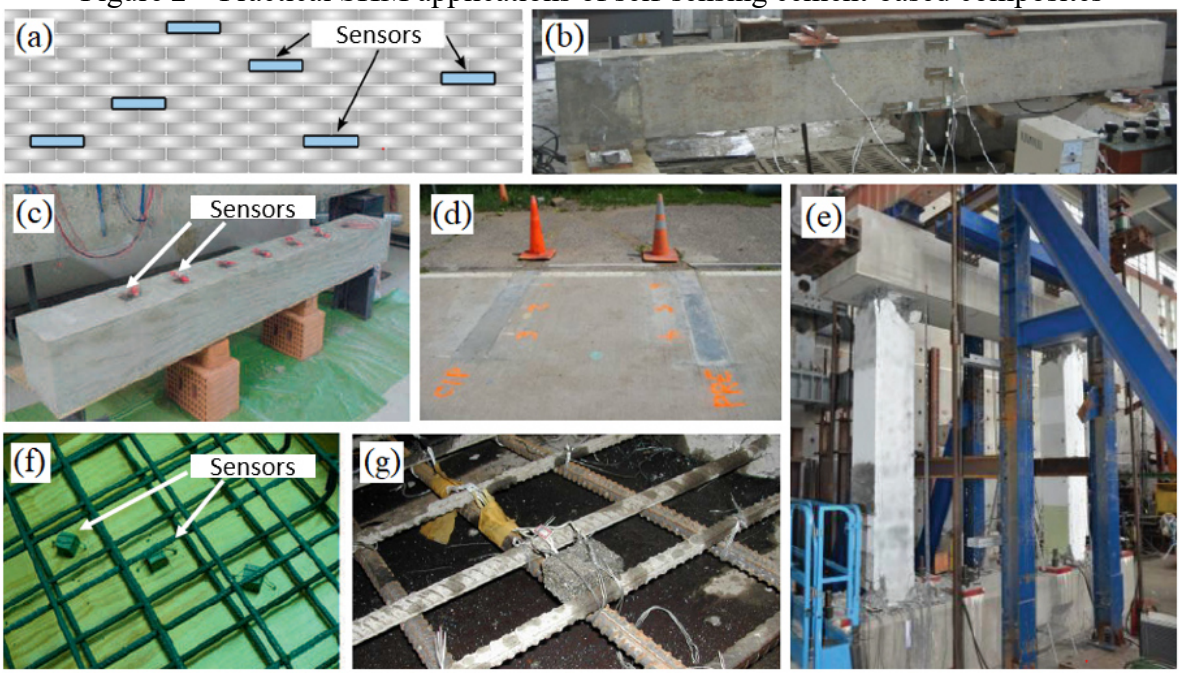

Source: a) Downey et al. [10], b) Xiao, Li and Ou [21], c) D'Alessandro et al. [22], d) Han et al. [23], e) Yeh, Chang e Liao [24], f) Ubertini and D'Alessandro [3], g) Ou [25]

The investigations reported in this chapter consist of a preliminary study developed in the Laboratory of Construction Materials of the Federal University of Viçosa to evaluate and confirm previous research results, refine experimental methods, test locally available construction materials and nanofillers, and create a substantial reference point for the main set of experiments presented in the following chapters.

2.2. EFFECTS OF DIFFERENT KINDS OF CBN ON THE PIEZORESISTIVE AND MECHANICAL PROPERTIES OF CEMENT-BASED COMPOSITES

2.2.1. Introduction

Carbon black is the generic name of a family of small particles of carbon which are formed during the thermal decomposition process of hydrocarbons. During the combustion of fuel oils, oil drops or gaseous hydrocarbons are incompletely burned, due to the gradient of temperature caused by various oxygen depletions. Carbon black nanoparticles (CBN) are smaller than 300 nm, but during the production process, they fuse to form aggregates, while clusters of aggregates may form agglomerates. In general, the degree of aggregate branching is known as the "structure" of carbon blacks. High structure blacks present extensive interlinking between primary particles, while low structure ones exhibit a small number of primary particles per aggregate [26-30].

The formation of CBN aggregates depends on different factors, such as type of fuel, maximum temperature and duration of combustion. Then, their size, morphology, chemical composition, microstructure and surface area are expected to vary significantly. In fact, there are many kinds of commercially available carbon blacks with various industrial applications [17, 29, 31].

The incorporation of CBN into cement matrices can provide the benefits of many conductive admixtures at a fraction of the cost, since they present a high surface area, small particle size, high electrical conductivity and low production cost [17, 32]. Many researchers have investigated potential applications of CBN to develop smart materials for strain-sensing and damage detection in civil structures. For instance, Li et al. [33], Monteiro et al. [17], Monteiro et al. [34], D'Alessandro et al. [35] and Lin et al. [36] investigated the mechanical and piezoresistive behavior of pastes and mortars with CBN under compressive and tensile stresses. Han et al. [37] investigated the mechanical and piezoresistive behavior of pastes containing a combination of two types of carbon nanofillers: CBN and multi-walled carbon nanotubes (MWCNT). Chen et al. [38], Ding et al. [39], Wen and Chung [40] investigated workability, piezoresistivity and internal damage of smart concrete elements containing CBN and carbon fiber (CF). The electrical properties of pastes with CBN under long-term wet and loading condition were studied by Li et al. [41]. The influence of water content on conductivity and piezoresistivity of cement composites containing CBN + CF, CBN + MWCNT and CBN were investigated by Han et al. [42], Zhang et al. [43] and Dong et al.

[44], respectively. Hussain et al. [45] used CBN and other conductive admixtures for production of self-monitoring concrete beams. Xiao et al. [21] and Xiao and Li [46] evaluated the sensing properties of cement-based sensors with CBN embedded in a bending concrete beam and concrete column, respectively. Ding et al. [47] investigated the self-sensing and mechanical properties of smart concrete columns incorporating CNT and CBN.

There are many types of commercially available CBN with characteristics directly related to the purpose for which they were produced [34]. Then, the mechanical and electrical properties of structural materials produced with these nanomaterials are directly associated with the chemical and physical interactions between the cement itious matrix and the CBN. Previous studies have investigated the effects of addition of various types of CBN in cement-based materials. Despite this, there is no systematic comparison between mechanical and electrical properties of cement-based materials produced with CBN of different characteristics. Then, this preliminary study aims to systematically investigate the influence of structure and surface area of CBN on the compressive strength, electrical resistivity and self-sensing ability of cement-based composites.

2.2.2. Experimental Methods

Four types of CBN with different specific surface area, electrical conductivity and structure were selected for production of self-sensing cement-based composites: a classical highly structured furnace carbon black N234 supplied by Birla Carbon and three kinds of conductive carbon blacks supplied by Cabot: Vulcan XC72, XC305 and XC605. The main structural parameters of the CBN used in this work are shown in Table 1. The average size of all primary CBN was around 20-30 nm.

Table 1 – Characteristics of the CBN investigated in this study

CBN type	Dibutyl phthalate (DBP) absorption number ($cm^3/100g$) [(a)]	Electrical resistivity (Ω.cm)	Specific surface area (m^2/g)
N234	125	3.3 - 3.9	120
Vulcan XC305	131	1.2 - 1.8	72
Vulcan XC605	148	1.7 - 2.1	90
Vulcan XC72	174	1.7 - 2.1	254

[(a)] Structure of CBN is defined as the number of particles making up the primary aggregate [48]. The greater the DBP absorption number, the greater the number of particles per aggregate and the higher the structure.

Five different kinds of mortars designated as REF, CBN125, CBN131, CBN148 and CBN174 were produced. No carbon black was added in the REF series. CBN125, CBN131, CBN148 and CBN174 were produced with N234, Vulcan XC305, Vulcan XC605 and Vulcan XC72 blacks, respectively. Consequently, the designation of each mortar series clearly indicates the structure (DBP number) of the carbon blacks used in their production. The mixture proportion was 1.00:1.35:0.65:0.04 (cement:sand:water:superplasticizer), by weight. In each one of the other series, a concentration of 8% of each different kind of CBN by weight of cement was incorporated. For each series, four prismatic specimens of 4 cm × 4 cm × 7.5 cm (Figure 3) were produced according to the procedures described in Section 2.2.2.1. During their production process, two copper plates (electrodes) measuring 1.5 cm × 5.0 cm × 0.1 cm were embedded in a straight line at equal distance of 2.0 cm from each other.

Figure 3 – Dimensions of the cement-based composites and location of electrodes

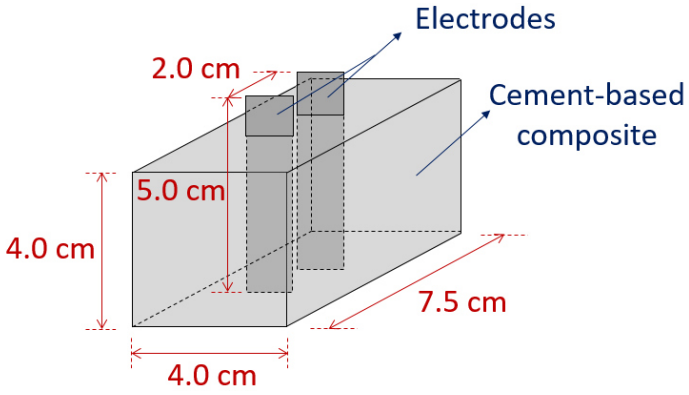

Source: Author (2020)

After a curing period of 28 days, one of the specimens was used to estimate the ultimate strength of the material. The other three composites were subjected to conventional uniaxial compression tests (according to procedures of ABNT NBR 13279 [49]) and to electrical and electromechanical tests described in Sections 2.2.2.2 to 2.2.2.5. In order to reduce any effect of ionic conduction through the pore water, the composites were oven dried for 24 hours at 100 - 105 ºC after the curing period and then cooled down to room temperature, according to recommendations of Mohsen et al. [50] and Kim et al. [51].

2.2.2.1. Cement-based composites preparation

The cement-based composites were produced with Portland cement CP II E-32 (a Brazilian Portland blast-furnace slag cement equivalent to the type I (SM) cement of ASTM

C595 [52]) with a density of 2.95 g/cm³ and natural sand with bulk specific gravity of 2.65 g/cm³ and maximum aggregate size of 1.2 mm. A commercially available polycarboxylate superplasticizer (SP) with a density of 1.12 g/cm³ was used as dispersant, as recommended by Han et al. [53].

Figure 4 indicates the main steps of production of the cement-based composites. At first, raw materials were weighed according to the designed mix proportions. After that, water, the nanomaterials and the superplasticizer were mixed for 1 minute. In order to improve the dispersion of the nanomaterials, the mixture was sonicated for 10 minutes using an ultrasonic probe with nominal frequency of 20 kHz and 50W of power. Then, the nanosuspension was mixed with cement for seven minutes with a conventional mortar mixer. Next, sand was added and mixed for additional four minutes. Finally, the fresh mixture was poured into oiled molds and compacted on a vibrating table for 10 seconds. After demolded, the composites were cured for 28 days in a moisture room at a temperature of (23 ± 2) ºC and relative humidity of 95%.

Figure 4 – Preparation of the cement-based composites

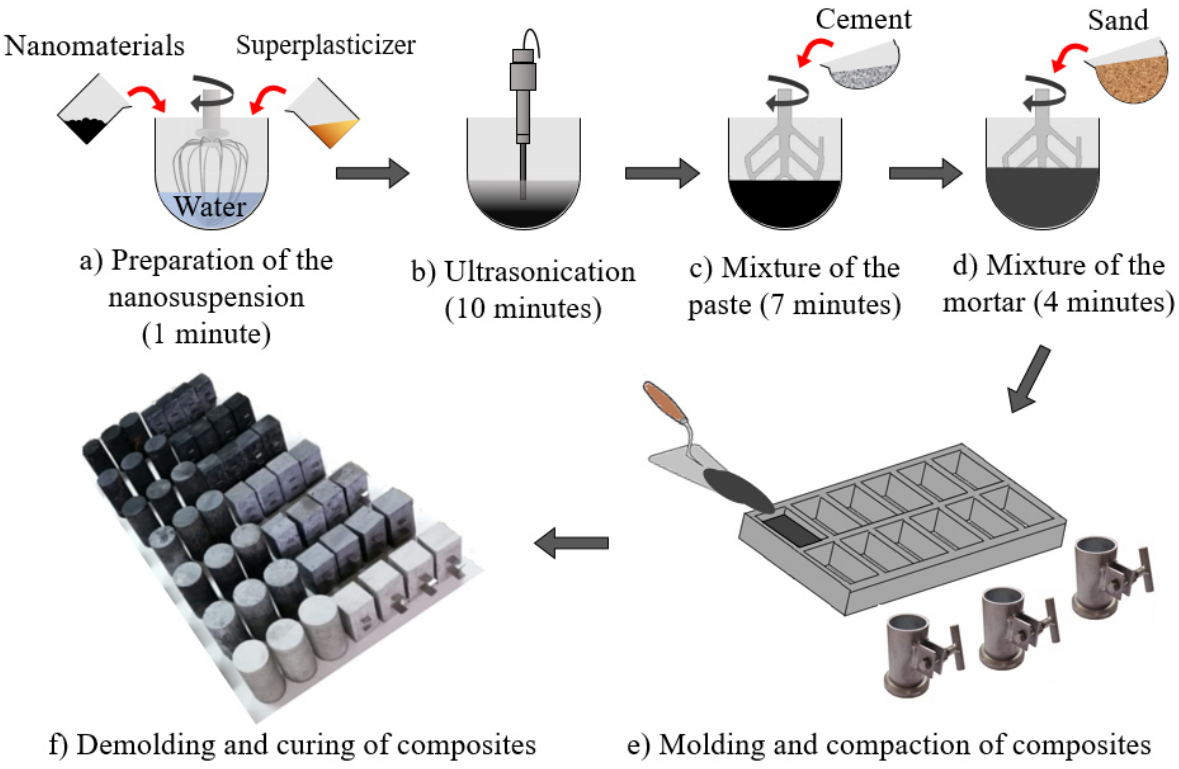

Source: Author (2020)

2.2.2.2. Direct current (DC) tests

DC tests were performed in order to evaluate the internal capacitance of the cementitious composites. Each mortar prism was connected in series to one 1000 Ω reference resistor and subjected to a DC electrical field, as shown in Figure 5. An Arduino Mega 2560 R3 microcontroller board was used to provide a 5 V stabilized source (v) for the circuit. Voltage was measured with a National Instruments compact DAQ-9178 chassis with a NI-9219 module and the LabVIEW software was used to create a data acquisition application.

Figure 5 – Experimental test setup for DC tests

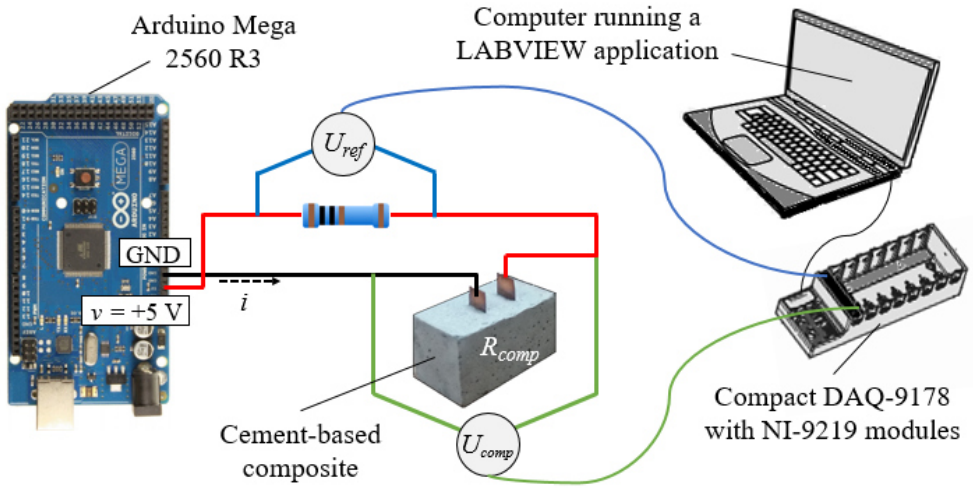

Source: Author (2020)

The electric current i flowing in this circuit was determined with Eq. 1, in which U_{ref} is the voltage drop across the reference resistor and R_{ref} is the electrical resistance of this resistor (1000 Ω).

Eq. 1
$$i = \frac{U_{ref}}{R_{ref}}$$

When the sample presented an inherent time-based drift, the electric current was determined until the drift levels out [8, 17-19]. In these situations, a nonlinear regression analysis was carried out to describe the capacitive response of these composites, based on the current vs. time (i vs. t) curve obtained from the DC test. The first-order exponential decay model of Eq. 2 was considered for the regression analysis. The constants K_1, K_2, and K_3 were systematically varied in order to minimize the sum of square errors. Based on these constants, the contact resistance of the electrodes R_{cont}, the composite's internal resistance R and capacitance C could be determined, considering the theoretical model proposed by Ubertini et al. [16] and D'Alessandro et al. [54] and presented in Eq. 3.

Eq. 2 $$i = K_1 + K_2 \exp\left(-\frac{t}{K_3}\right)$$

Eq. 3 $$i = \frac{v}{R + R_{cont} + R_{ref}}\left[\frac{R}{R_{cont} + R_{ref}} \exp\left(-\frac{\left(R + R_{cont} + R_{ref}\right) t}{CR\left(R_{cont} + R_{ref}\right)}\right) + 1\right]$$

When the electrical current i reached a plateau due to complete polarization of the composite, its electrical resistance R_{comp} was estimated with Eq. 4.

Eq. 4 $$R_{comp} = \frac{U_{comp}}{i}$$

where U_{comp} is the potential difference between the electrodes of the composite.

The electrical resistance R_{comp} can be used to estimate an electrical resistivity ρ for the system composite + electrodes, as shown in Eq. 5. It is important to note that this parameter represents not only the true electrical resistivity of the nanomodified mortar. Two other smaller electrical resistances are also related to this parameter: the electrical resistance of the electrodes and the contact resistance between mortar and electrodes. However, electrodes resistance and contact resistance only accounts for a small fraction of the electrical resistance of the whole specimen [55].

Eq. 5 $$\rho = \frac{R_{comp}\, L}{A}$$

where L is the distance between the electrodes and A is the effective area of the voltage pole.

2.2.2.3. Biphasic DC tests

The electrical resistance of the mortar prisms was also determined with the biphasic DC electrical measurement approach suggested by Downey et al. [18], which is an efficient way to determine fractional changes in the electrical resistance of cement-based composites used for strain sensing and damage detection in concrete structures.

In the present work, a periodic measure/discharge cycle in the form of a 6 Hz square wave ranging from -5 V to + 5 V with a duty cycle of 50% was used to determine the electrical resistance of the cementitious composite. The periodic signal was generated by the Arduino Mega 2560 R3 microcontroller board, as shown in Figure 6. Again, each composite was connected in series to one 1000 Ω reference resistor. A DAQ-9178 chassis, a NI-9219 module and the LabVIEW software were used to develop an application for acquisition of the potential differences U_{ref} and U_{comp} at instants of time of 80% of the positive constant part of the biphasic signal [18] and real-time plotting of data calculated with Eq. 1 and Eq. 4.

Figure 6 – Experimental test setup for biphasic DC tests

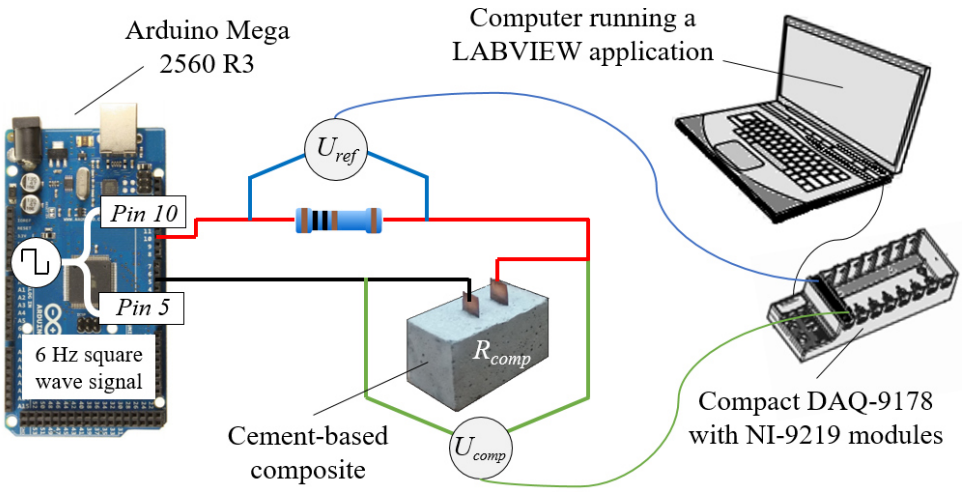

Source: Author (2020)

2.2.2.4. Piezoresistive tests

An electromechanical test was developed in a mechanical testing press for evaluation of the piezoresistive response of the cement-based composites, considering the load-time history presented in Figure 7. It consisted of a "cycle test", in which loading and unloading cycles with a maximum compressive load of 30% of the estimated ultimate load (f_u) were applied at about 600 N/s, followed by a "step test" with load steps at 10%, 20% and 30% of f_u. Then, the piezoresistive tests were within the elastic regime. The ultimate load was estimated through a compression test of one of the four specimens of the series. The plates of the press were covered with a plastic film to prevent unwanted electrical conduction.

Figure 7 – Load history of piezoresistive tests

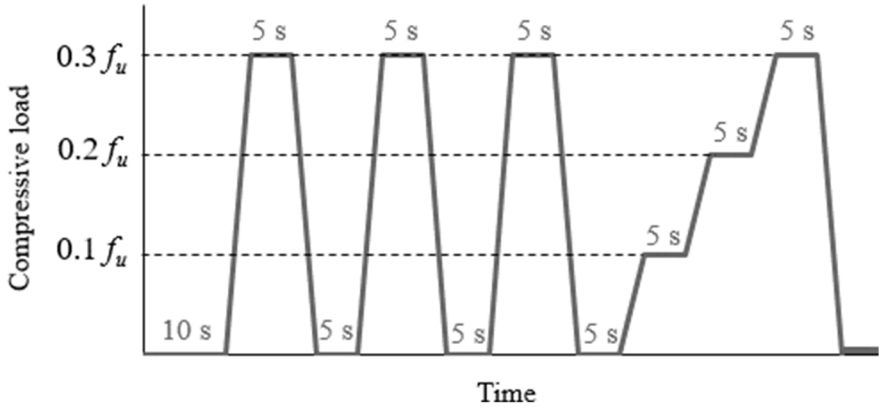

Source: Author (2020)

During the test, the electrical resistance of the composite was determined with the methods described in Section 2.2.2.3. In order to measure the real longitudinal strain at two

opposite faces of the specimen, the composites were equipped with the clip-gauge shown in Figure 8. Voltage drops and strains were collected by the DAQ-9178 chassis with two NI-9219 modules. Real-time charts were used in a LabVIEW application to plot fractional changes in the electrical resistance and axial deformation of the specimen during the test.

Figure 8 – Experimental setup for evaluation of piezoresistive response of the composites

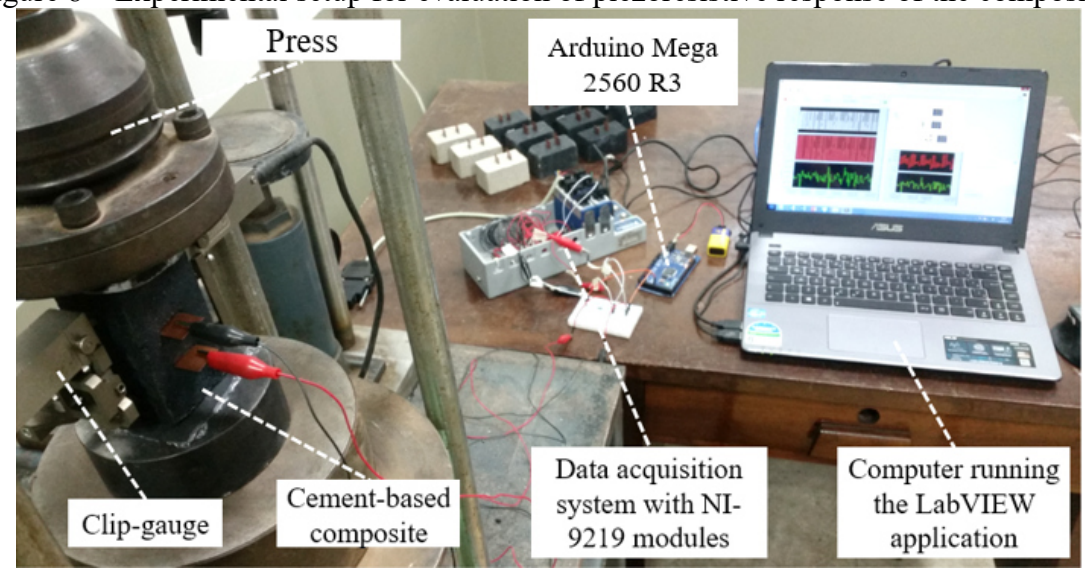

Source: Author (2020)

When the composite was subjected to the compressive load, the resistivity of the composite decreased. As dimensional changes of the composite were very small, the fractional change of electrical resistivity was approximately equal to the fractional change of electrical resistance FCR of the material [56]. Data from the loading part of the cycle tests was used to determine the relationship between the fractional change in electrical resistivity (FCR) and both compressive strain ε and compressive stress σ, considering the definition of gauge factor (GF) and stress sensitivity (SS), respectively, as shown in Eq. 6 and Eq. 7.

Eq. 6
$$GF = \frac{FCR}{\varepsilon} = \frac{\frac{\Delta R}{R_0}}{\varepsilon} \approx \frac{\frac{\Delta \rho}{\rho_0}}{\varepsilon}$$

Eq. 7
$$SS = \frac{FCR}{\sigma} = \frac{\frac{\Delta R}{R_0}}{\sigma} \approx \frac{\frac{\Delta \rho}{\rho_0}}{\sigma}$$

where R_0 and ρ_0 are the initial electrical resistance and resistivity of the composite, respectively, and ΔR and $\Delta \rho$ are the variation of electrical resistance and resistivity of the composites due to the load, respectively.

2.2.2.5. Evaluation of ohmic behavior

Experiments were conducted to determine the relationship between the electric current going through the cement-based sensor and the potential difference across the composite under unloading condition. Each composite and a 1000 Ω reference resistor were added in series to a source of constant voltage provided by a Keithley 6517B electrometer. Another LabVIEW application was used to provide 20 different constant supply voltage levels during 0.083 seconds, ranging from - 9V to + 9V. For each voltage level, the electric current after this sweep time was also measured with the Keithley 6517B electrometer. A sweep time of 0.083 seconds was chosen because it is the duration of the positive constant part of the 6 Hz biphasic signal considered in the resistance measurements of Section 2.2.2.3.

2.2.3. Results and discussion

Results of the DC tests show that the incorporation of any type of CBN decreased the electrical resistivity of the mortars and changed their capacitive behavior. The values of the ratio U_{comp}/i calculated with Eq. 4 for the three samples (S1, S2 and S3) of each series are shown in Figure 9. Within each series, all samples exhibited U_{comp}/i values of the same order of magnitude. Small differences between results of similar specimens can be attributed to slight variations in the electrodes spacing. The highest values were obtained for mortars without CBN (between 4.0×10^5 V/A and 1.2×10^6 V/A), which suggests a very high electrical resistance.

Mortars of the CBN125 series were produced with a furnace black with electrical resistivity of 3.3-3.9 Ω.cm and structure of 125 cm³/100g, which provided composites that presented significantly lower values of U_{comp}/i in DC tests (ranging from 8.0×10^3 V/A to 1.3×10^4 V/A). Despite this improvement in the electrical conductivity, Figure 9 indicates that these composites presented an increase of the U_{comp}/i ratio over time, which is related to the accumulation of electrical charge under an applied constant electrical field [3]. It means that N234 furnace blacks were not able to make a cement-based composite simply resistive, but also slightly capacitive. In fact, a clear decay of electric current over time was observed in the three samples of this series during the DC tests, as shown in Figure 10. The regression models developed with Eq. 2 and Eq. 3 were also presented in Figure 10. The time constants

τ of 4.33 s, 9.36 s and 10.31 s of samples S1, S2 and S3, respectively, characterize the capacitive behavior of this series.

Figure 9 – U_{comp}/i ratio vs. time curves obtained from the DC measurement approach of a) REF, b) CBN125, c) CBN131, d) CBN148 c) CBN174 series

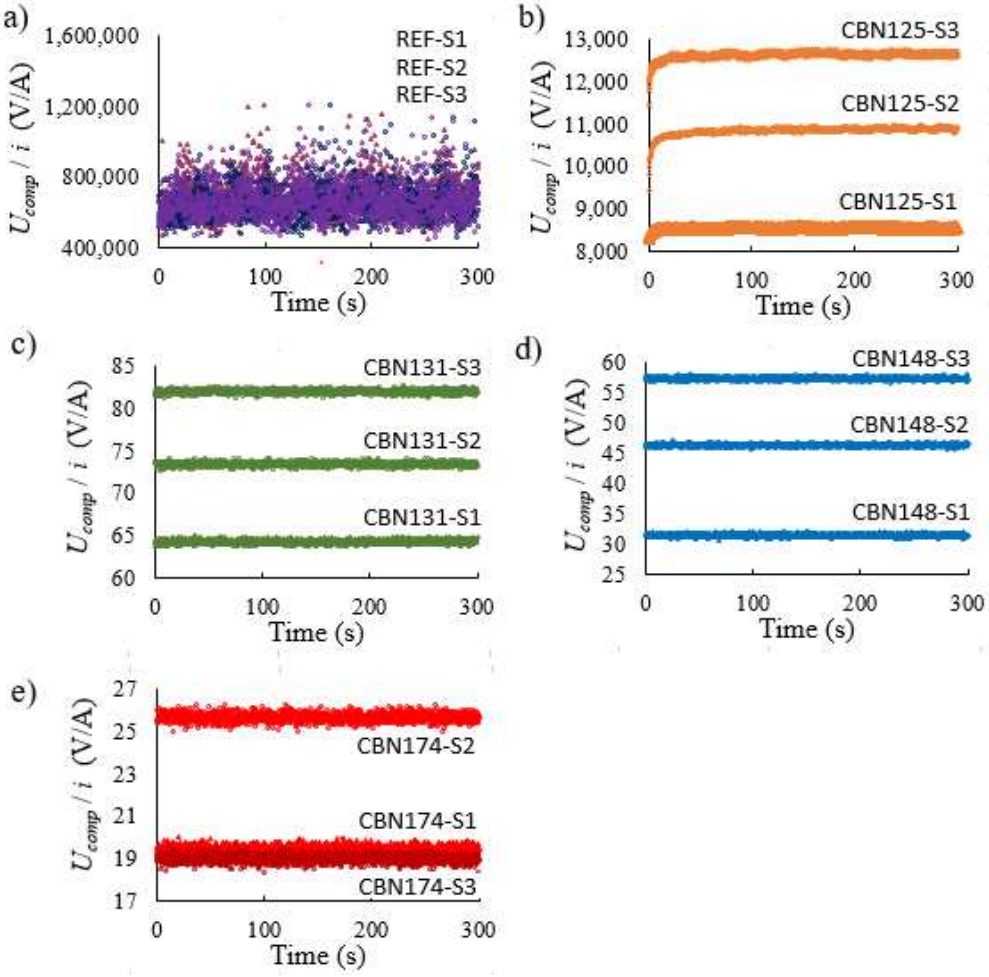

Source: Author (2020)

Figure 10 – DC current-time curves of samples a) S1, b) S2 and c) S3 of the CBN125 series

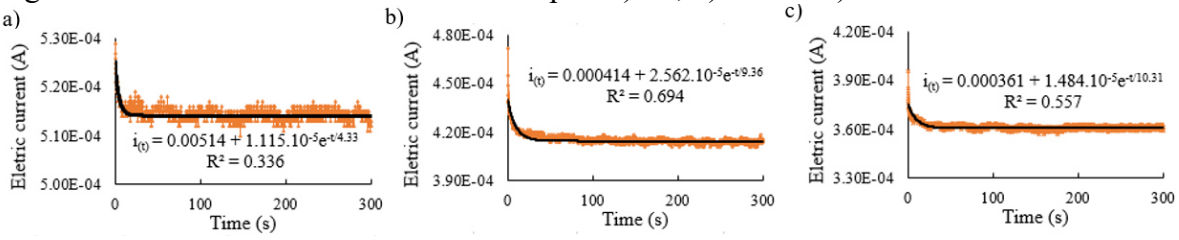

Source: Author (2020)

The internal capacitance depicted in Figure 10 disappeared when CBN with higher conductivity and structure were used. CBN131, CBN148 and CBN174 series were produced with CBN with electrical resistivity of about 50% of that of N234 blacks and structures 5%-

40% higher than the structure of N234 blacks. Since a same concentration of CBN was added in all series, these characteristics were the main responsible for the improvement of the conductive network inside the mortar (electrical resistivity values between 19 Ω and 85 Ω) and the elimination of the internal capacitance of the material.

The improvement of electrical conductivity with XC72, XC305 and XC605 blacks can also be realized in Figure 11, in which the electrical resistivity of composites obtained from the DC and biphasic DC tests are shown.

Figure 11 – Electrical resistivity of composites produced with different kinds of CBN

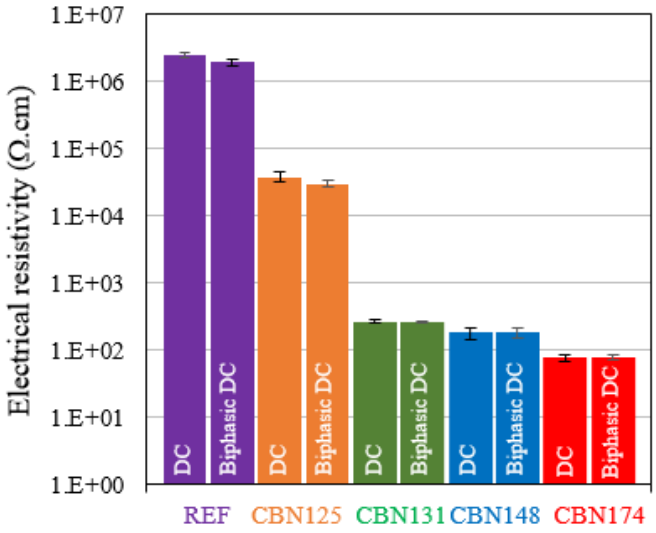

Source: Author (2020)

High structured and more conductive CBN (XC72, XC305 and XC605) provided composites with low values of electrical resistivity in both tests. The lowest values of electrical resistivity were observed in composites of the CBN174 series, which were produced with CBN with the highest structure (174 $cm^3/100g$) and specific surface area (254 m^2/g), characteristics that improve the contact between nanofillers and the electronic conduction. The difference between the resistivity results of DC and biphasic DC measurement approaches is related to an internal capacitance of the composite. A significant difference is indicated only in REF and CBN125 series (Figure 11).

Results of piezoresistive tests and FCR vs. strain data are shown in Figure 12 and Figure 13, respectively. Only the REF series did not present a good piezoresistive response under repeated compressive loadings. Regardless the type of CBN, piezoresistive tests presented good repeatability and no significant hysteresis. In order to better observe the piezoresistive response, linear regression analyses with zero intercept were performed to find

the models that provide the best fit to FCR vs. strain datasets. The developed models and their coefficients of determination R^2 are also presented in Figure 13.

Figure 12 – Piezoresistivity in a) REF, b) CBN125, c) CBN131, d) CBN148 and e) CBN174 series

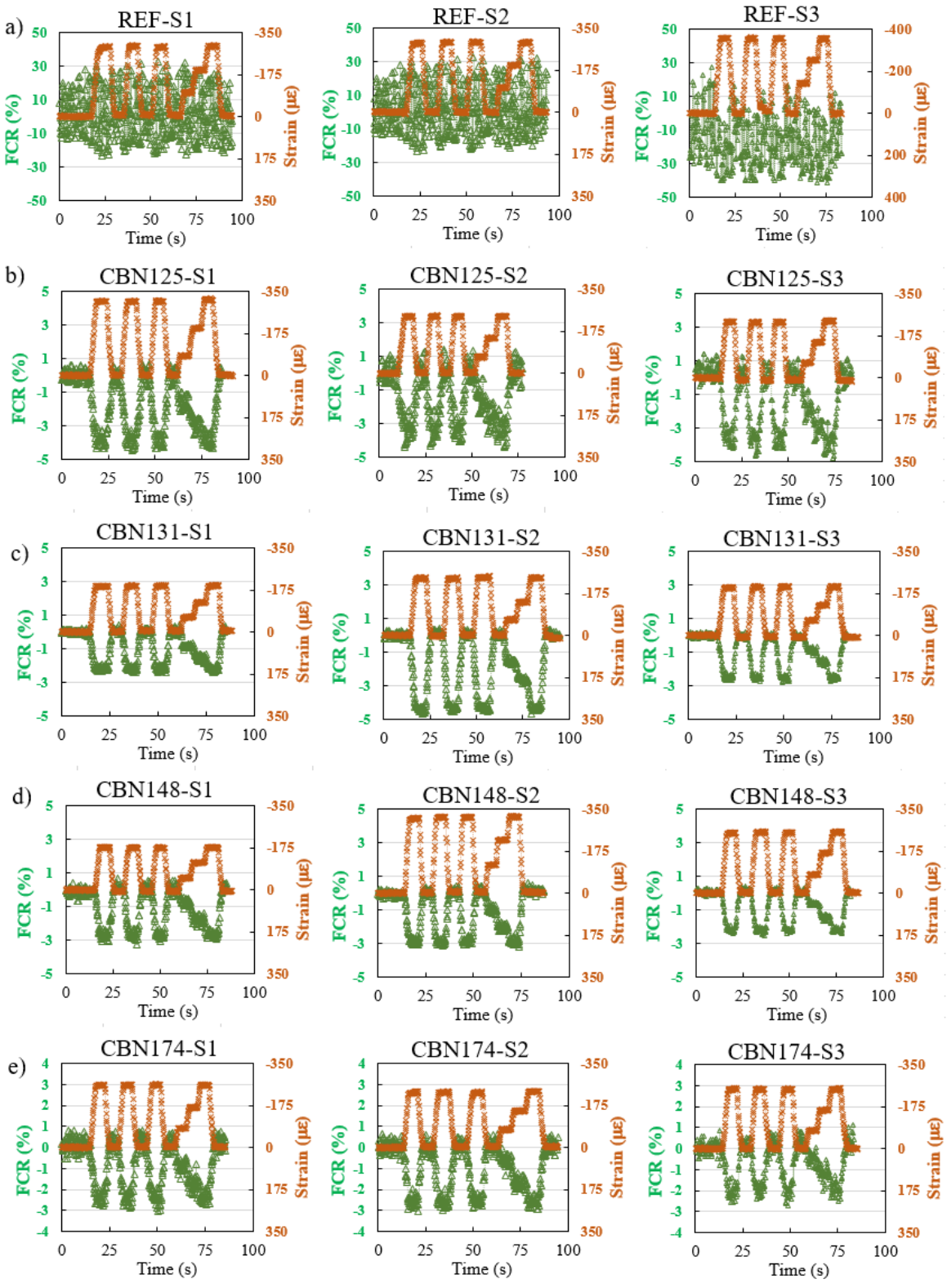

Source: Author (2020)

Figure 13 – FCR vs. strain curves of a) REF, b) CBN125, c) CBN131, d) CBN148 and e) CBN174 series

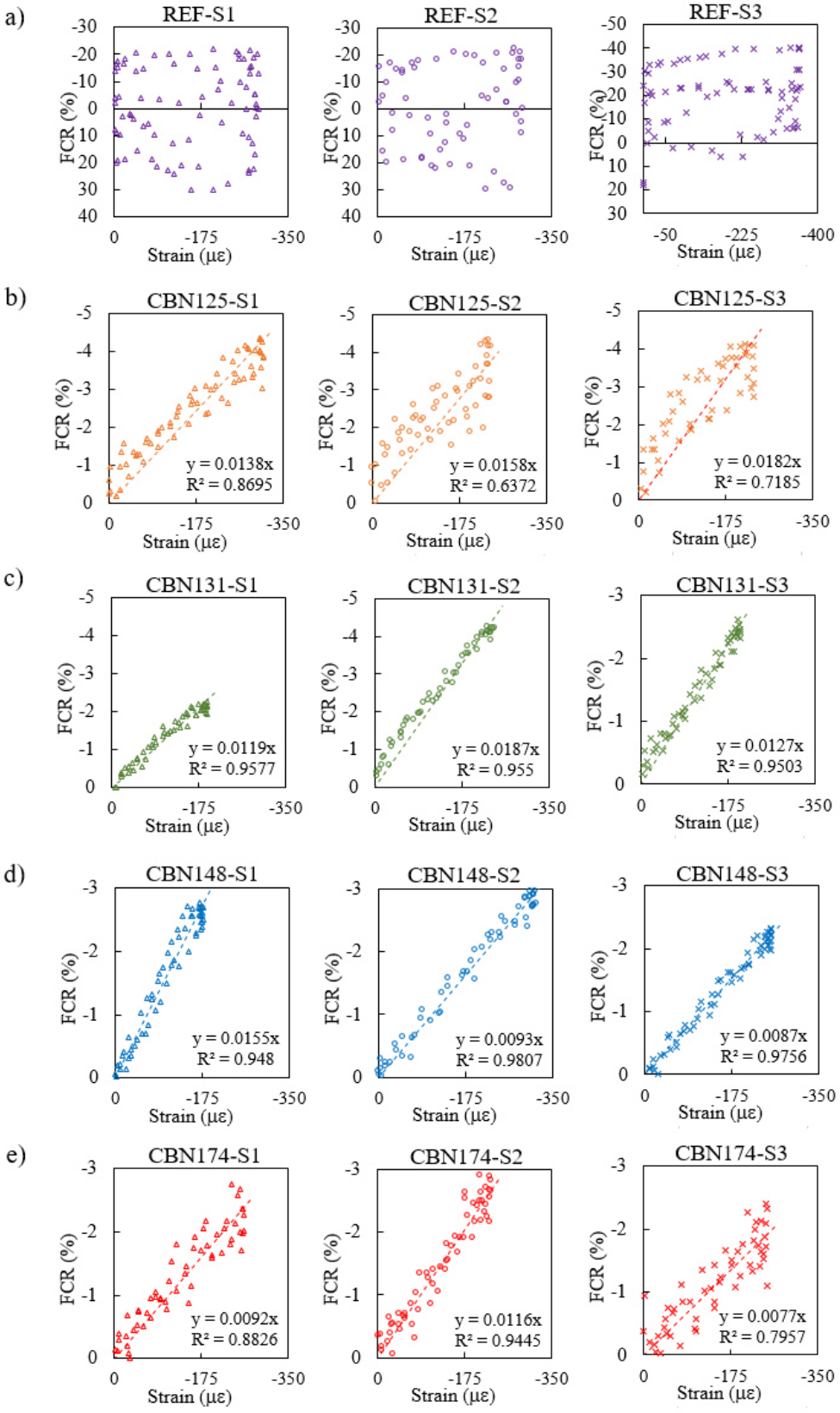

Source: Author (2020)

Average values of gauge factor, coefficients of determination and stress sensitivity of each series are presented in Figure 14. CBN125 series presented the lowest average R^2 value (0.74), but the highest amplitude of FCR values and, consequently, the highest average gauge factor (159) and average stress sensitivity (0.0100 MPa^{-1}). On the other hand, CBN174 series presented a good average R^2 value (0.87), but the lowest average gauge factor (95) and stress sensitivity (0.0084 MPa^{-1}).

Figure 14 – GF, R^2 and SS of mortars with different types of CBN

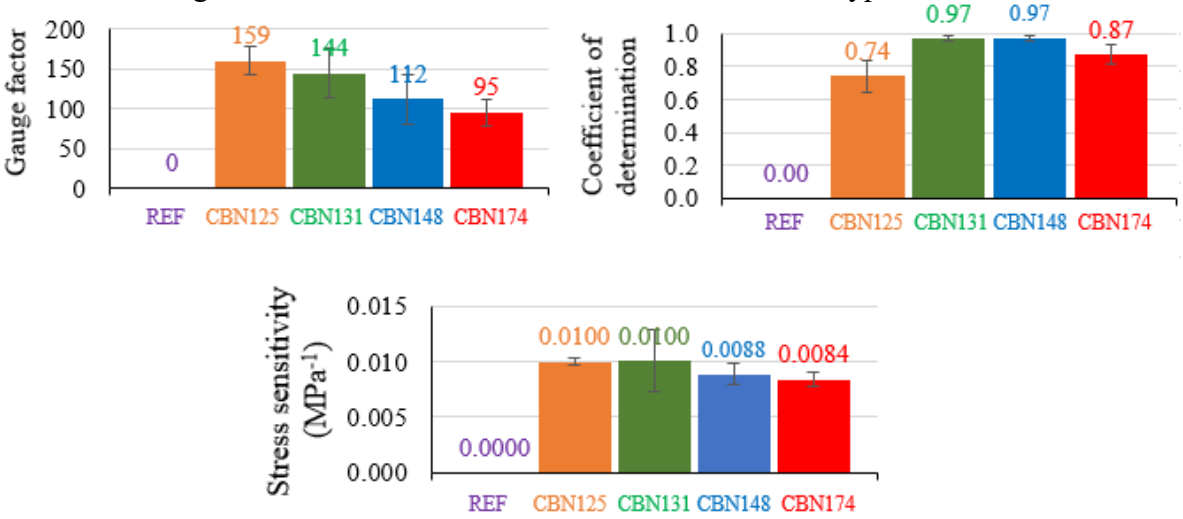

Source: Author (2020)

Tunneling and contact conduction are the basic mechanisms that originate electronic conduction in these composites. However, strain-induced changes in their electrical resistivity are directly related to the variations in tunneling resistance due to changes of inter-particle distances [2, 3, 33]. Results of this work indicate that CBN with moderate electrical conductivity and structure (CBN125 series) provided the best improvements to the sensing properties of the mortars. The increase of the CBN aggregates structure improved the conductive network inside the cementitious matrix and increased contact conduction. On the other hand, the decrease of the CBN aggregates structure improved the variations of tunneling resistance between nanofillers due to compressive loading. Consequently, the electrical resistivity of mortars with CBN with moderate structure is easier to be changed by compressive loading. In addition, XC72 blacks have a specific surface area of 254 m^2/g, which is significantly greater than the specific surface area of N234 blacks (120 m^2/g). A high surface area increases the probability of contact between neighboring functional fillers, which contributes for the domination of the contact conduction over the tunneling conduction.

The electric current vs. voltage curves of cement-based sensors are shown in Figure 15. These curves were obtained at voltage levels close to the range in which the cement-based sensors of CBN125, CBN131, CBN148 and CBN174 series will work in test setups similar to those described in Sections 2.2.2.2 and 2.2.2.3. Regardless the type of CBN, a linear dependence of the electric current as a function of the voltage was observed in the composites, which suggests the dominance of contacting conduction in all samples [57, 58, 13]. Such behavior is in accordance with Ohm's law and findings of Han et al. [57], Mao et al. [59] and Benamara et al. [60] (apud Han et al. [13]) for nanomodified cement composites.

Figure 15 – Electric current vs. voltage curves of cement-based sensors of a) CBN125, b) CBN131, c) CBN148 and d) CBN174 series

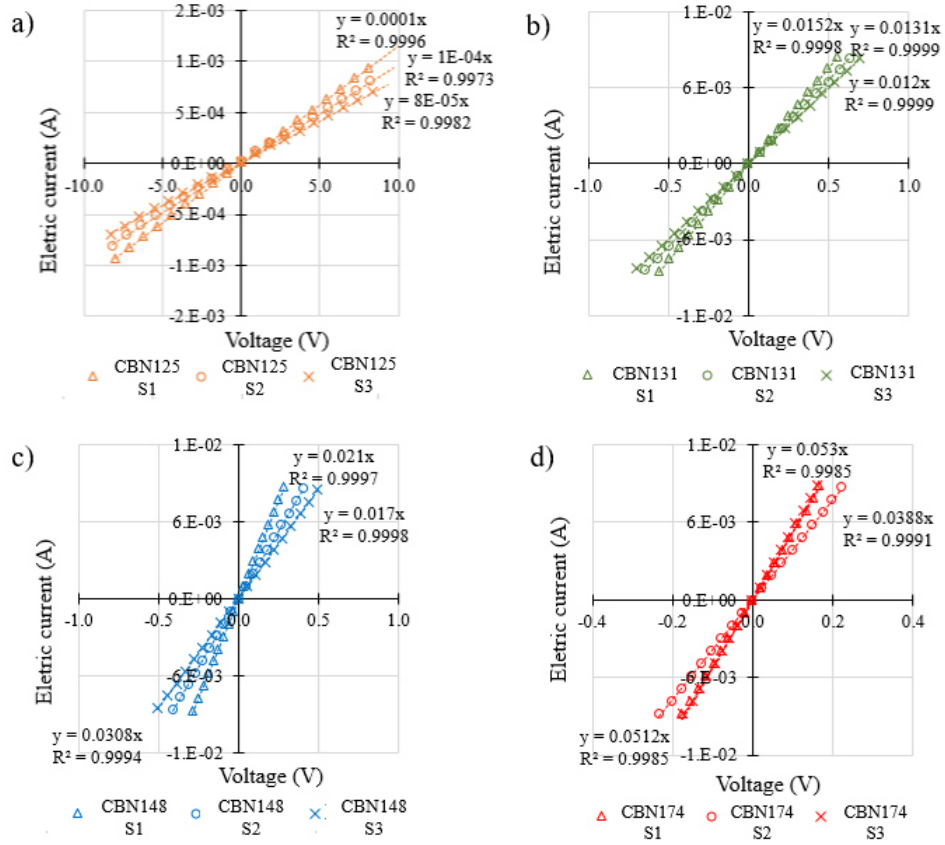

Source: Author (2020)

The incorporation of a high concentration of any type of CBN caused decreases in the compressive strength of the mortars (Figure 16), as previously reported by Yawen et al. [61] and Dong et al. [62]. Strength reductions have been attributed to poor cohesion between the cementitious matrix and CBN aggregates and adsorption of CBN on the surface of cement, which hinders the hydration process. Dong et al. [62] also mention that CBN tend to absorb a fraction of water leading to decreases of mechanical strength.

Figure 16 – Compressive strength of mortars with different types of CBN

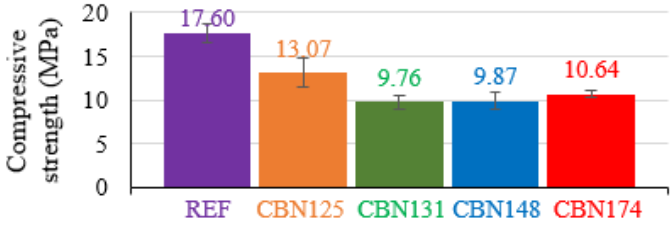

Source: Author (2020)

XC72 blacks have the highest specific surface area. In addition, XC72, XC305 and XC605 blacks have high structures. Such characteristics suggest that greater levels of water adsorption by the functional fillers had a negative influence on the rate of cement hydration. Among the CBN used in this work, N234 blacks have the lowest structure and a moderate surface area, which suggests why they provided the lower mechanical strength reductions.

2.2.4. Conclusion

The results of this preliminary study show that the structure, conductivity and specific area of nanofillers must be taken into account in the design of cementitious composites. The following conclusions were derived from this study:

(1) Any type of CBN reduced the electrical resistivity and compressive strength of mortars, provided composites with good piezoresistive response and with linear dependence of the electric current as a function of the voltage.

(2) A high electrical conductivity, low internal capacitance, good linearity and repeatability on piezoresistive response, lowest gauge factor, lowest stress sensitivity and moderate compressive strength were verified in composites containing carbon blacks with very high structure (174 $cm^3/100g$) and low resistivity (1.7 - 2.1 Ω.cm). A moderate decrease of electrical resistivity, considerable internal capacitance, reasonable linearity and repeatability on piezoresistive response, highest gauge factor, highest stress sensitivity and good compressive strength were observed in composites containing carbon blacks with the lowest structure (125 $cm^3/100g$) and the highest resistivity (3.3 - 3.9 Ω.cm).

(3) The increase of CBN aggregates structure, surface area and conductivity improved the conductive network inside the composite and reduced its internal capacitance. Despite this, it decreased its compressive strength and piezoresistive response due to reduction of changes of tunneling distance between functional fillers in compression tests.

2.3. EFFECTS OF CBN CONCENTRATION ON THE PIEZORESISTIVE RESPONSE OF CEMENT-BASED COMPOSITES AT DRIED AND WET CONDITIONS

2.3.1. Introduction

The electrical resistivity of cementitious materials ranges from 1×10^4 Ω.cm to 1×10^8 Ω.cm [5]. The production of self-sensing composites requires the reduction of the electrical resistivity of the material by adding a concentration of conductive nanofillers above a critical value called percolation threshold [2, 3, 11]. If the fraction of functional fillers exceeds the percolation threshold, there is a domination of the electronic conduction over the ionic conduction. In this case, the composites have noticeable self-sensing behavior, which is related to the materials' piezoresistivity phenomenon [2, 14, 32].

Cement-based composites with intrinsic self-sensing behavior can be produced with carbon black nanoparticles (CBN), nanomaterials with high electrical conductivity and specific surface area and low production cost [17, 32]. Li, Xiao and Ou [33] verified a sharp decrease in the electrical resistivity of cement pastes when fractions of 12% to 20% of CBN (by weight of cement) were added. Regarding the piezoresistive behavior, composites with a CBN concentration of 15% presented an excellent gauge factor (55.28). Monteiro, Cachim and Costa [34] verified a good piezoresistive response in mortars with CBN content of 7% and 10%, reaching gauge factors values of 30.28 and 24.13 and stress sensitivity values of 0.00286 MPa^{-1} and 0.00172 MPa^{-1}, respectively. Cement pastes with 15% CBN produced by Li, Xiao and Ou [41] presented gauge factors ranging from 52.7 to 59.6 and stress sensitivity around 0.006 MPa^{-1}. Using a CBN content of 6.5%, Monteiro et al. [17] developed self-sensing mortars with gauge factors between 40 and 60 and stress sensitivity between 0.0025 MPa^{-1} and 0.0035 MPa^{-1}. Gauge factors from 25 to 160 were obtained for mortars with 1% CBN by Huang et al. [32]. The high scatter of sensing properties is mainly related to different mixture compositions and characteristics of CBN.

Experimental tests of mortars with carbon fiber (CF) developed by Chung et al. [14] indicated that the water content only influences the electrical resistivity of the cementitious composites when a low CF content is used. Yoo et al. [56] also verified that the variation of pore water content causes relatively insignificant changes of electrical resistivity of mortars with multi-walled carbon nanotubes (MWCNT) when the concentration of functional fillers was beyond the percolation threshold value.

The influence of water content on conductivity and piezoresistive of cement pastes with silica fume, CBN and CF was investigated by Han et al. [42]. They found that the electrical resistivity and strain sensitivity of cement-based material with both CF and CBN increases as the water content increases. Similar results were recently reported by Zhang et al. [43] for cement mortars with both CBN and MWCNT. An opposite behavior was observed in the mortars with MWCNT produced by Song and Choi [63]: when the water content of mortars with MWCNT decreased, their electrical resistivity and stress sensitivity increased. Differently, Han, Yu and Ou [64] observed that the stress sensitivity of mortars with MWCNT firstly increased and then decreased with the increase of water content. They stated that the adsorption of water molecules enhances the field emission effect on the nanotube tip and improves the electrical conductivity of the composite. Dong et al. [44] also observed that the increase of water content affected the sensitivity of cementitious composites containing 3% of CBN, by firstly increasing and then decreasing their gauge factor. In addition, they reported that the electrical resistance of the composites increased with water content, due to the water that enclosed CBN.

Effects of water content on the electrical resistivity, intrinsic capacitance, gauge factor and stress sensitivity of cement-based composites containing different CBN contents were not previously investigated. Distinct conclusions about this topic have been reported for cement-based composites with other types of carbon nanomaterials. Then, the present preliminary study aims to improve the understanding of the effect of water content on the electrical properties of mortars with CBN. In addition, there is no self-sensing cement-based material developed with Brazilian construction materials and Brazilian conductive fillers, which is also a reasonable justification to develop this preliminary study.

2.3.2. Experimental Methods

Cement-based composites were produced with N234 blacks with specific surface area of 120 m^2/g, dibutyl phthalate (DBP) absorption number of 124.7 $cm^3/100g$, average particle size of 20 nm and made by Birla Carbon in Cubatão (São Paulo, Brazil). Four different types of mortar compositions designated as 0CBN, 4CBN, 8CBN, and 12.5CBN were produced. They were doped with 0%, 4%, 8% and 12.5% of CBN by mass of cement, respectively. The sand to cement ratio and water to cement ratio of all mixes were 2.29 and 0.54 by mass, respectively. The superplasticizer was added in 0%, 1.6%, 3.3%, and 5% by mass of cement in 0CBN, 4CBN, 8CBN, and 12.5CBN mortars, respectively.

For each series, four prismatic specimens (S1, S2, S3 and S4) of 4 cm × 4 cm × 7.5 cm were produced according to the procedures described in Section 2.2.2.1. In each composite, two copper plates of 1.5 cm × 5.0 cm × 0.1 cm were embedded in a straight line at equal distance of 2.0 cm from each other. After 28 days, one of the specimens was used to estimate the ultimate strength of the material. The other specimens were subjected to the electrical and electromechanical tests described in Sections 2.2.2.2 to 2.2.2.4.

In order to verify the effect of water content on the electrical properties of the composites, two humidity conditions were considered for testing after the curing period. In the first humidity condition, specimens were tested after being taken from the moisture room. Their water content was about (4.0 ± 0.5)%. In the second condition, composites were tested after being oven dried for 24 hours at 100 - 105 ºC and cooled down to room temperature, according to recommendations of Mohsen et al. [50] and Kim et al. [51]. Then, eight different series were evaluated in this preliminary study (Table 2).

Table 2 – Characteristics of the composites of each series of this preliminary study

Series	CBN concentration [(a)]	Water content
0CBN/W	0	(4.0 ± 0.5)%
4CBN/W	0.04	
8CBN/W	0.08	
12.5CBN/W	0.125	
0CBN/D	0	~ 0 %
4CBN/D	0.04	
8CBN/D	0.08	
12.5CBN/D	0.125	

[(a)] Fraction by mass of cement

2.3.3. Results and discussion

Results of DC tests are summarized in Figure 17. It is evident that the increase of CBN content continually decreased the mortar's electric resistivity and capacitive behavior. There are clear evidences of reduction of ionic conduction effects due to the drying process. For instance, the U_{comp}/i ratios of three dried samples without CBN (0CBN/D-S1, 0CBN/D-S2 and 0CBN/D-S3) are 10 - 20 times greater than the U_{comp}/i ratios of non-dried samples without CBN (0CBN/W-S1, 0CBN/W-S2 and 0CBN/W-S3). It suggests that the electrical resistivity of ordinary mortars is strongly affected by humidity conditions.

Figure 17 – U_{comp}/i ratio vs. time curves obtained from the DC measurement approach of a) composites with water content of (4.0 ± 0.5)% and b) oven-dried composites

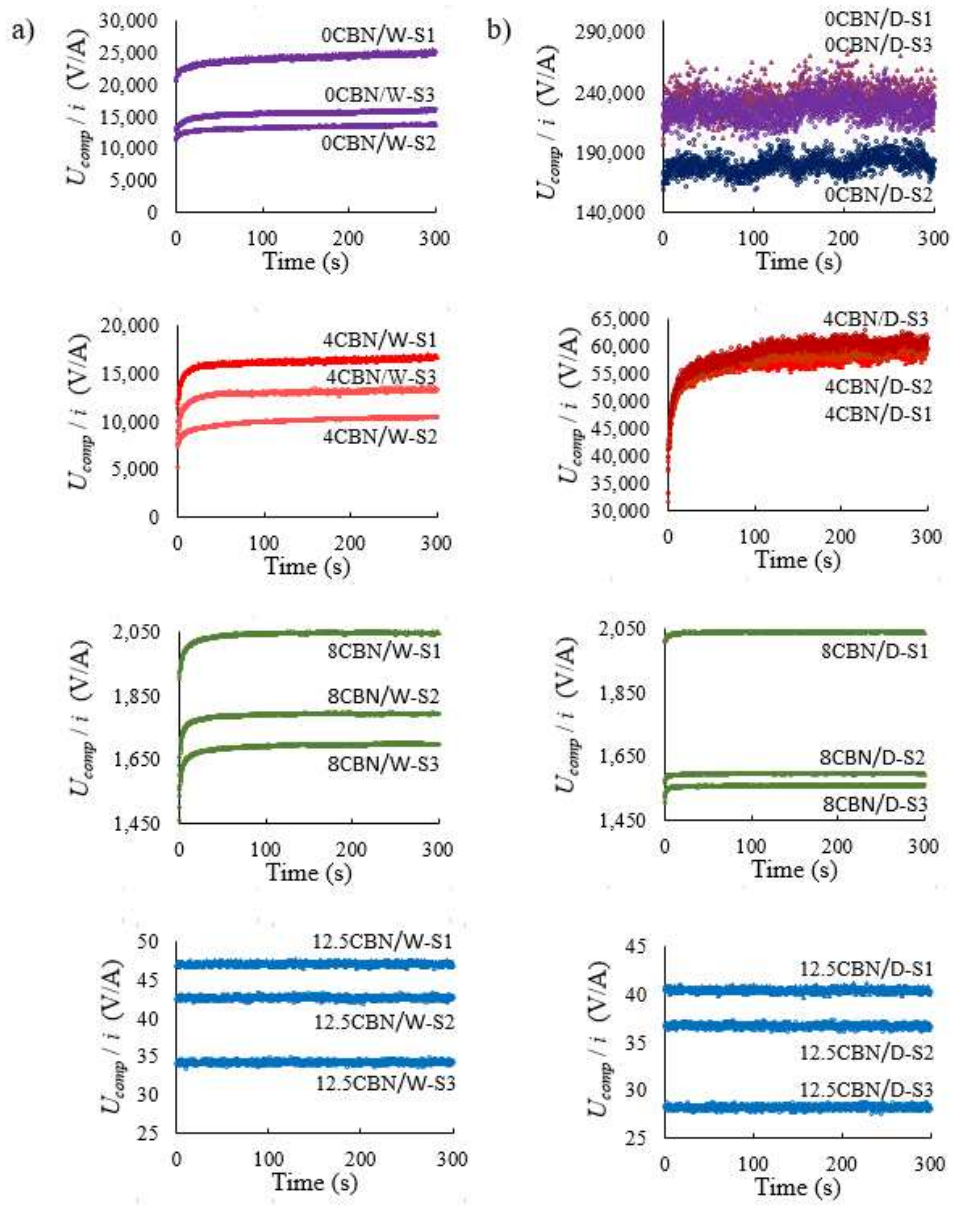

Source: Author (2020)

The incorporation of CBN contents of 4% and 8% improved the electrical conductivity of mortars. Despite this, values of U_{comp}/i increased over time in most of the series with these CBN concentrations, which indicates an intrinsic capacitive effect [3]. In fact, a decay of electric current over time was noted in the three samples of 0CBN, 4CBN and 8CBN series in wet condition (Figure 18) and the samples of 4CBN, 8CBN series in dry condition (Figure 19). Samples of the 0CBN series did not demonstrate a capacitive behavior after the drying process because their electrical resistivity was excessively high.

Electric current vs. time regression models obtained from Eq. 2 and Eq. 3 are also presented in Figure 18 and Figure 19. These models were used to determine the time constants of each circuit, which were plotted against the CBN concentration in Figure 20. Results show that larger amounts of CBN (12.5% cases) reduced the mortars' intrinsic capacitive effect and decreased the influence of the drying process on the capacitive behavior.

Figure 18 – DC current vs. time curves of samples S1 (left), S2 (center), and S3 (right) of a) 0% CBN, b) 4% CBN and c) 8% CBN series, for a water content of (4.0 ± 0.5)%

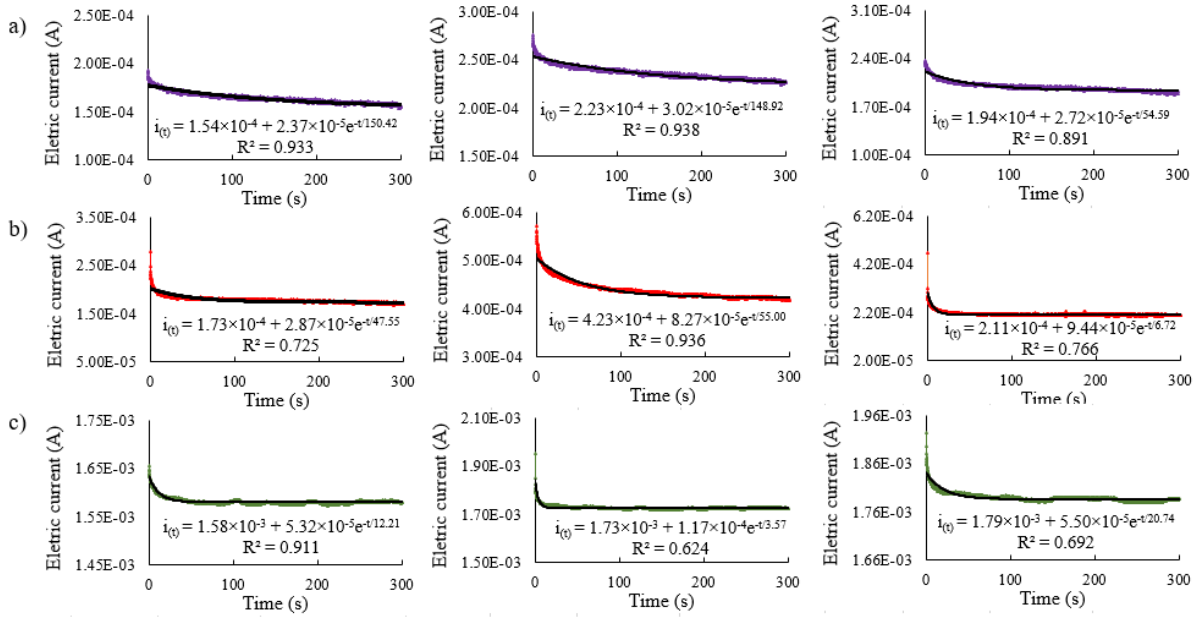

Source: Author (2020)

Figure 19 – DC current vs. time curves of samples S1 (left), S2 (center), and S3 (right) of a) 4% CBN and b) 8% CBN series, after the drying process

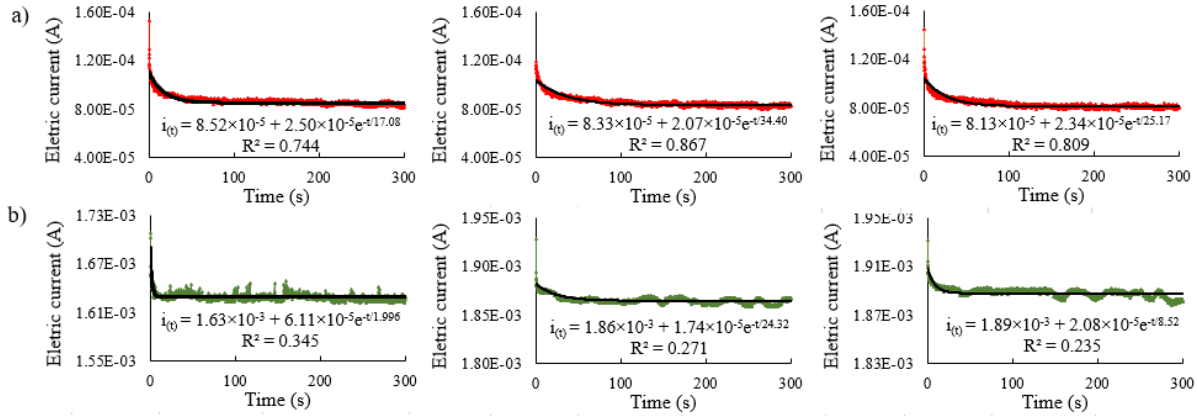

Source: Author (2020)

Figure 20 – Time constants in DC tests as a function of mortar's CBN concentration

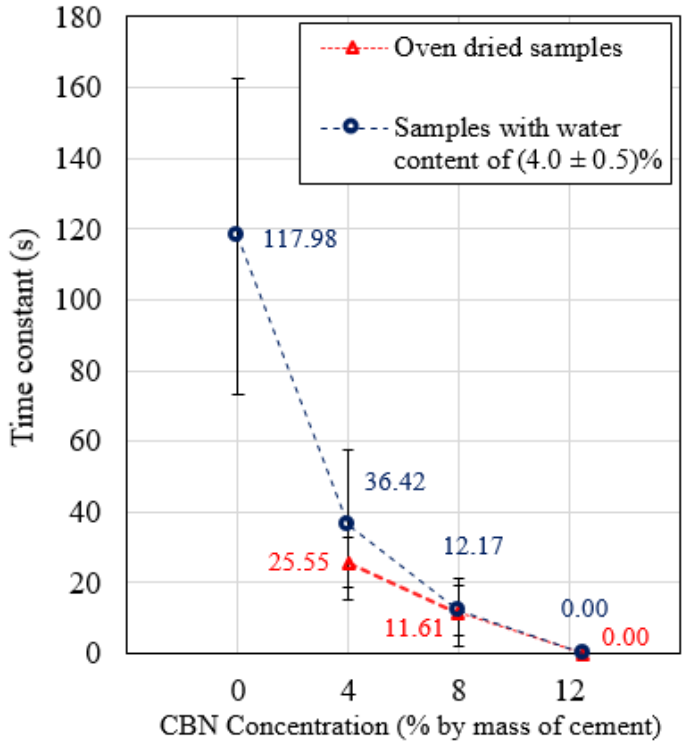

Source: Author (2020)

The incorporation of CBN contents of 12.5% (by mass of cement) eliminated the internal capacitance (Figure 17) and provided composites with DC or biphasic DC electrical resistivity up to four orders of magnitude lower than the resistivity of dried ordinary mortars (Figure 21). Difference between the electrical resistivity obtained through DC and biphasic DC measurement approach was only significant in 0CBN and 4CBN series, which demonstrated stronger internal capacitance.

Figure 21 – Electrical resistivity of composites produced with different contents of CBN

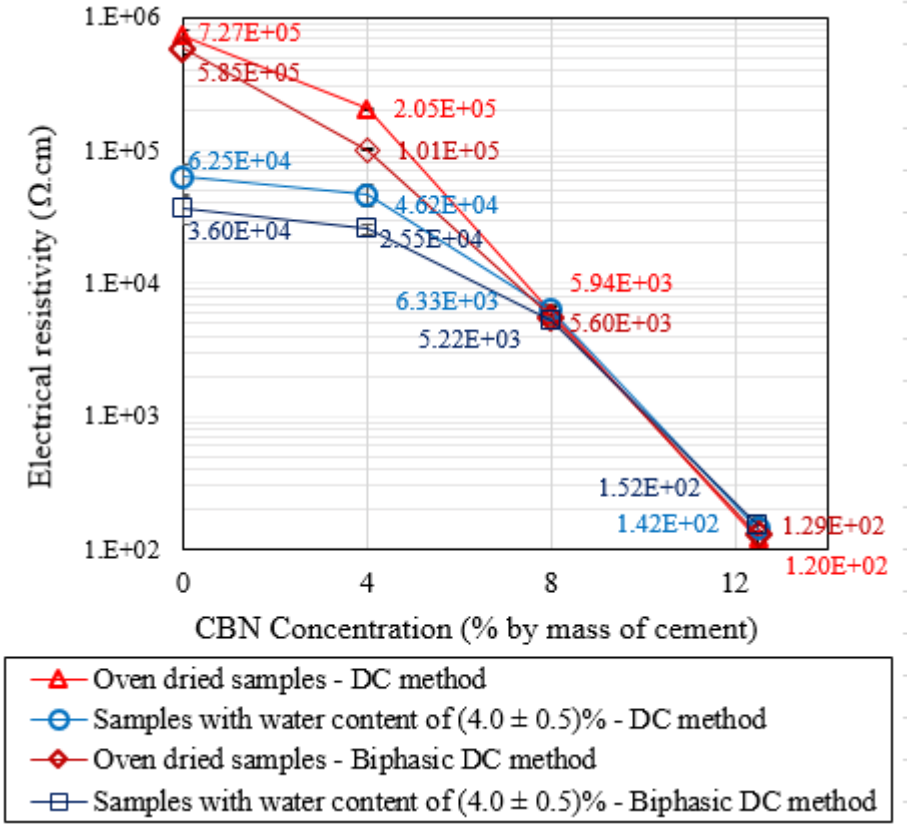

Source: Author (2020)

Data of Figure 21 provided a better understanding of the influence of water content on the electrical resistivity of mortars with CBN. Results show that the influence of water content on the electrical resistivity of cement-based composites is directly related to the nanofillers concentration. When the filler content was below the percolation threshold (0CBN and 4CBN series), the reduction of the water content significantly increased the electrical resistivity of the material, which is in accordance with the results of Chung et al. [14] and Yoo et al. [56] for mortars with carbon fibers (CF). In this situation, the ionic conduction was dominant (insulation zone) and the drying process eliminated the conduction associated with the motion of ions (mainly Ca^{2+} and OH^{-}) in the pore solution [58].

An opposite result was obtained when the CBN content was significantly higher than the percolation threshold (12.5CBN series): the reduction of water content decreased the electrical resistivity of the material, which is consistent with results of Han et al. [42] (mortars with both CBN and CF) and Zhang et al. [43] (mortars with both CBN and MWCNT). In this situation, electronic conduction due to direct contact of neighboring CBN aggregates is the dominant conduction mechanism (conductive zone). The water adsorbed on CBN caused an increase of the contact resistance between aggregates [43]. The drying process eliminated

part of this water, improved the contact electronic conduction and decreased the electrical resistivity of the material.

After performing an analysis of variance at the 5% significance level, it was observed that the electrical resistivity of 8CBN composites in dry and wet condition can be considered statistically equal (a P-value of 0.363 was obtained, which confirms the null hypothesis that the compared averages are statistically equal). In this case, the CBN content is pretty close to the percolation threshold and the tunneling conduction is the dominant mechanism in the electrical conductivity of the material (percolation zone). Since evaporation of pore water did not affect the electrical resistivity, it is possible to infer that the drying process did not provide substantial changes on tunneling conduction.

These results are slightly different from those obtained by Han et al. [64] for cement pastes with MWCNT. They mentioned that the adsorption of water molecules enhanced the field emission effect on the nanotube tip and improved the electrical conductivity of composites in the percolation zone. In the present work, the results indicate that the water content significantly affected ionic conduction and electronic conduction due to physical contact between CBN, but did not statistically affect the tunneling effect.

Figure 22 and Figure 23 show the piezoresistive response and FCR vs. strain curves of composites with water content of (4.0 ± 0.5)%, respectively, while Figure 24 and Figure 25 show the same items for the oven-dried composites. All non-dried composites exhibited some piezoresistive response, which is probably associated with dominant ionic conduction in 0CBN series and dominant electronic conduction in the other cases. It shows that even cement-based materials with no conductive filler have a piezoresistive response. However, the piezoresistive response of these materials is highly dependent on their water content. In addition, the electrical resistivity of wet composites of the 0CBN series on the beginning of the piezoresistive test was higher than the electrical resistivity at the end of the test, which is related to the motion of water within the pores during the loading and unloading cycles.

Among the oven-dried composites, a piezoresistive response was not verified only in composites of the 0CBN and 4CBN series, which is related to the great increase of electrical resistivity of these composites due to the elimination of the pore water. Oven-dried composites of the 8CBN and 12.5CBN series presented good repeatability and no hysteresis. Linear regression analyses with zero intercept were performed to determine the models that provide the best fit to FCR vs. strain curves. Figure 23 and Figure 25 also show these models and their coefficients of determination R^2.

Figure 22 – Piezoresistive response of composites with water content of (4.0 ± 0.5)%

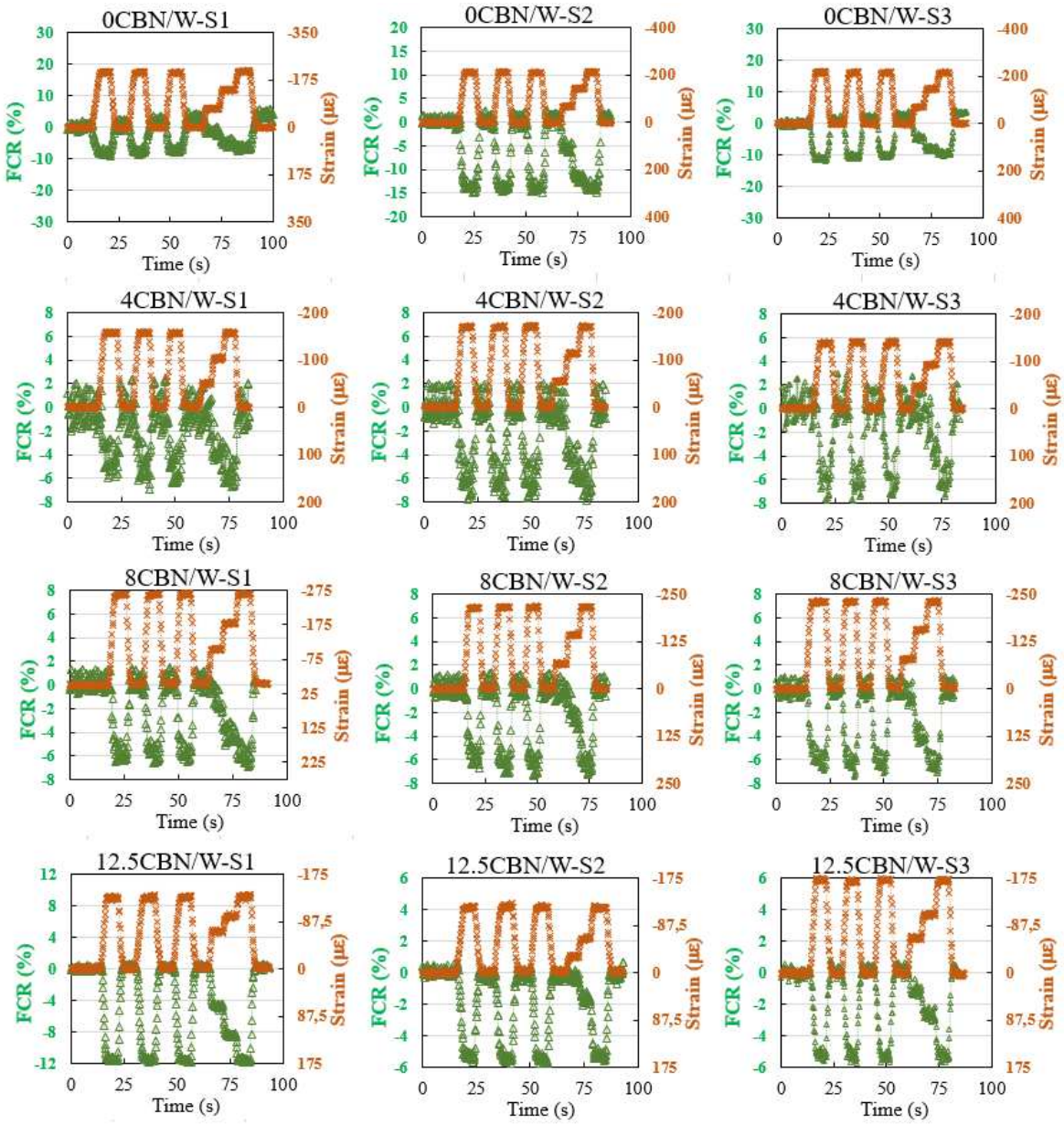

Source: Author (2020)

Figure 23 – FCR vs. strain curves of composites with water content of (4.0 ± 0.5)%

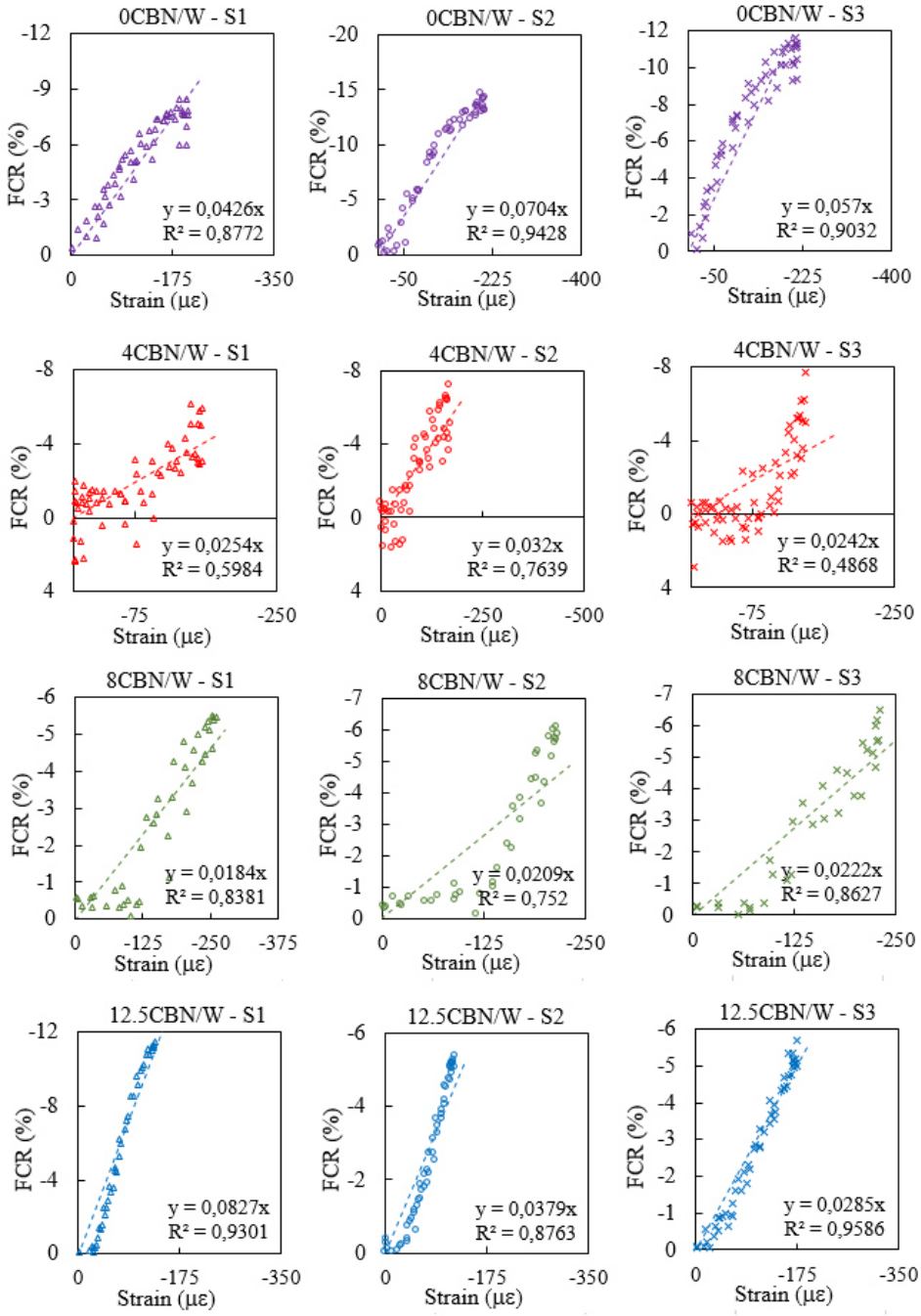

Source: Author (2020)

Figure 24 – Piezoresistive response of oven-dried composites

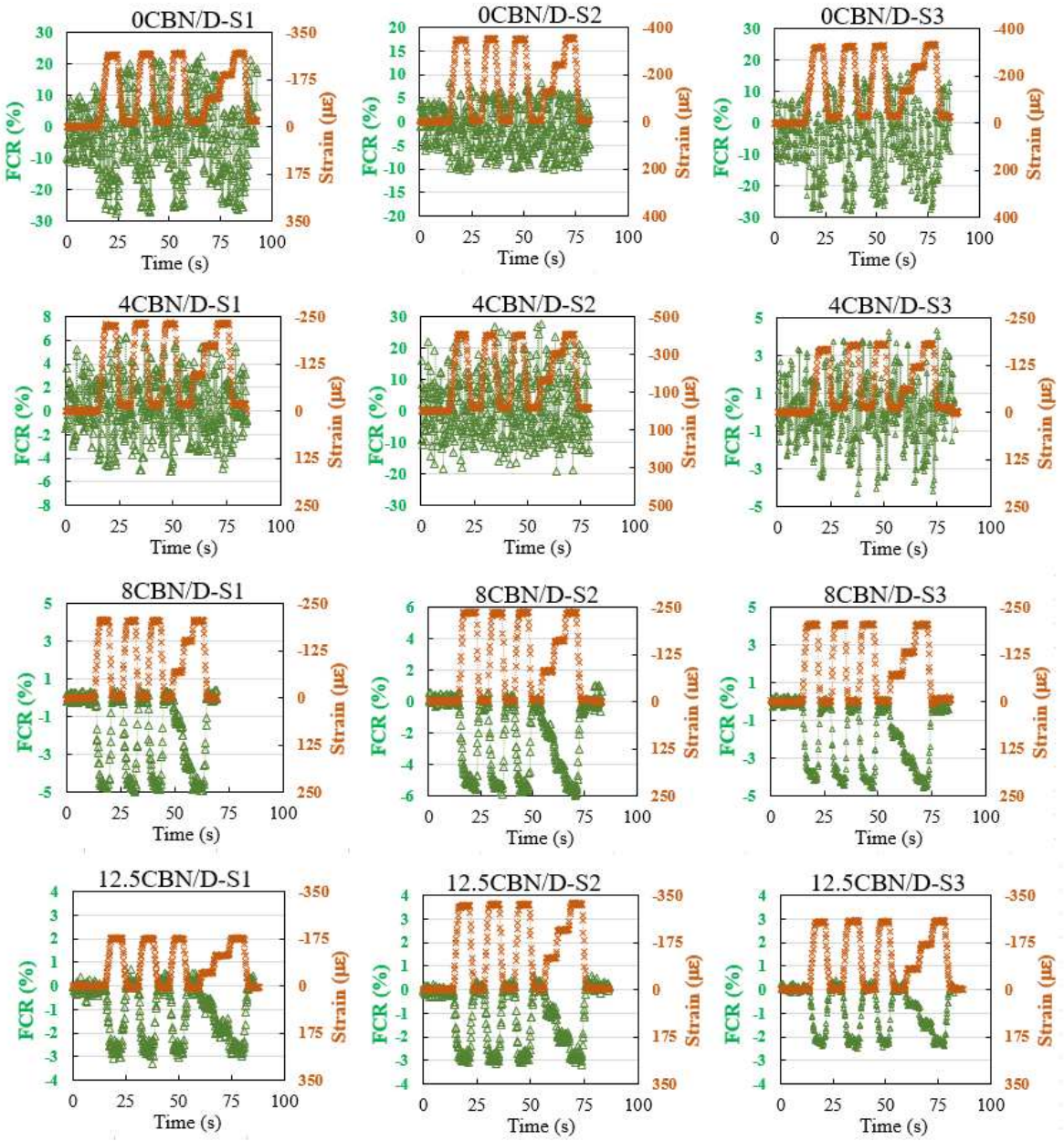

Source: Author (2020)

Figure 25 – FCR vs. strain curves of oven-dried composites

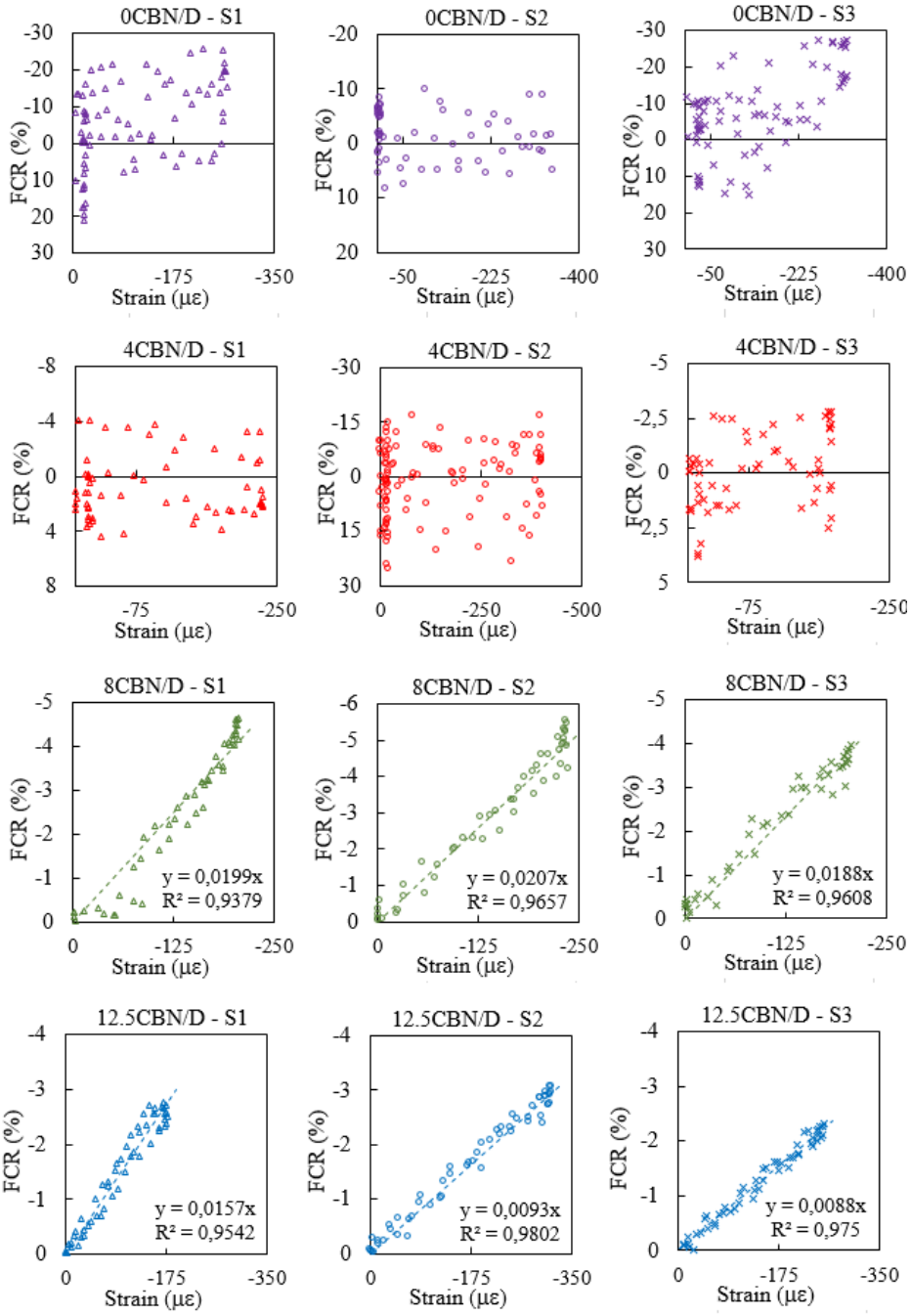

Source: Author (2020)

Results of piezoresistive tests of the three samples of each series were used to determine their average gauge factor, coefficient of determination and stress sensitivity (Figure 26). In 0CBN, 4CBN and 12.5CBN series, the average gauge factor and stress sensitivity of samples with high water content were higher than those of dried samples, which indicates that pore water provided ionic conduction and improved the sensing ability of the material. In the 8CBN series, gauge factor and stress sensitivity did not change with the

drying process, which was corroborated through analyses of variance at the 5% significance level. When comparing the average gauge factors of 8CBN samples in dry and wet condition, a P-value of 0.604 was obtained, which confirms the null hypothesis that the compared averages are statistically the same. A P-value of 0.071 was obtained in the analysis of variance of stress sensitivity of 8CBN series, which also confirms the null hypothesis that the average stress sensitivities are equal. Then, these results also suggest that the drying process did not provide considerable changes on tunneling conduction.

Figure 26 – Gauge factor, R^2 and stress sensitivity of mortars as a function of the CBN concentration

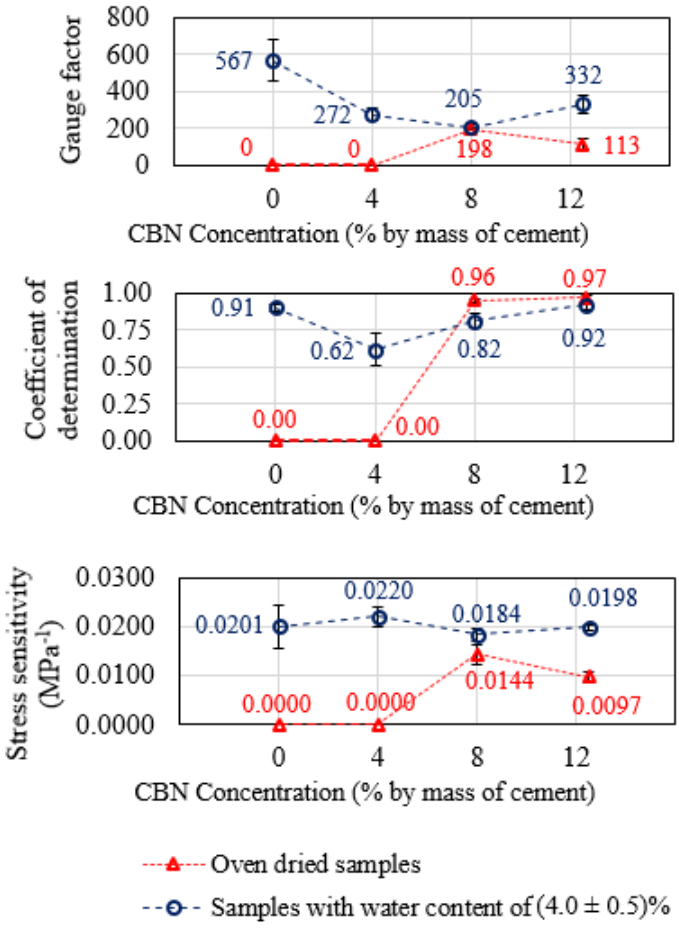

Source: Author (2020)

The gauge factor and stress sensitivity of dried samples of 0CBN and 4CBN series were set to zero because they did not exhibit piezoresistive response. Dried samples of 8CBN and 12.5CBN series exhibited an excellent linearity and repeatability (coefficients of determination of 0.96 and 0.97, respectively). Despite this, 12.5CBN samples had lower gauge factor and stress sensitivity because they had a larger amount of functional fillers contacting each other and a more stable conductive network.

2.3.4. Conclusion

In this preliminary study, self-sensing cement-based materials developed with Brazilian construction materials and Brazilian conductive nanofillers were firstly investigated. It provided a better understanding of the influence of water content on the electrical resistivity of mortars with CBN. The following conclusions were derived from this study:

(1) The increase in CBN concentration reduced the intrinsic capacitance of mortars and decreased the influence of the drying process on their capacitive behavior.

(2) The influence of water content on the electrical resistivity of cement-based composites is related to the CBN content. When the CBN content is below the percolation threshold and ionic conduction is dominant, the reduction of the water content significantly increased the electrical resistivity of the material. When the CBN content was significantly higher than the percolation threshold and the contact conduction was dominant, the reduction of water content decreased the electrical resistivity.

(3) The drying process did not provide substantial changes on tunneling conduction, since the electrical conductivity, gauge factor and stress sensitivity of wet and dry composites with CBN content close to the percolation threshold were statistically the same.

(4) When the CBN concentration was not close to the percolation threshold, the average gauge factor and stress sensitivity of wet samples were higher than those of dried samples, which indicates that pore water provided ionic conduction and improved the sensing ability of the material.

(5) In the percolation threshold, the influence of water content on the piezoresistive behavior and electronic conduction in cement-based composites containing CBN seems to be minimized and values of gauge factor and stress sensitivity were optimized.

2.4. MICROSTRUCTURAL INVESTIGATION OF THE EFFECTS OF CBN ON THE HYDRATION PROCESS AND MECHANICAL AND PIEZORESISTIVE PROPERTIES OF MORTARS

2.4.1. Introduction

Carbon black nanoparticles (CBN) significantly affect the mechanical and electrical properties of cement-based materials due to their high specific surface area, low electrical resistivity and small average particle size [17, 32, 34].

Various effects of CBN on the mechanical properties of pastes, mortars and concretes are reported in the literature. Yawen et al. [61] and Dong et al. [62] observed decreases in mechanical properties of pastes produced with CBN concentration ranging from 0.1% to 6%, by weight of cement. These reductions were mainly attributed to the adsorption of CBN on the surface of cement, which hinders the hydration process [61]. In addition, there is poor cohesion between the cement matrix and the nanofillers, which tend to absorb a fraction of water leading to decreases of mechanical strength [62].

On the other hand, Rezania et al. [65] reported reductions of mechanical properties of concretes for CBN contents between 0.4% and 1.2%, followed by improvements in these parameters for CBN contents higher than 1.2%. Monteiro et al. [34] verified improvements of compressive strength and tensile strength of mortars with addition of CBN contents of 1%, 4% and 7%. When the concentration of CBN was higher than 10%, they observed segregation and extremely low strength values. Dehghanpour, Yilmaz and Ipek [66] also verified a progressive improvement of mechanical properties of concretes with 3%, 6% and 10% of CBN. Strength improvements have been attributed to a physical phenomenon based on the filler effect and to the strengthening of the interface bondage between hydrates and CBN due to the high chemical activity of nano-size functional fillers [61].

The high electrical conductivity of CBN decrease the electrical resistivity of cement-based materials to values close to the resistivity of semiconductors [4, 32-34, 40, 41]. When the conductive filler concentration is close to the percolation threshold, the electronic tunneling conduction is dominant, which provides an excellent piezoresistive behavior to the composite [2, 13, 14]. Consequently, they can be used as a sensor for strain monitoring of concrete structures, since the electrical resistivity of CBN composites changes significantly when they are subjected to deformation due to variations of the distance between neighboring CBN and changes of conductive pathways [17, 33].

Li, Xiao and Ou [33, 41] reported that additions of CBN contents between 12% and 20% drastically decreased the resistivity of pastes. They realized an excellent piezoresistive behavior for a CBN content of 15%, which provided composites with gauge factors between 52.7 and 59.6 and stress sensitivity of about 0.006 MPa^{-1}. A good piezoresistive response was also observed in mortars with various CBN concentrations: 1% (with gauge factors between 25 and 160) [32], 6.5% (with gauge factors between 40 and 60 and stress sensitivity between 0.0025 MPa^{-1} and 0.0035 MPa^{-1}) [17], 7% and 10% (with gauge factors between 30.28 and 24.13 and stress sensitivity between 0.00286 MPa^{-1} and 0.00172 MPa^{-1}) [34].

Previous studies report different optimal contents of CBN for improvement of mechanical strength or improvement of piezoresistivity of cement-based materials. There is no previous research focused on the microstructural evaluation of the effects of CBN on both parameters, in order to detect an optimal content that provides low electrical resistivity and good piezoresistive response, without significant loss of mechanical strength. In addition, according to the authors knowledge, none of the previous studies [17, 32-34, 36, 37, 39-42, 44, 46, 47, 61, 62, 65, 66] about the incorporation of CBN in cement-based materials evaluated their microstructure with X-ray diffraction and Raman spectroscopic techniques. Therefore, the preliminary study reported in the following sections consists of an experimental program for microstructural evaluation of the influence of CBN on both mechanical and piezoresistive properties of mortars, using a combination of techniques of scanning electron microscopy (SEM), X-ray diffraction (XRD) and Raman spectroscopy.

2.4.2. Experimental Methods

The conductive nanofillers used in this study were Raven P5 Ultra carbon blacks with specific surface area of 100 m^2/g, dibutyl phthalate (DBP) absorption number of 117 $cm^3/100g$, particle size of 20 nm and supplied by Birla Carbon. In order to develop a microstructural analysis of the influence of CBN on the mechanical and piezoresistive properties of mortars, series with eight different CBN concentrations were considered: 0%, 0.375%, 0.75%, 1.5%, 3%, 4%, 5% and 6% (by weight of cement). The mix proportions (in mass) of each composition are indicated in Table 3.

Eight mortar prisms measuring 4 cm × 4 cm × 7.5 cm were produced for each series, following the prescriptions of Section 2.2.2.1. During the production process, a small amount of paste was poured in sealed plastic vials and stored in the moisture room at (23 ± 2) ºC and relative humidity of 95%, as recommended by Garg, Wang and Martin [67]. Two

1.5 cm × 5.0 cm × 0.1 cm copper plates were embedded in four prisms in a straight line, at equal distance of 2.0 cm from each other, while no electrodes was embedded in the others.

Table 3 – Mix proportions (in mass)

Series	Cement	Sand	Water	CBN	SP
REF	1.00	0.90	0.45	0.00000	0.0000
CBN0.375%	1.00	0.90	0.45	0.00375	0.0005
CBN0.75%	1.00	0.90	0.45	0.00750	0.0009
CBN1.5%	1.00	0.90	0.45	0.01500	0.0024
CBN3%	1.00	0.90	0.45	0.03000	0.0076
CBN4%	1.00	0.90	0.45	0.04000	0.0128
CBN5%	1.00	0.90	0.45	0.05000	0.0194
CBN6%	1.00	0.90	0.45	0.06000	0.0275

After a 28-days curing time, samples were oven dried for 24 hours at (100 ± 5) ºC and cooled down to room temperature before the piezoresistive tests, following recommendations of Mohsen et al. [50] and Kim et al. [51]. After the same curing period, the samples in the sealed plastic vials were uncovered and subjected to the SEM, XRD and Raman analyses described in Sections 2.4.2.1, 2.4.2.2 and 2.4.2.3, respectively. In this experimental program, the wavenumber range of 110 - 1330 cm^{-1} was chosen in Raman analysis for evaluation of portlandite peaks located at 354 - 359 cm^{-1} [68-72]. Moreover, an exposure time of three seconds and one accumulation per spectrum were used. In each series, one of the prisms with copper electrodes (designated as S4) was used to estimate the ultimate strength of the composite. The other composites with embedded electrodes (designated as S1, S2 and S3) were subjected to the piezoresistive test described in Section 2.2.2.4. Next, one of the specimens without electrodes was also used to estimate the mortar compressive strength (f_u). The others were used to determine the static modulus of elasticity and the compressive strength of the material, according to the procedures described in Section 2.4.2.4.

2.4.2.1. Scanning electron microscopy (SEM)

Scanning electron microscopy (SEM) and energy-dispersive spectrometry (EDS) were performed in the SEM Laboratory of the Physics Department of the Universidade Federal de Viçosa. A JEOL's JSM-6010LA microscope operating at 20 kV was used to obtain secondary electron images of the samples.

2.4.2.2. X-ray diffraction (XRD)

XRD tests were performed in the XRD Laboratory of the Physics Department of the Universidade Federal de Viçosa, using a D8Discover diffractometer with CuKα radiation (λ = 1.5418 Å), working voltage of 40kV and electric current of 40 mA. Samples were scanned from 20º to 65º (2θ), with a 0.05º step size and an accumulated time per step of 1 s.

2.4.2.3. Raman spectroscopy

Raman spectra were collected with a Renishaw inVia spectrometer with an Ar+ laser of 633 nm (1 mW) as excitation source, available in the Raman Spectroscopy Laboratory of the Physics Department of the Universidade Federal de Viçosa. A randomly chosen area of the sample was brought into focus with 20× objective lens. A Raman map of the area was elaborated, with spectra collected at 81 different locations distributed in a square grid with measurement points spaced 25 μm apart horizontally and vertically. Using the software Wire 3.1, the collected data was subjected to a post-processing treatment for baseline correction, as proposed by Garg, Wang and Martin [67].

2.4.2.4. Mechanical tests

The static modulus of elasticity and compressive strength of the specimens were determined according to the prescriptions of ABNT NBR 8522 [73]. Axial compression tests were performed in an EMIC 23-600 universal testing machine available in the Structures Laboratory of the Civil Engineering Department of the Universidade Federal de Viçosa. Clip-gauges were used to measure the longitudinal strain of the specimens. An automated test method was used to apply compressive loads according to the methodology A of the ABNT NBR 8522 [73], as indicated in Figure 27. A constant loading rate of 0.50 MPa/s was used. Considering the stress-strain curve of the test, the static modulus of elasticity E was calculated as the slope of the straight line that links the points of compressive stress (in MPa) of σ_a (0.5 MPa) and σ_b (30% of f_u). This calculation is indicated in Eq. 8, in which the longitudinal strains ε_a and ε_b (in m/m) were measured during the last load cycle, when the specimen was under the compressive stress σ_a and σ_b, respectively.

Eq. 8
$$E = \left(\frac{\sigma_b - \sigma_a}{\varepsilon_b - \varepsilon_a} \right) 10^{-3}$$

Figure 27 – Load-history of tests of determination of static modulus of elasticity

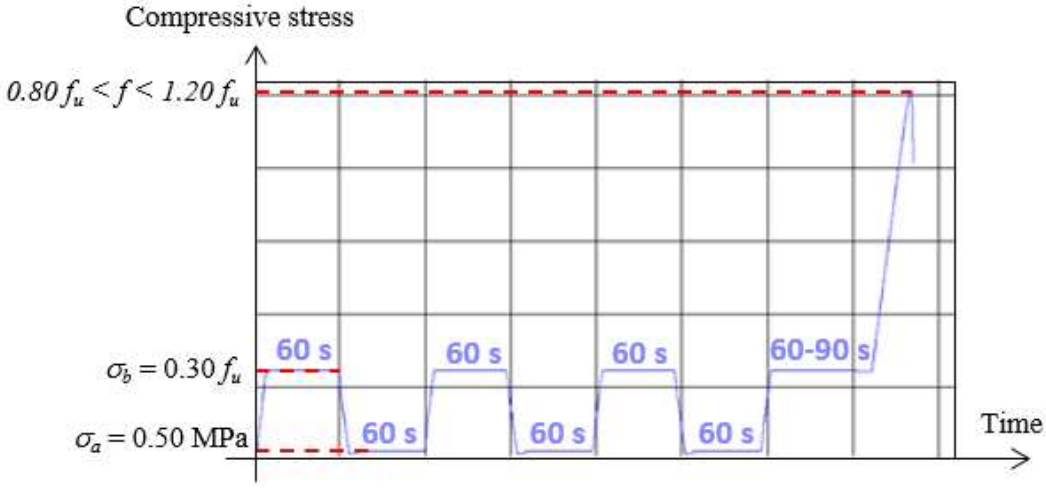

Source: Author (2020)

2.4.3. Results and discussion

The effects of CBN concentration on the compressive strength of mortars is evidenced in Figure 28. CBN concentrations smaller than 3% provided increases in the compressive strength of the material, while higher CBN contents provided lower strength values. For example, a strength decrease of about 86% was verified when the CBN concentration increased from 3% to 6%. A quadratic regression analysis was carried out to determine the model that provides the best fit to the experimental data. A coefficient of determination of 0.99 was obtained, which indicates that a good relationship between CBN content and mortar compressive strength could be established. The developed quadratic model indicates that the optimal CBN concentration seems to be close to 2.06%, which would provide compressive strengths close to 44.1 MPa.

Figure 28 – 28-days compressive strength of mortars with different CBN contents

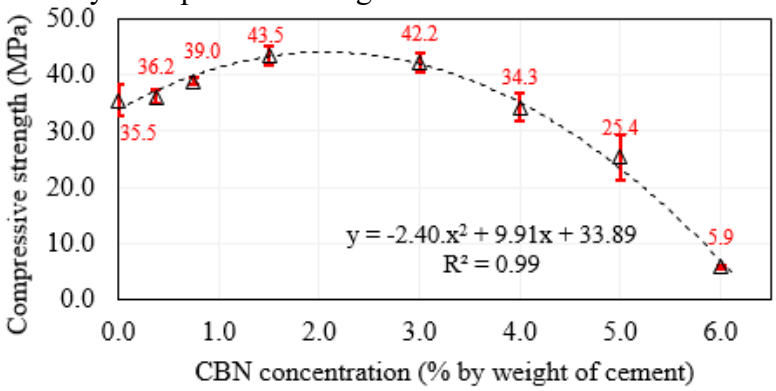

Source: Author (2020)

Monteiro et al. [34] also verified that the compressive strength of mortars first increased and then decreased with the increase of CBN content. However, they found an optimal content close to 4% and mentioned that contents higher than 10% revealed the presence of segregation and extremely low strength values. A sharp decrease of compressive strength for CBN contents of 6% was also reported by Yawen et al. [61] for cement pastes.

A similar behavior was verified when the mortars' elasticity modulus was plotted against the CBN concentration (Figure 29). Improvements in modulus of elasticity were obtained for CBN contents up to 1.5%. Samples with the highest filler concentration presented a modulus of elasticity 72.0% lower than the control samples. Another regression analysis was carried out and a good quadratic relationship between CBN content and modulus of elasticity could be established (the coefficient of determination was 0.83). The obtained quadratic equation suggests that the optimal CBN concentration seems to be close to 2.14%, which would provide a modulus of elasticity close to 18.8 GPa.

Figure 29 – 28-days modulus of elasticity of mortars with different CBN contents

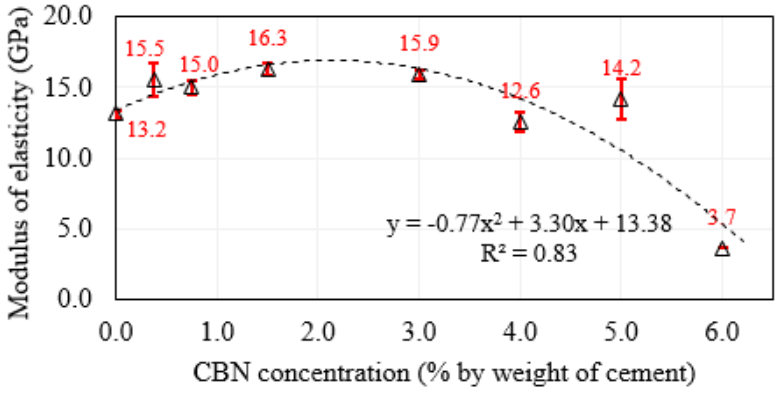

Source: Author (2020)

A relationship between CBN content and modulus of elasticity of mortars was only previously reported by Monteiro et al. [34], at the age of 120 days. They observed an increase of modulus of elasticity only for CBN contents lower than 4%. For higher concentrations, the modulus of elasticity was lower than that of control samples. Improvements of 28-days compressive strength and 120-days modulus of elasticity obtained by Monteiro et al. [34] were 21.3% and 41.3%, respectively.

Since no ultrasonication dispersion method was used, they suggested the development of future studies focused on lowering the CBN fraction by using filler dispersion procedures. In the present work, ultrasonication and CBN with smaller particle

size were used, which provided improvements of 28-days compressive strength and 28-days modulus of elasticity of 24.2% and 42.4%, respectively, for a filler concentration 50% lower.

Since the relationship between compressive strength and modulus of elasticity of cement-based materials with CBN has never been established in previous works, a nonlinear regression analyses was performed to find the model that provides the best fit to the experimentally obtained mechanical properties. A functional form commonly used by structural design codes to correlate concrete mechanical properties was used and a good coefficient of determination (0.949) was obtained, as shown in Figure 30.

Figure 30 – Relationship between 28-days compressive strength and modulus of elasticity of mortars with CBN.

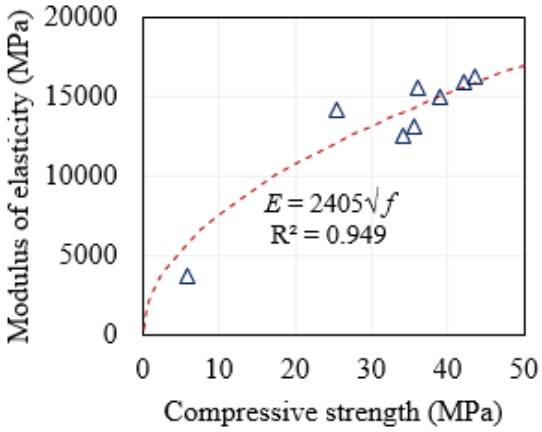

Source: Author (2020)

A morphological evaluation of the influence of CBN on the cementitious matrix was carried out using the SEM images shown in Figure 31. One can see that lower CBN concentrations (Figure 31a-d) decreased the porosity of the control sample, which explains the gains of compressive strength and stiffness presented in Figure 28 and Figure 29. This microstructural analysis suggests that lower contents of CBN refine pores at the nanoscale when an adequate dispersion method is used, as previously mentioned by Yawen et al. [61].

In contrast, CBN6% sample (Figure 31h) presented large volume of voids caused by excess CBN in the matrix. In this case, the large amount of nanofillers absorb significant amount of water [42, 43] and make it more difficult for the remaining water molecules to reach the cement particles, which impairs the development of hydration products. For a better understanding of the hydration process, two different techniques for microstructural investigation were used: XRD and Raman spectroscopy. It should be noted that these techniques were not used in previous studies dealing with CBN in cementitious matrices [17, 32-34, 36, 37, 39-43, 46, 61, 62, 65, 66].

Figure 31 – SEM images of a cementitious matrix with different CBN contents at 28 days

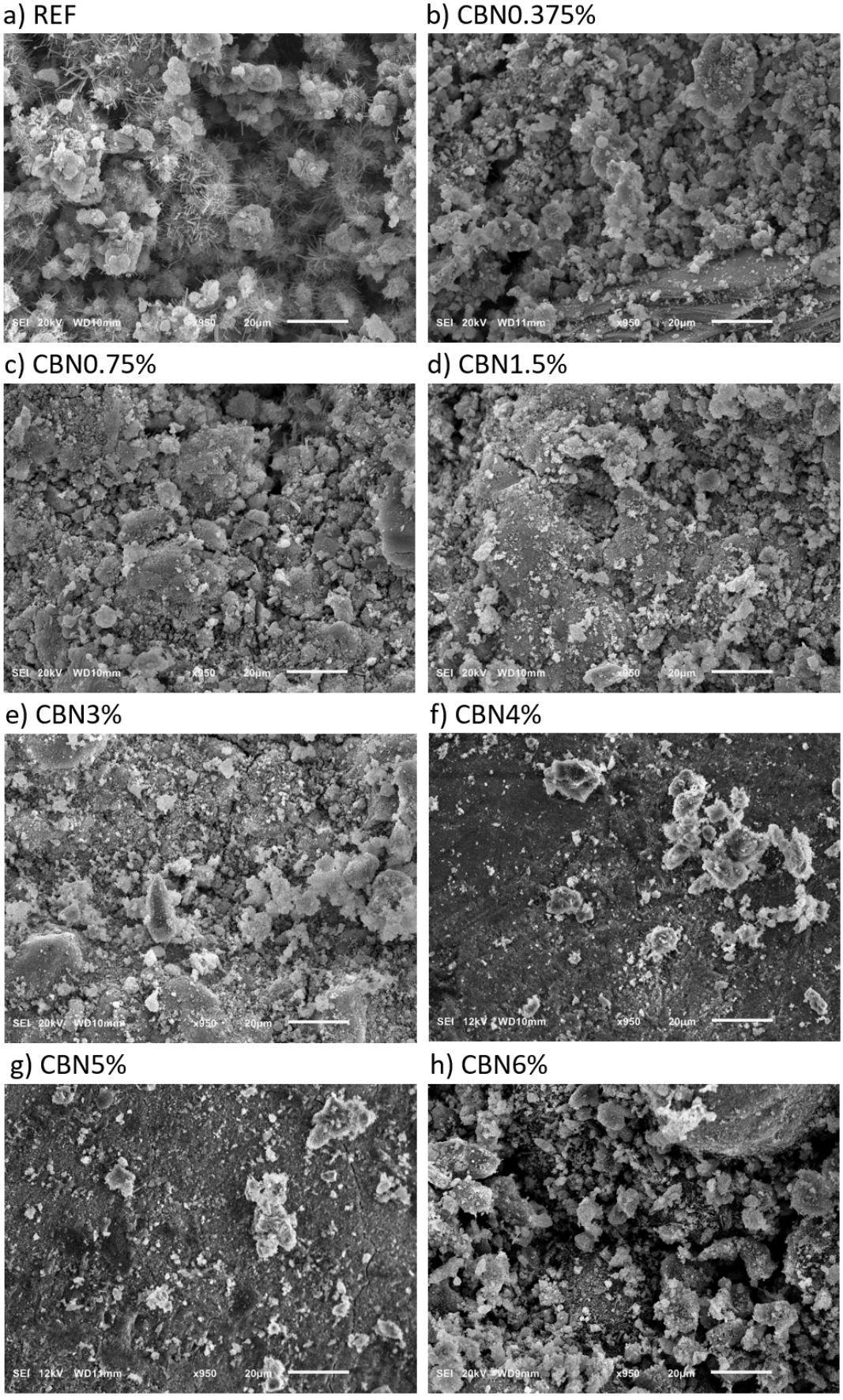

Source: Author (2020)

XRD spectra and Raman maps for portlandite peaks located at 356.63 cm^{-1} of the eight samples are presented in Figure 32 and Figure 33, respectively. The brighter spots of the Raman maps indicate locations with higher 356.63 cm^{-1} peak intensities. Figure 34 shows a typical Raman spectrum (after baseline correction) collected from sample CBN0.375%, in a measurement location with high portlandite concentration. When the CBN increased from 0% to 3%, there are an increase of the intensity of peaks of portlandite at 2θ = 18º, 48º and 51º in the XRD diffratograms and an intensification of brighter areas in the portlandite Raman maps. Since portlandite is a by-product of the cement hydration, the results prove that small CBN contents improved the hydration process and increased the mortar compressive strength and stiffness, as shown in Figure 28 and Figure 29. In fact, XRD diffratograms and Raman maps also suggest lower amounts of portlandite in series with higher CBN concentration (CBN4%, CBN5% and CBN6%). In addition, the high intensity of peaks of alite (2θ = 23º, 29.4º, 32.2º, 38.9º and 41.3º), belite (2θ = 32.2º, 39.5º and 41.3º) and ettringite (2θ = 23º) in the XRD diffratogram of the CBN6% sample also indicate a delay of cement hydration.

Figure 32 – XRD spectra of a cementitious matrix with different CBN contents at 28 days

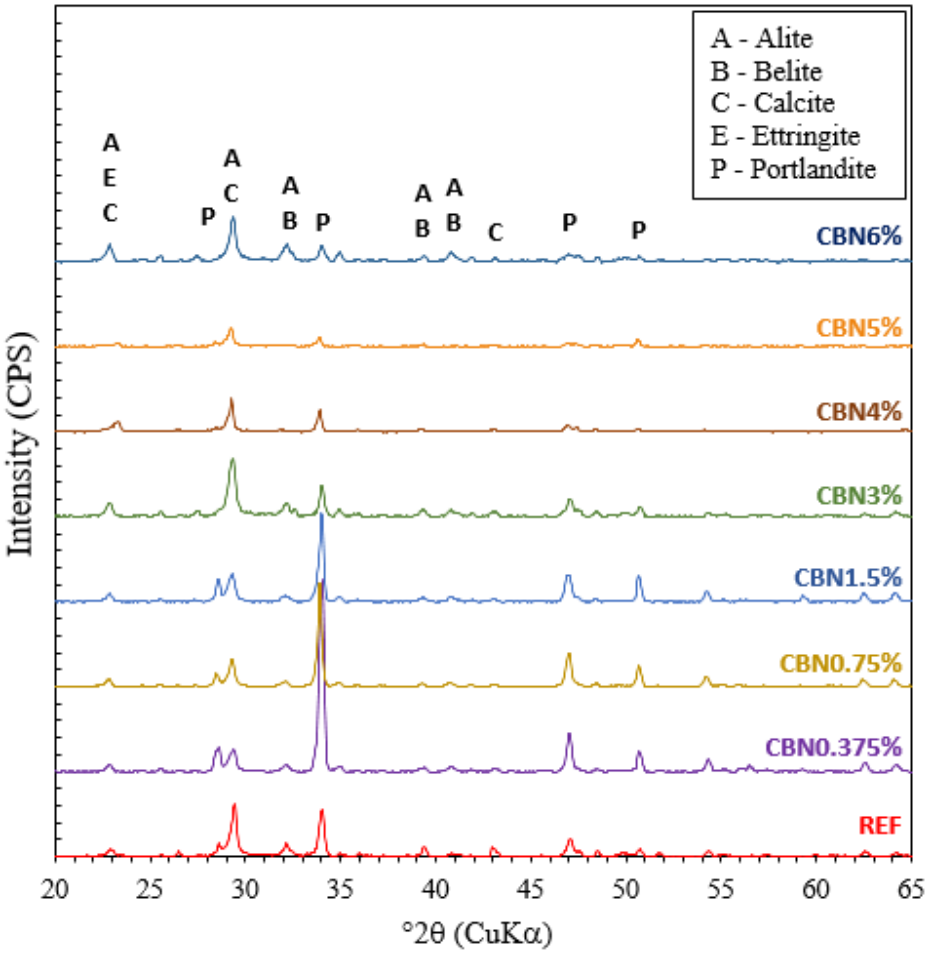

Source: Author (2020)

Figure 33 – Raman maps for portlandite peaks at 356.63 cm^{-1} (brighter spots indicate higher peak intensities) of a cementitious matrix with different CBN contents at 28 days

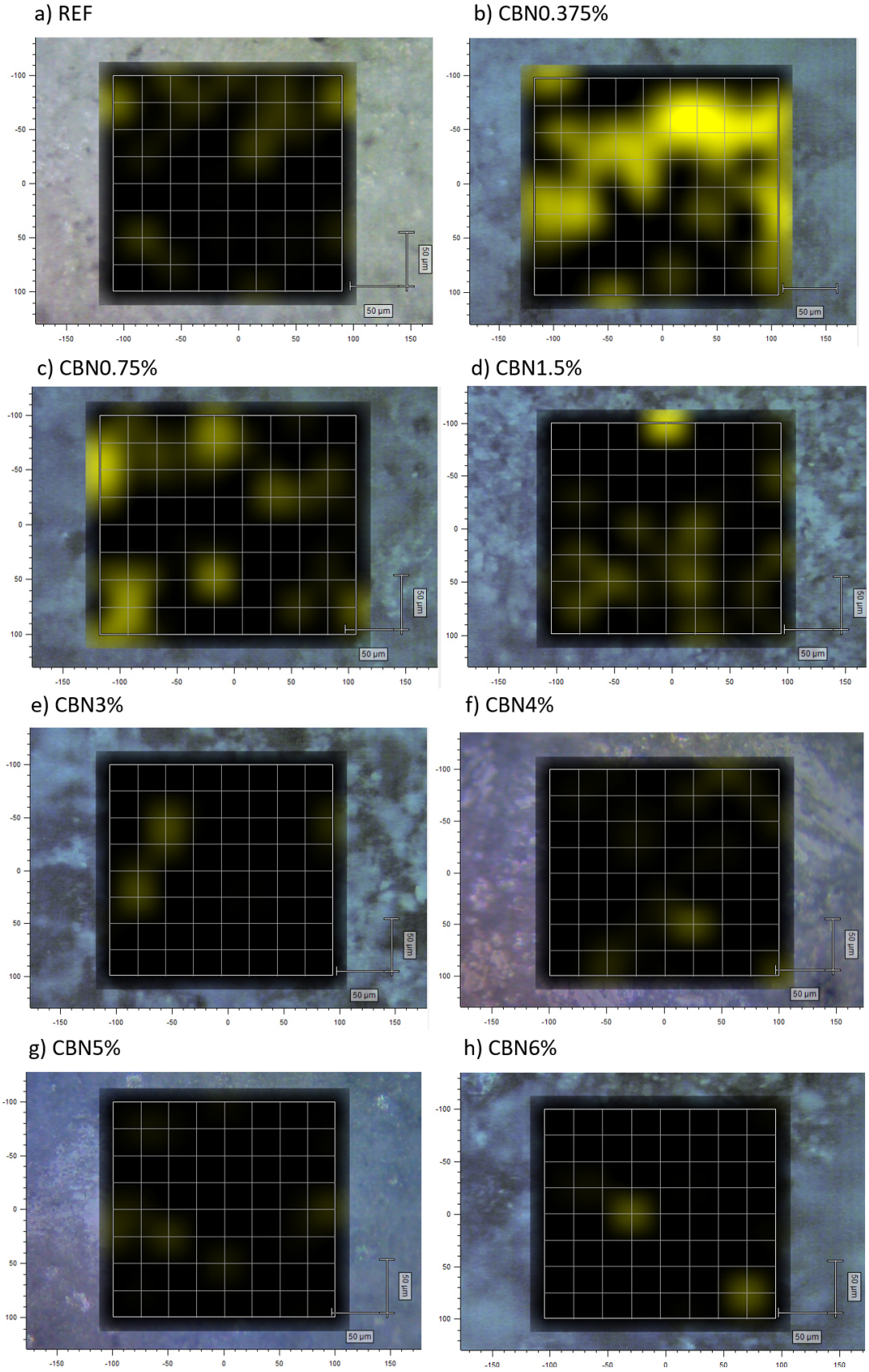

Source: Author (2020)

Figure 34 – Typical Raman spectrum collected in measurement locations with high portlandite concentration

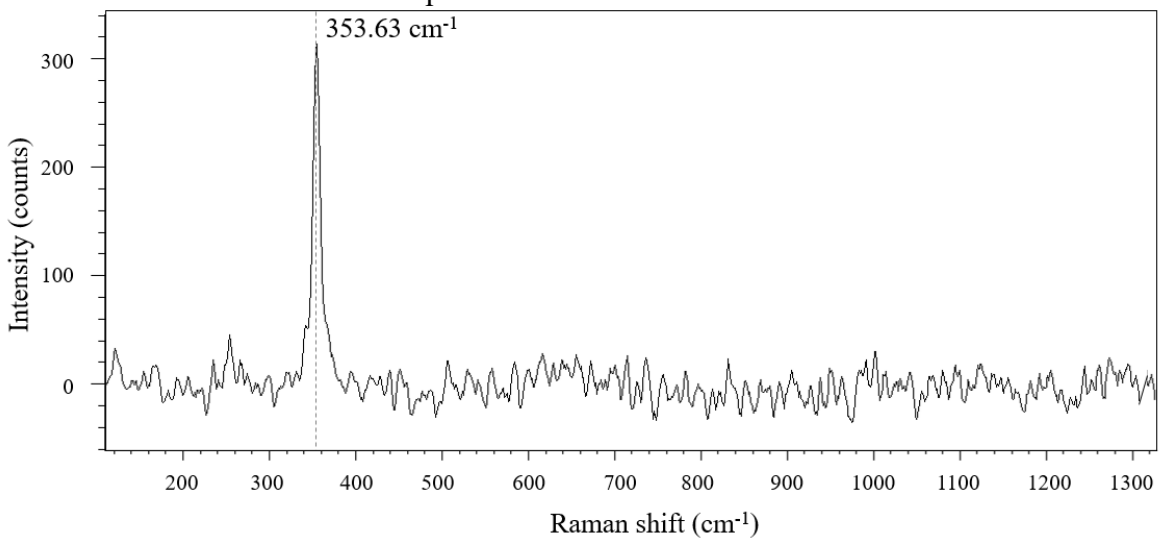

Source: Author (2020)

The increase of CBN concentration significantly affected the electrical resistivity of the composites (Figure 35). A behavior similar to that observed in the mechanical tests was obtained for electrical resistivity: it firstly increased and then decreased with CBN concentration. It increased for CBN contents from 0.375% to 3%, and then sharply decreased. The electrical resistivity of mortars with a CBN concentration of 6% is about four orders of magnitude lower than the electrical resistivity of plain mortars.

Figure 35 – Electrical resistivity of mortars with different CBN contents at 28 days

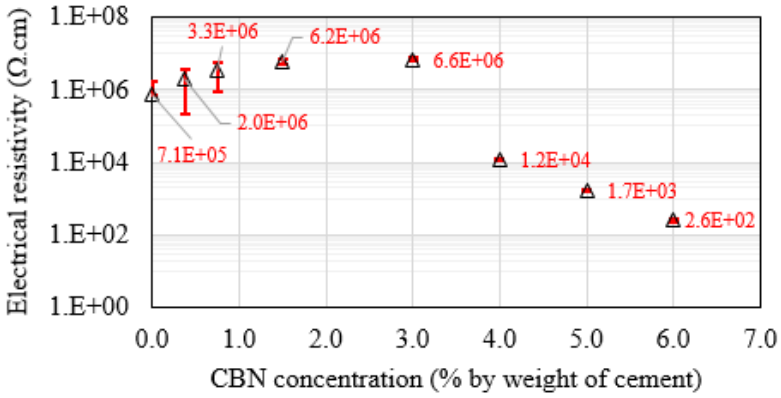

Source: Author (2020)

Curiously, an increase of electrical resistivity was observed when the CBN content increased from 0% to 3%. It can be attributed to the higher densification of the cementitious matrix due to the filler effect and improvement of the hydration process suggested by the results of SEM, XRD and Raman spectroscopy techniques. These smaller functional filler

contents were not able to generate electronic conduction. The conductive network was only created when CBN contents greater than 6% were used.

The piezoresistive behavior of the mortars and the relationship between FCR and strain are shown in Figure 36 and Figure 37. Series with CBN content lower than 3% did not present a piezoresistive response, since there is no proportional relationship between strain and FCR. The series with CBN content of 4% presented a strong piezoresistive effect, but a nonlinear relationship between strain and FCR was obtained. The best piezoresistive responses were obtained in series with 5% and 6% of CBN. In these series, excellent linearity and repeatability were observed, with gauge factors of 500, 487 and 561 for the three specimens with CBN content of 6% and 129, 82 and 121 for the three specimens with CBN content of 5%.

Figure 36 – Piezoresistive response of the composites at 28 days

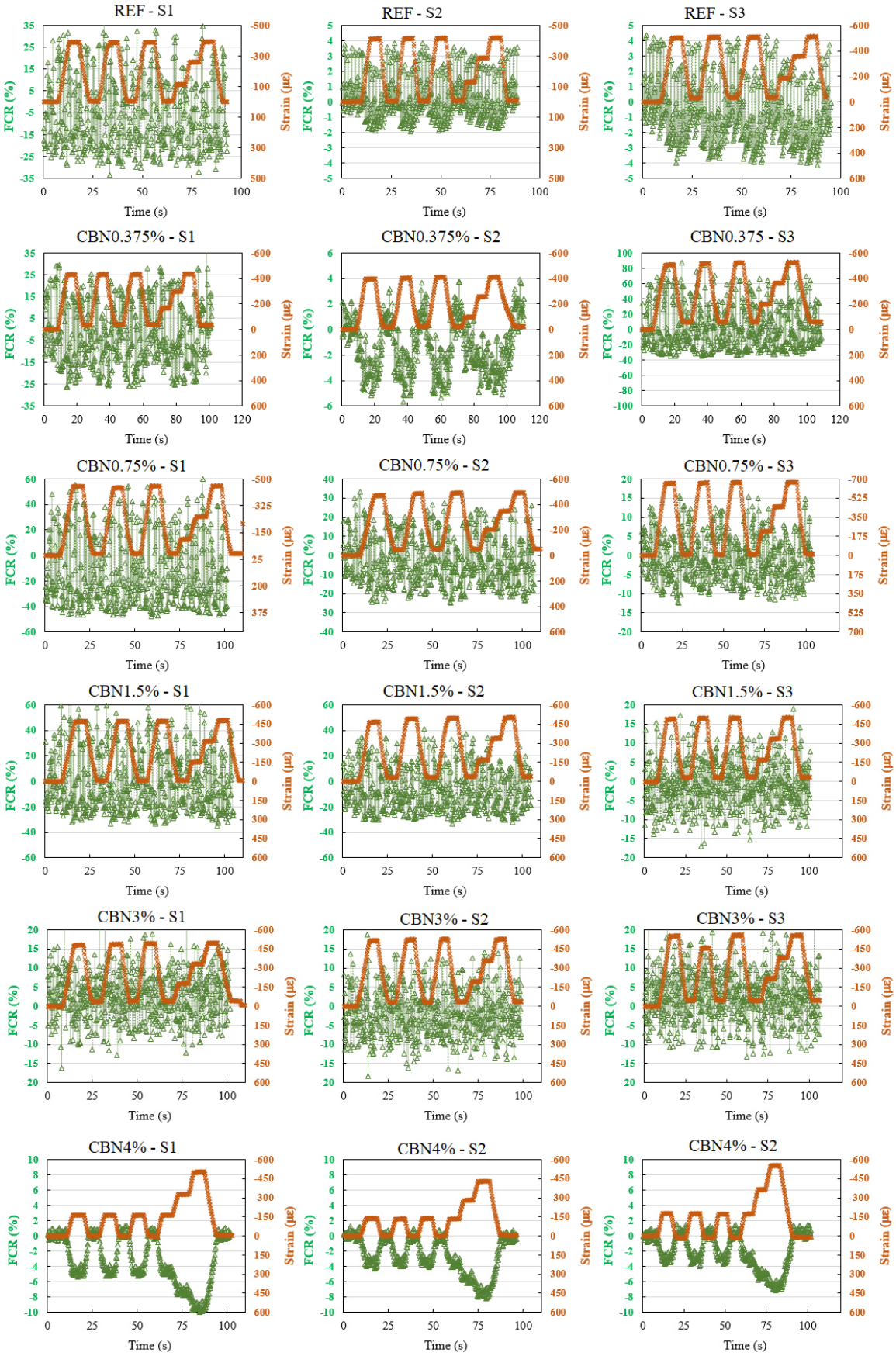

(to be continued)

Figure 36 – Piezoresistive response of the composites (continued)

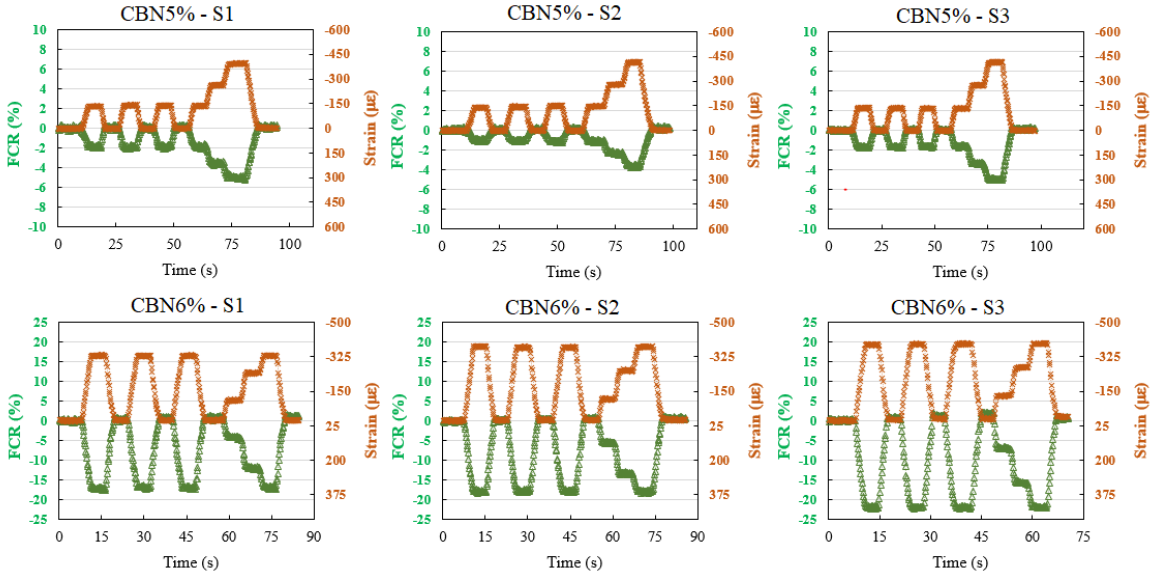

Source: Author (2020)

Figure 37 – Relationship between FCR and strain of self-sensing composites

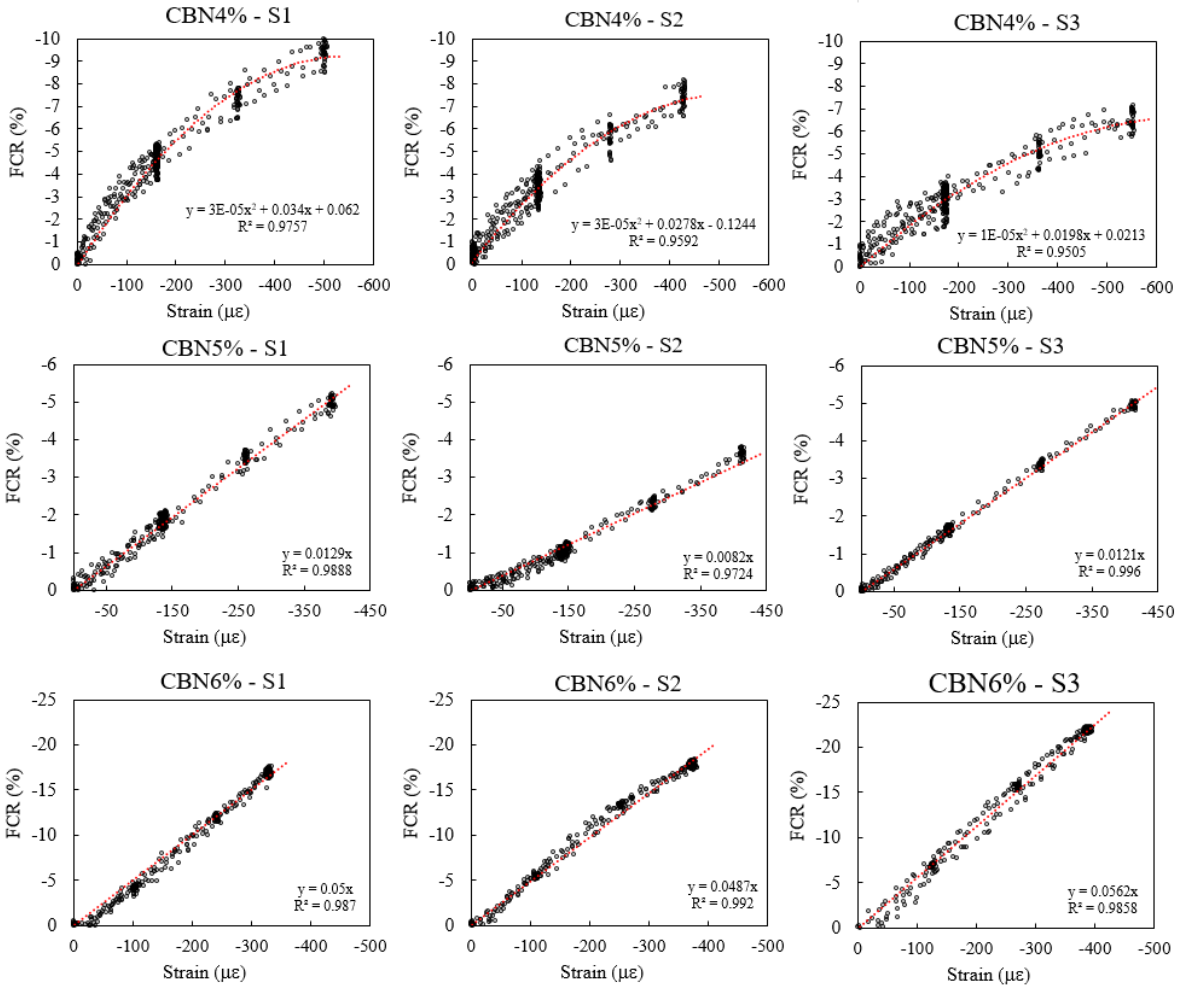

Source: Author (2020)

2.4.4. Conclusion

The present preliminary study brings the following conclusions:

(1) Compressive strength, static modulus of elasticity and electrical resistivity of mortars increased for CBN contents between 0% and 3%, but decreased when the CBN concentration ranges from 3% to 6%.

(2) A good relationship between compressive strength and static modulus of elasticity of mortars with CBN was established in this work, considering the square root functional model commonly used by structural design codes to correlate these mechanical properties.

(3) The best improvements of compressive strength and static modulus of elasticity were provided by CBN contents between 2% and 3%, while nanofiller concentrations of 5% and 6% provided the best improvements of sensing properties. A concentration of 5% of CBN provided low electrical resistivity and excellent piezoresistive response, without very significant strength and stiffness losses.

(4) SEM images show that lower contents of CBN refined the cementitious matrix pores at the nanoscale and higher contents of CBN increased the volume of voids. Then, smaller CBN concentrations provided a densification of the cementitious matrix.

(5) Raman spectroscopy and XRD analysis have been effectively used to investigate cement hydration on mortars with CBN. XRD diffratograms suggested significant amounts of alite, belite and ettringite in specimens with higher nanofiller concentration. Raman maps and XRD spectra also indicated higher formation of portlandite in specimens with CBN contents between 0.375% and 3%, which is related to improvements of the hydration process.

REFERENCES

[1] Y. XU e J. HE, Smart civil structures, Boca Raton: CRC Press, 2017.

[2] B. HAN, S. DING e X. YU, “Intrinsic self-sensing concrete and structures: A review,” *Measurement,* vol. 59, pp. 110-128, 2015.

[3] F. UBERTINI e A. D'ALESSANDRO, “Concrete with self-sensing properties,” em *Eco-Efficient Repair and Rehabilitation of Concrete Infrastructures*, Woodhead Publishing, 2018, pp. 501-530.

[4] I. YOU, D. YOO, S. KIM, M. KIM e G. ZI, “Electrical and self-sensing properties of ultra-high-performance fiber-reinforced concrete with carbon nanotubes,” *Sensors,* vol. 17, p. 2481, 2017.

[5] T. HOU e J. LYNCH, "Conductivity-based strain monitoring and damage characterization of fiber reinforced cementitious structural components," em *12th Annual International Symposium on Smart Structures and Materials*, San Diego, California, 2005.

[6] D. YOO, I. YOU, H. YOUN e S. LEE, "Electrical and piezoresistive properties of cement composites with carbon nanomaterials," *Journal of Composite Materials,* pp. 1-16, 2018.

[7] G. YILDIRIM, S. M.H., A. AL-DAHAWI, O. ÖZTÜRK, A. O. e M. SAHMARAN, "Piezoresistive behavior of CF- and CNT-based reinforced concrete beams subjected to static flexural loading: Shear failure investigation," *Construction and Building Materials,* nº 168, pp. 266-279, 2018.

[8] A. MEONI, A. D'ALESSANDRO, A. DOWNEY, S. LAFLAMME e F. UBERTINI, "Strain monitoring in masonry structures using smart bricks," em *Proceedings of Sensors and Smart Structures Technologies for Civil, Mechanical, and Aerospace Systems*, Denver, Colorado, 2018.

[9] S. BAI, L. JIANG, N. XU, M. JIN e S. JIANG, "Enhancement of mechanical and electrical properties of graphene/cement composite due to improved dispersion of graphene by addition of silica fume," *Construction and Building Materials,* vol. 164, pp. 433-441, 2018.

[10] A. DOWNEY, A. D'ALESSANDRO, S. LAFLAMME e F. UBERTINI, "Smart bricks for strain sensing and crack detection in masonry structures," *Smart Materials and Structures,* vol. 27, nº 1, pp. 1-10, 2017.

[11] P. XIE, P. GU e J. BEAUDOIN, "Electrical percolation phenomena in cement composites containing conductive fibres," *Journal of Materials Science,* vol. 31, pp. 4093-4097, 1996.

[12] S. HWANG, Y. PARK, K. YOON e D. BANG, "Chapter 18: Smart materials and structures based on carbon nanotube composites.," em *Carbon nanotubes-synthesis, characterization, applications*, InTech, 2011, p. 371–396.

[13] B. HAN, X. YU e J. OU, Self-Sensing Concrete In Smart Structures, Waltham, MA, USA: Elsevier Inc., 2015.

[14] D. CHUNG, "Electrical applications of carbon materials," *Journal of Materials Science,* vol. 39, pp. 2645-2661, 2004.

[15] S. ZHU e D. CHUNG, "Analytical model of piezoresistivity for strain sensing in carbon fiber polymer–matrix structural composite under flexure," *Carbon,* vol. 45, pp. 1606-1613, 2007.

[16] F. UBERTINI, S. LAFLAMME e A. D'ALESSANDRO, "Smart cement paste with carbon nanotubes," em *Innovative Developments of Advanced Multifunctional Nanocomposites in Civil and Structural Engineering*, 2016, pp. 97-120.

[17] A. MONTEIRO, A. LOREDO, P. COSTA e M. C. P. OESER, "A pressure-sensitive carbon black cement composite for traffic monitoring," *Construction and Building Materials,* vol. 154, pp. 1079-1086, 2017.

[18] A. DOWNEY, A. D'ALESSANDRO, F. UBERTINI, S. LAFLAMME e R. GEIGER, "Biphasic DC measurement approach for enhanced measurement stability and multi-channel sampling of self-sensing multi-functional structural materials doped with carbon-based additives," *Smart Materials and Structures,* vol. 26, nº 6, pp. 1-13, 2017.

[19] A. D'ALESSANDRO, A. MEONI, F. UBERTINI e A. MATERAZZI, "Strain measurement in a reinforced concrete beam using embedded smart concrete sensors," em *Italian Concrete Days*, Milão, Lecco, 2018.

[20] X. FU, E. MA, D. CHUNG e W. ANDERSON, "Self-monitoring in carbon fiber reinforced mortar by reactance measurement," *Cement and Concrete Research,* vol. 27, pp. 845-852, 1997.

[21] H. XIAO, H. LI e J. OU, "Strain sensing properties of cement-based sensors embedded at various stress zones in a bending concrete beam," *Sensors and Actuators A: Physical,* vol. 167, pp. 581-587, 2011.

[22] A. D'ALESSANDRO, F. UBERTINI, E. GARCÍA-MACÍAS, R. CASTRO-TRIGUERO, A. DOWNEY, S. LAFLAMME, A. MEONI e A. L. MATERAZZI, "Static and dynamic strain monitoring of reinforced concrete components through embedded carbon nanotube cement-based sensors," *Shock and Vibration,* pp. 1-11, 2017.

[23] B. HAN, K. ZHANG, T. BURNHAM, E. KWON e X. YU, "Integration and road tests of a self-sensing CNT concrete pavement system for traffic detection," *Smart Materials and Structures,* vol. 22, 2013.

[24] F. YEH, K. CHANG e W. LIAO, "Experimental investigation of self-sensing carbon fiber reinforced cementitious composite for strain measurement of an RC portal frame," *International Journal of Distributed Sensor Networks,* pp. 1-13, 2015.

[25] J. OU, "Research and practice of intelligent sensing technologies in civil structural health monitoring in the mainland of China," *Nondestructive Evaluation and Health Monitoring of Aerospace Materials, Composites, and Civil Infrastructure,* vol. 6176, 2006.

[26] E. CUERDA-CORREA, J. DOMÍNGUEZ-VARGAS, F. OLIVARES-MARÍN e J. HEREDIA, "On the use of carbon blacks as potential low-cost adsorbents for the removal of on-steroidal anti-inflammatory drugs from river water," *Journal of Hazardous Materials,* vol. 177, pp. 1046-1053, 2010.

[27] Y. HSIEH e M. TSAI, "Physical and chemical analyses of unburned carbon from oil-fired fly ash," *Carbon,* vol. 41, pp. 2317-2324, 2003.

[28] A. APARECIDO-FERREIRA, G. RIBEIRO, E. ALVES e J. SAMPAIO, "Determination of a soft gap in the density states of granular carbon," *Physical Rev. B,* vol. 84, pp. 0242041-0242046, 2011.

[29] N. HAUPTMAN, M. GUNDE, M. KUNAVER e M. BESTER-ROGAC, "Influence of dispersing additives on the conductivity of carbon black pigment dispersion," *Journal of Coatings Technology and Research,* vol. 8, pp. 553-561, 2011.

[30] M. BERA, P. GUPTA e P. MAJI, "Structural/Load-Bearing Characteristics of Polymer–Carbon Composites," em *Carbon-Containing Polymer Composites*, Singapore, Springer, 2018, pp. 457-502.

[31] M. FERNANDES, J. SKJEMSTAD, B. W. J. JOHNSON e P. BROOKS, "Characterization of carbonaceous combustion residues. I. Morphological, elemental and spectroscopic features," *Chemosphere,* vol. 51, pp. 785-795, 2003.

[32] Y. HUANG, H. LI e S. QIAN, "Self-sensing properties of Engineered Cementitious Composites," *Construction and Building Materials,* vol. 174, p. 253–262, 2018.

[33] H. LI, H. XIAO e J. OU, "Effect of compressive strain on electrical resistivity of carbon black-filled cement-based composites," *Cement and Concrete Composites,* vol. 28, pp. 824-828, 2006.

[34] A. O. MONTEIRO, P. B. CACHIM e P. J. COSTA, "Self-sensing piezoresistive composite loaded with carbon black particles," *Cement and Concrete Composites,* vol. 81, pp. 59-65, 2017.

[35] A. D'ALESSANDRO, A. MEONI e F. UBERTINI, "Innovative Composites with Carbon Nanofillers for Self-Sensing," *Nano Hybrids and Composites,* vol. 19, pp. 12-22, 2018.

[36] V. LIN, M. LI e J. L. V. LYNCH, "Mechanical and electrical characterization of self-sensing carbon black ECC," *Nondestructive Characterization for Composite Materials, Aerospace Engineering, Civil Infrastructure, and Homeland Security,* vol. 7983, 2011.

[37] B. HAN, Y. WANG, S. DING, X. YU, L. ZHANG, Z. LI e J. OU, "Self-sensing cementitious composites incorporated with botryoid hybrid nano-carbon materials for smart infrastructures," *Journal of Intelligent Material Systems and Structures,* vol. 28, pp. 1-29, 2016.

[38] Z. CHEN, Y. DING, F. PACHECO-TORGAL e Y. ZHANG, "Self-sensing concrete with nanomaterials," em *Nanotechnology in Eco-Efficient Construction* , Woodhead Publishing Series in Civil and Structural Engineering, 2013, pp. 53-74.

[39] Y. DING, Z. CHEN, Z. HAN, Y. ZHANG e F. TORGAL, "Nano-carbon black and carbon fiber as conductive materials for the diagnosing of the damage of concrete beam," *Construction and Building Materials,* vol. 43, p. 233–241, 2013.

[40] S. WEN e D. CHUNG, "Partial replacement of carbon fiber by carbon black in multifunctional cement–matrix composites," *Carbon,* vol. 45, p. 505–513, 2007.

[41] H. LI, H. XIAO e J. OU, "Electrical property of cement-based composites filled with carbon black under long-term wet and loading condition," *Composites Science and Technology,* vol. 68, p. 2114–2119, 2008.

[42] B. HAN, L. ZHANG e J. OU, "Influence of water content on conductivity and piezoresistivity of cement-based material with both carbon fiber and carbon black," *Journal of Wuhan University of Technology-Mater Sci Ed,* vol. 25, pp. 147-151, 2010.

[43] L. ZHANG, S. DING, B. HAN, X. YU e Y. NI, "Effect of water content on the piezoresistive property of smart cement-based," *Composites Part A,* vol. 119, p. 8–20, 2019.

[44] W. DONG, W. LI, N. LU, F. QU, K. VESSALAS e D. SHENG, "Piezoresistive behaviours of cement-based sensor with carbon black subjected to various temperature and water content," *Composites Part B,* vol. 178, p. 107488, 2019.

[45] A. HUSSAIN, Y. DING, G. LIU e A. NAQI, "Study on self-monitoring of multiple cracked concrete beams with multiphase conductive materials subjected to bending," *Smart Materials and Structures,* vol. 28, nº 9, 2019.

[46] H. XIAO e H. LI, "A study on the application of CB-filled cement-based composite as a strain sensor for concrete structures," *Smart Structures and Materials 2006: Sensors and Smart Structures Technologies for Civil, Mechanical, and Aerospace Systems,* vol. 6174, pp. 1-8, 2006.

[47] S. DING, Y. RUAN, X. YU, B. HAN e Y. NI, "Self-monitoring of smart concrete column incorporating CNT/NCB composite fillers modified cementitious sensors," *Construction and Building Materials,* vol. 201, p. 127–137, 2019.

[48] J. SANCHEZ-GONZALEZ, A. MACIAS-GARCIA, M. ALEXANDRE-FRANCO e V. GOMEZ-SERRANO, "Electrical conductivity of carbon blacks under compression," *Carbon,* vol. 43, p. 741–747, 2005.

[49] ABNT, *NBR 13279: Mortars applied on walls and ceilings - Determination of the flexural and the compressive strength in the hardened stage,* Rio de Janeiro, Brazil, 2005.

[50] M. MOHSEN, A. NASSER, K. RASHID, S. AHMED e A. KHALDOON, "Effect of mixing duration on flexural strength of multi walled carbon nanotubes cementitious composites," *Construction and Building Materials,* vol. 126, pp. 586-598, 2016.

[51] H. KIM, I. PARK e H. LEE, "Improved piezoresistive sensitivity and stability of CNT/cement mortar composites with low water–binder ratio," *Composite Structures,* vol. 116, pp. 713-719, 2014.

[52] ASTM, *C595 / C595M-19: Standard Specification for Blended Hydraulic Cements,* ASTM International, West Conshohocken, PA, 2019.

[53] B. HAN, K. ZHANG, X. YU, E. KWON e J. OU, "Fabrication of Piezoresistive CNT/CNF Cementitious Composites with Superplasticizer as Dispersant," *Journal of Materials in Civil Engineering,* vol. 24, pp. 658-665, 2012.

[54] A. D'ALESSANDRO, F. UBERTINI e A. P. M. MATERAZZI, "Electrical modelling of carbon nanotube cement-based sensors for structural dynamic monitoring," em *AIP Conference Proceedings 1603*, 2014.

[55] Q. LIU, R. GAO, V. TAM, W. LI e J. XIAO, "Strain monitoring for a bending concrete beam by using piezoresistive cement-based sensors," *Construction and Building Materials,* vol. 167, pp. 338-347, 2018.

[56] D. YOO, I. YOU e S. LEE, "Electrical properties of cement-based composites with carbon nanotubes, graphene, and graphite nanofibers," *Sensors,* vol. 17, p. 1064, 2017.

[57] B. HAN, X. GUAN e J. OU, "Electrode design, measuring method and data acquisition system of carbon fiber cement paste piezoresistive sensors," *Sensors and Actuators A,* vol. 135, p. 360–369, 2007.

[58] B. HAN, L. ZHANG e J. OU, Smart and Multifunctional Concrete Toward Sustainable Infrastructures, Gateway East, Singapore: Springer Nature, 2017.

[59] Q. MAO, B. ZHAO, D. SHENG e Z. LI, "Resistance changement of compression sensible cement specimen under different stresses," *Journal of Wuhan University of Technology - Mater Sci ,* vol. 11, pp. 41-45, 1996.

[60] Z. BENAMARA, N. MECIRDI, B. AKKAL, H. MAZARI, M. CHELLALI, A. TALBI, B. GRUZZA, K. BEN, C. ROBERT-GOUMET, G. MONIER e L. BIDEUX, "Electrical characterization and electronic transport modelization in the InN/InP structures," *Sensor Letters,* vol. 7, pp. 712-715, 2009.

[61] D. YAWEN, S. MINGQING, L. CHENGUO e L. ZHUOQIU, "Electromagnetic wave absorbing characteristics of carbon black cement-based composites," *Cement And Concrete Composites,* vol. 32, pp. 508-513, 2010.

[62] W. DONG, W. LI, L. SHEN e D. SHENG, "Piezoresistive behaviours of carbon black cement-based sensors with layer-distributed conductive rubber fibres," *Materials & Design,* vol. 182, pp. 1-12, 2019.

[63] C. SONG e S. CHOI, "Moisture-dependent piezoresistive responses of CNT-embedded cementitious composites," *Composite Structures,* vol. 170, pp. 103-110, 2017.

[64] B. HAN, X. YU e J. OU, "Effect of water content on the piezoresistivity of MWNT/cement," *Journal of Materials Science,* vol. 45, p. 3714–3719, 2010.

[65] M. REZANIA, M. PANAHANDEH e S. B. F. RAZAVI, "Experimental study of the simultaneous effect of nano-silica and nanocarbon black on permeability and mechanical properties of the concrete," *Theoretical and Applied Fracture Mechanics,* vol. 104, p. 102391, 2019.

[66] H. DEHGHANPOUR, K. YILMAZ e M. IPEK, "Evaluation of recycled nano carbon black and waste erosion wires in electrically conductive concretes," *Construction and Building Materials,* vol. 221, p. 109–121, 2019.

[67] N. GARG, K. WANG e S. MARTIN, "A Raman spectroscopic study of the evolution of sulfates and hydroxides in cement–fly ash pastes," *Cement And Concrete Research,* vol. 53, pp. 91-103, 2013.

[68] L. BLACK, C. BREEN, J. YARWOOD, S. DENG, J. PHIPPS e G. MAITLAND, "Hydration of tricalcium aluminate (C3A) in the presence and absence of gypsum - studied by Raman spectroscopy and X-ray diffraction," *Journal of Materials Chemistry,* vol. 16, p. 1263–1272 , 2006.

[69] K. GARBEV, P. STEMMERMANN, L. BLACK, C. BREEN, J. YARWOOD e B. GASHAROVA, "Structural Features of C–S–H(I) and Its Carbonation in Air - A RamanSpectroscopic Study. Part I: Fresh Phases," *Journal of the American Ceramic Society,* vol. 90, pp. 900-907, 2007.

[70] M. FRÍAS e S. MARTÍNEZ-RAMÍREZ, "Use of micro-Raman spectroscopy to study reaction kinetics in blended white cement pastes containing metakaolin," *Journal of Raman Spectroscopy,* vol. 40, p. 2063–2068, 2009.

[71] C. DENG, C. BREEN, J. YARWOOD, S. HABESCH, J. PHIPPS, B. CRASTERB e G. MAITLAND, "Ageing of oilfield cement at high humidity: a combined FEG-ESEM and Raman microscopic investigation," *Journal of Materials Chemistry,* vol. 12, p. 3105–3112, 2002.

[72] M. CHOLLET e M. HORGNIES, "Analyses of the surfaces of concrete by Raman and FT-IR spectroscopies: comparative study of hardened samples after demoulding and after organic post-treatment," *Surface and Interface Analysis ,* vol. 43, p. 714–725, 2011.

[73] ABNT, *NBR 8522: Concrete - Determination of the static elasticity and strain modulus,* Rio de Janeiro, Brazil, 2008.

CHAPTER 3: RESIDUAL MECHANICAL PROPERTIES OF MORTARS CONTAINING CARBON NANOMATERIALS EXPOSED TO HIGH TEMPERATURES

3.1. INTRODUCTION

High temperatures pose serious problems to the structural performance and durability of concrete structures. The deterioration of cement-based materials exposed to fire conditions is directly related to changes in the chemical composition and physical structure of cement paste and aggregates, combined with thermal and elastic incompatibilities between these components [1-4]. Nano-scale reinforcement has been recently proposed as an alternative for improving the mechanical strength and ductility of cementitious materials at elevated temperatures, since it can refine the pore structure, accelerate the hydration process or inhibit the development of cracks at the nano-level [4-6].

Among the nanomaterials used for improving the thermal resistance of cementitious matrices, nano-silica (NS) has been the most extensively studied nano-inclusion. Most of the previous studies [7-16] have mentioned different benefits of NS in cement-based materials under high temperatures, such as increase of residual mechanical strength, reduction in crack width and length, and prevention of spalling.

Carbon-based nanomaterials have also been proposed for improvement of the mechanical behavior of cementitious materials at high temperatures, due to their excellent strength, fractural toughness and thermal stability [5]. While polypropylene fibers into cementitious matrices decompose at a temperature of 167 - 170 °C, the thermal stability of carbon nanomaterials is estimated to be up to 500 - 700 °C in air [17].

Some studies [5, 18-24] reported increases of residual mechanical properties and ductility of cement-based materials with multi-walled carbon nanotubes (MWCNT), graphene oxide (GO) or graphene sulfonate nanosheets (GSNs). These carbon-based nanofillers developed a crack bridging action or reduced the number of capillary pores, improved the distribution of thermal stresses, worked as channels for the release of autoclaving steam and prevented the damage caused by the high-pressure steam. Sikora et al. [6] reported that nanoclay (NC), nanometakaolin (NM), nanoalumina (NA), nano-iron oxide (NIO) and nano-titania (NT) also provide improvements on the structural behavior of cementitious materials exposed to high temperatures.

Although many studies [25-29] have investigated the mechanical properties of cement-based materials with nano-carbon black (CBN) at room temperature, there is no previous research focused on the experimental investigation of the residual mechanical properties of cement-based materials with CBN exposed to high temperatures. In addition, there is a lack of comparisons between the performances of different nanofillers for improvement of thermal resistance of cementitious composites. Comparison between data of distinct papers is difficult due to the vast differences in testing procedures, heating and cooling regimes, materials properties and mix proportions [6]. Therefore, the contribution of this chapter is threefold: 1) residual compressive strength and microstructure of mortars with CBN exposed to high temperatures were firstly investigated; 2) elastic and dynamic modulus of mortars with different contents of CBN or MWCNT after thermal exposure were reported; 3) a comprehensive comparison between the post-fire performances of these different carbon-based nanomaterials was made.

3.2. EXPERIMENTAL METHODS

3.2.1. Materials and mix proportions

Two different carbon-based nanofillers were used in this study: (i) CBN supplied by Birla Carbon, with specific surface area of 120 m^2/g, DBP absorption number of 124.7 $cm^3/100g$ and average particle size of 20 nm; (ii) MWCNT supplied by LG, with specific surface area of 236-276 m^2/g, DBP absorption number of 1020 $cm^3/100g$, diameter of 7 - 15 nm and length of 10 - 50 μm. Characteristics of cement, sand and superplasticizer were previously presented in Section 2.2.2.1.

CBN and MWCNT have different patterns of relationship curves between the concentration of nanofillers and the composites' mechanical or electrical properties. MWCNT have a higher aspect ratio, which provides significant changes in the characteristics of the composites at a much lower concentration level [30, 31]. Then, in the present study, the CBN content ranges from 3% to 9%, while the MWCNT content ranges from 0.4% to 1.2% (Table 4).

The water/cement ratio was 0.45 (in mass), while the sand/cement ratio was 1.00 (in volume). Superplasticizer was added to provide an appropriate dispersion of the nanofillers in water [32] and a consistency index greater than 220 mm (ABNT NBR 13276 [33]), which ensures good compaction.

Table 4 – Nanofiller and superplasticizer concentration and flow of mortars

Mortar type	Nanofiller	Nanofiller concentration[(a)]	Superplasticizer concentration[(a)]	Flow (mm)
REF	No nanofiller	0.00	0.0000	389
0.4CNT	MWCNT	0.004	0.0050	354
0.8CNT		0.008	0.0125	266
1.2CNT		0.012	0.0250	225
3CBN	CBN	0.030	0.0076	291
6CBN		0.060	0.0275	313
9CBN		0.120	0.0450	230

(a) Fraction by mass of cement

3.2.2. Preparation of specimens

For each mortar type presented in Table 4, twelve Ø5 x 10 cm cylindrical specimens were produced according to the prescriptions of Section 2.2.2.1. In addition, two extra cylinders instrumented with type K thermocouples were casted for temperature monitoring, as described in Section 3.2.3. During the production of each type of mortar, small amount of paste was poured in sealed plastic vials, according to recommendations of Garg, Wang and Martin [34]. Then, the specimens were stored during 28 days in a moisture room in controlled conditions (temperature of (23 ± 2) ºC and relative humidity of 95%) for curing. After the curing period, samples were oven dried for 24 hours at 100 - 105 ºC and then cooled down to room temperature, according to prescriptions of Mohsen et al. [35] and Kim et al. [36].

3.2.3. Heating and cooling regimes

All specimens were weighed and placed in an electric furnace equipped with a temperature controller for adjustment of rate of heating and hold times. A quarter of the samples were not exposed to high temperatures, a quarter of them were exposed to a maximum temperature of 200 ºC, another quarter was exposed to 400 ºC and the remaining samples were exposed to 600 ºC. Samples molded in the plastic vials were also exposed to these different temperature levels.

The average heating rate was 5 ºC/min. Figure 38 depicts the experimental setup for heating and cooling of specimens. A NI-9219 module, an application created with the LabVIEW software and three type K thermocouples were used to monitor the temperature in the furnace chamber and the temperature in the core of two different mortar cylinders: one of them without nanofillers and the other with the maximum nanofiller concentration.

Figure 38 – Experimental setup for heating and cooling of specimens

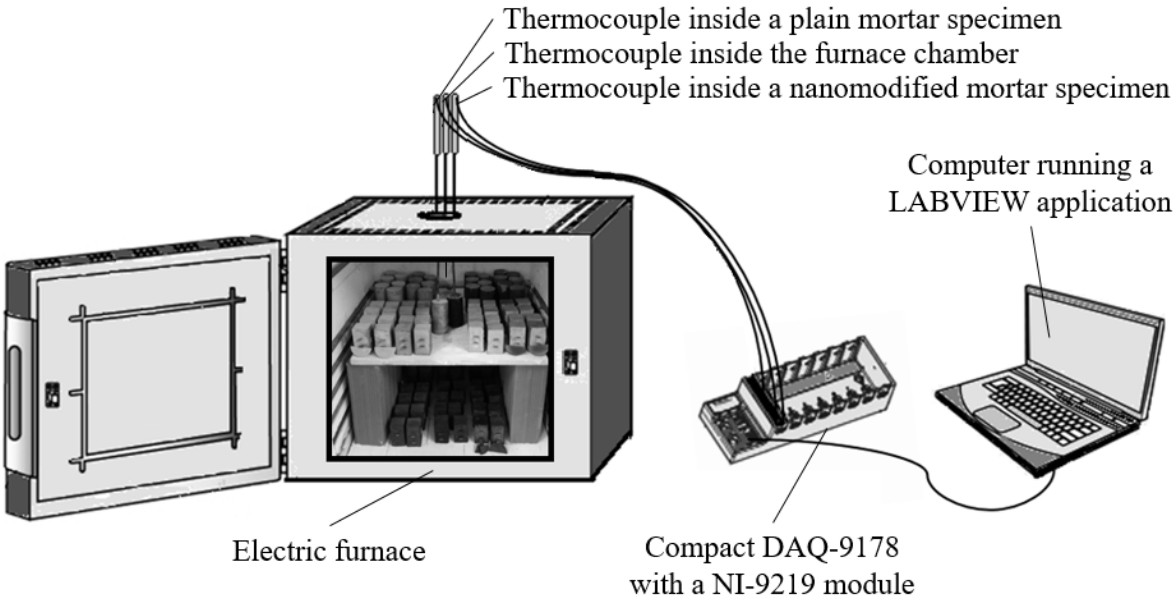

Source: Author (2020)

Once reached, the maximum temperature inside the furnace chamber was maintained for the time interval enough to ensure a constant temperature over the entire cross-section of both specimens. After that, the door of the furnace was opened and the specimens were slowly cooled to room temperature. The temperatures measured by the three thermocouples are shown in Figure 39, for each different target temperature level. Finally, the specimens were weighed again in order to determine their mass loss.

Figure 39 - Heating and cooling regimes of the specimens

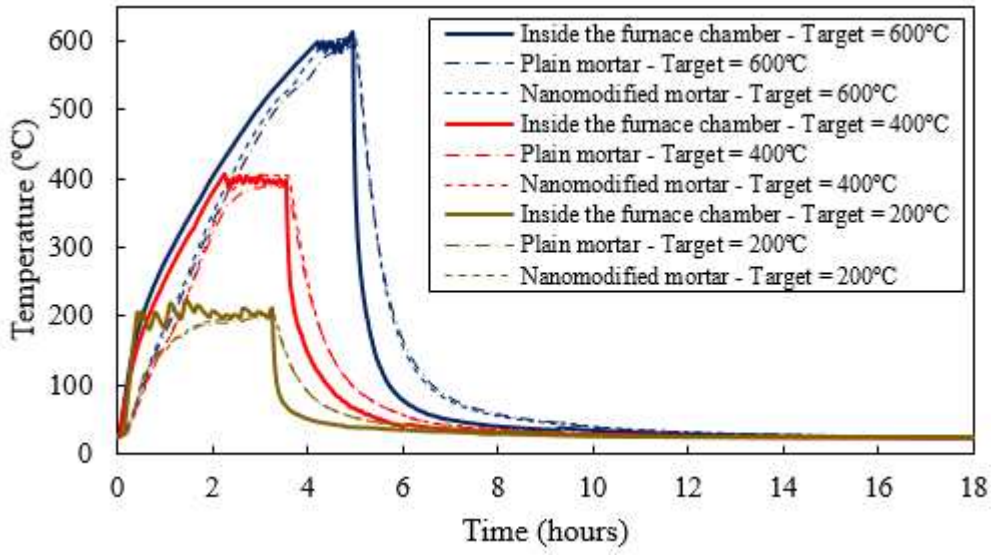

Source: Author (2020)

3.2.4. Experimental test procedures

The specimens exposed to the different temperature levels were subjected to the experimental tests of compressive strength and static modulus of elasticity indicated in Section 2.4.2.4 (ABNT NBR 8522 [37]) and dynamic modulus of elasticity (ABNT NBR 15630 [38]). For determination of the dynamic modulus of elasticity, a portable ultrasonic nondestructive digital indicating tester (PUNDIT) was used to determine the velocity of ultrasonic pulses. The samples in the sealed plastic vials were subjected to the SEM analyses described in Section 2.4.2.1.

Relative factors of residual mechanical properties (compressive strength, dynamic or static modulus of elasticity) of each specimen exposed to elevated temperatures were calculated. The relative residual mechanical property factor of a specimen *j* (Φ_j) is defined as the ratio between the value of its residual mechanical property (k_j^{res}) and the average mechanical property of their similar reference specimens, which were not exposed to a heating and cooling regime ($k_m^{25°C}$), as defined in Eq. 9:

Eq. 9
$$\Phi_j = \frac{k_j^{res}}{k_m^{25°C}}$$

3.3. RESULTS AND DISCUSSION

The compressive strength and relative residual strength factors of all series of specimens exposed to elevated temperatures are shown in Figure 40. The compressive strength of all specimens decreased when the temperature increased from 25 ºC to 600 ºC. Specimens with higher amount of CBN (9%) and MWCNT (1.2%) presented significant loss in compressive strength (48% and 44%, respectively) when the temperature increased from 25 ºC to 400 ºC. The preliminary studies of the present research indicated that very high concentrations of nanofillers significantly impair the development of hydration products. Consequently, a small increase of temperature was enough to cause significant degradation of the cement paste due to the initial dehydration of calcium silicate hydrates (CSH) [6].

The morphology of the cement pastes before and after exposure to high temperatures is shown in the SEM images of Figure 41. In fact, for lower exposure temperatures, the presence of stable hydrates is less noticeable in cementitious matrices with high amount of carbon nanofillers (9% of CBN and 1.2% of MWCNT). On the other hand, Figure 41 shows a greater amount of stable hydrates (indicated by red rectangles) in samples without carbon

nanofillers that were not exposed to high temperatures or exposed to a maximum temperature of 200 ºC. Consequently, mortar specimens without nanofillers presented higher compressive strength values in this temperature range. EDS dot maps and spectra (e.g. those indicated in Figure 41a) were used to develop a qualitative evaluation of the presence of portlandite crystals intermixed with the CSH phase.

Figure 40 – Compressive strength and relative residual strength factors of plain mortars and mortars with a) MWCNT or b) CBN exposed to high temperatures

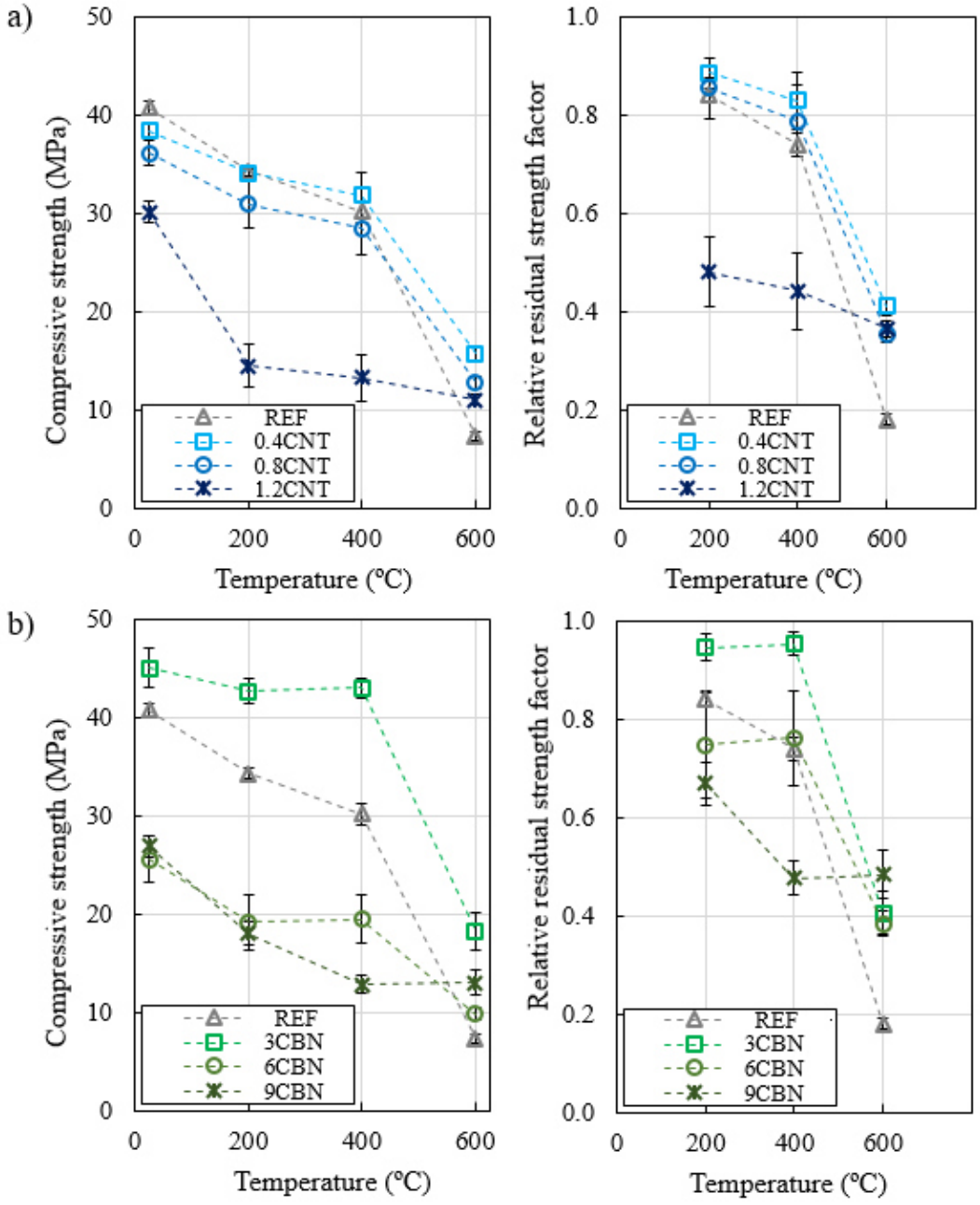

Source: Author (2020)

Figure 41 – SEM/EDS results of plain and nanomodified cementitious matrices exposed to different temperature levels

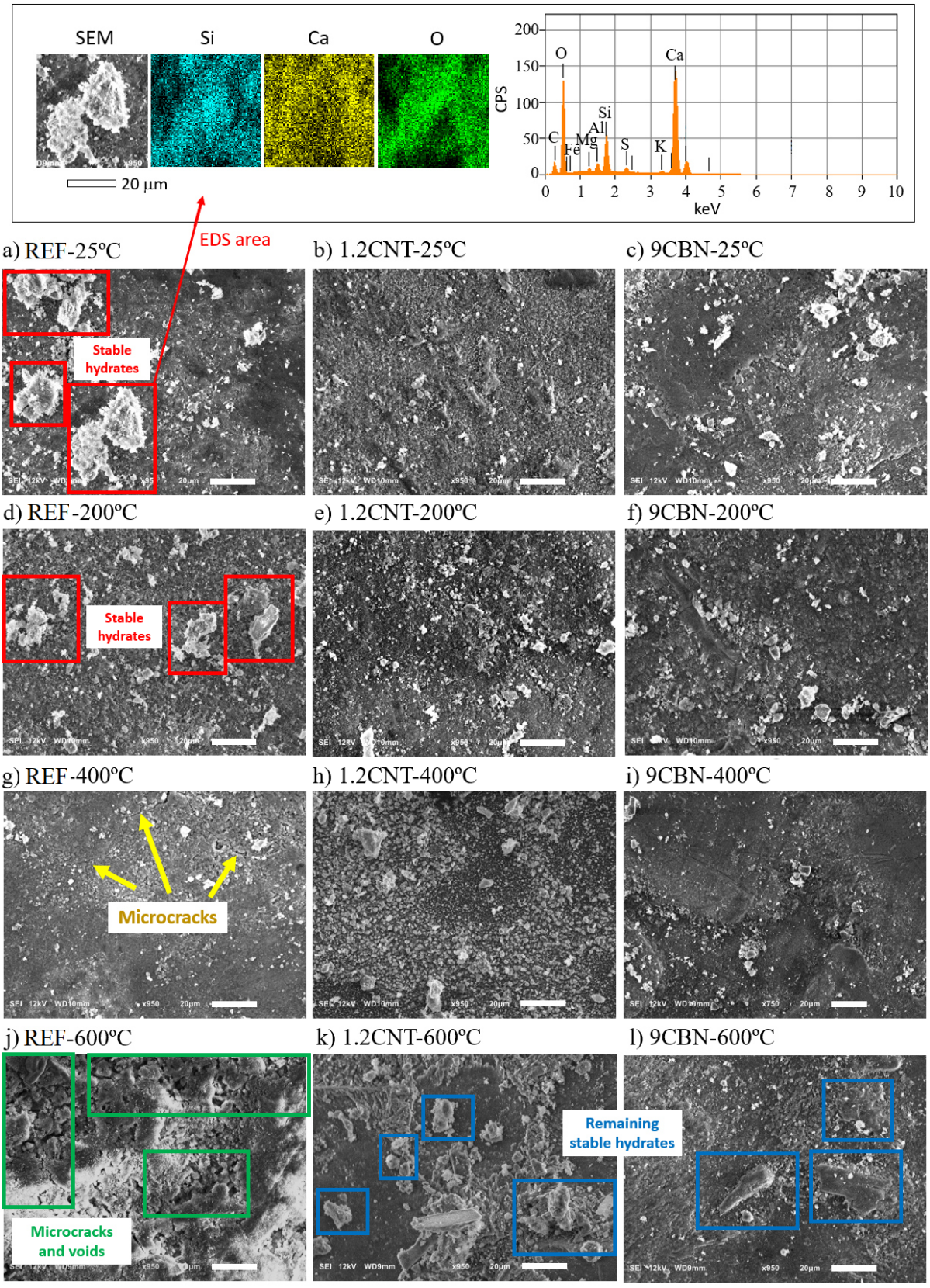

Source: Author (2020)

Specimens with lower concentration of CBN (3% and 6%) or MWCNT (0.4% and 0.8%) presented high residual compressive strength values up to 400 ºC. For example, a concentration of CBN of 3% provided a minimal strength loss of 5% after exposure to 400 ºC. This strength loss is five times lower than the strength loss of plain mortars exposed to 400 ºC (25%). Composites with 0.4% of MWCNT exposed to 400 ºC presented a strength loss of 13%, which is approximately three times lower than that of plain mortars exposed to 400 ºC. It suggests that small concentrations of CBN and MWCNT provide a significant improvement of the thermal resistance of cement mortars. Mortars with lower concentration of carbon nanofillers only faced a sharp strength decrease in the range of 400 - 600 ºC, which is mainly associated to the first phase of destruction of the calcium silicate hydrate (CSH) gel and some volumetric expansion of aggregates due to the quartz crystal transition at around 573 ºC [2, 5, 6].

Among all specimens exposed to 600 ºC, mortars without nanofillers presented the smallest residual compressive strength. In this situation, even mortars with high content of CBN and MWCNT presented average relative residual strength factors (0.48 and 0.37, respectively) higher than that of plain mortars (0.18). While plain mortars lost approximately 82% of their strength after exposure to 600 ºC, mortars with the different contents of CBN and MWCNT lost about 55% and 60% of their original compressive strength, respectively.

SEM images of samples exposed to 400 ºC (Figure 41**)** reveal a primary change in the microstructure of pastes without nanofillers: CSH crystals were not clearly evidenced and small micro-cracks were verified (indicated by yellow arrows). Massive changes in the morphology of the cement pastes were observed in samples without nanofillers exposed to 600 ºC: increase of voids and micro-cracks (indicated by green rectangles) and presence of disrupted CSH crystals. SEM images of samples with carbon nanofillers did not exhibit a similar formation of voids and micro-cracks due to this increase of temperature. In addition, some hydrates remained stable after exposure to 600 ºC (indicated by blue rectangles), which can explain their higher values of average relative residual strength factors.

The effects of high temperatures on the static modulus of elasticity and relative residual static modulus factors of plain and nanomodified mortars are shown in Figure 42. The static modulus of elasticity of most of the specimens was not significantly affected by a temperature exposure up to 200 ºC, since they present relative residual static modulus factors higher than 0.85. Only mortars produced with a concentration of 1.2% of MWCNT presented a significant decrease of static modulus of elasticity (49%) due to an increase of temperature from 25 ºC to 200 ºC.

Figure 42 – Static modulus of elasticity and relative residual static modulus factor of plain mortars and mortars with a) MWCNT or b) CBN exposed to high temperatures

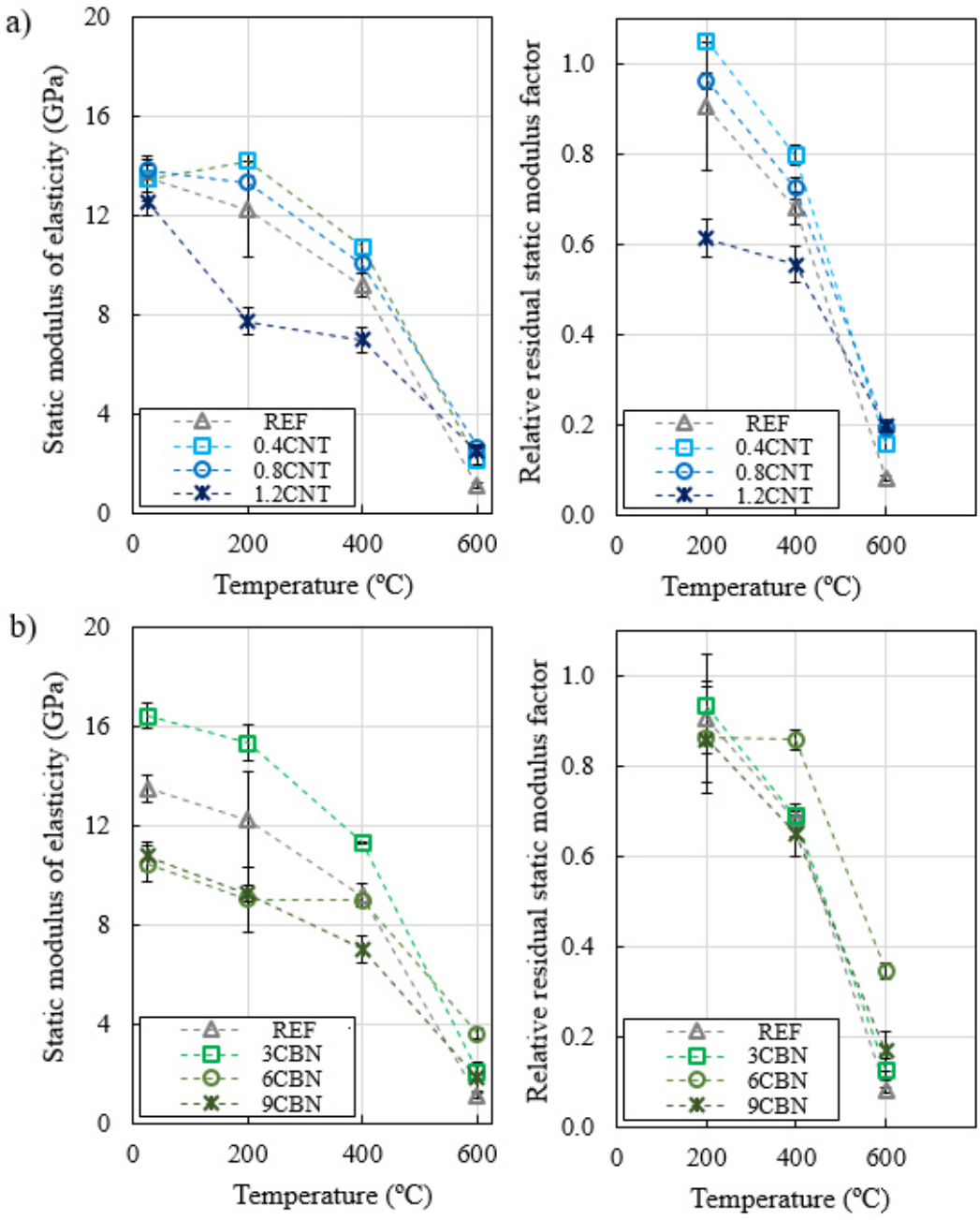

Source: Author (2020)

All specimens exhibited an interesting gradual strength loss from 200 ºC to 600 ºC and the losses of static modulus were more significant than the losses of compressive strength up to 400 ºC. The incorporation of a concentration of 0.4% and 0.8% of MWCNT or 3% of CBN provided mortars with a higher static modulus at room temperature and after exposure to any temperature level. In addition, a concentration of 3% of CBN provided the greatest stiffness increases to plain mortars (about 22% for any exposure temperature). As previously

mentioned for compressive strength, mortars exposed to 600 ºC without nanofillers exhibited the smallest values of static modulus of elasticity. Mortars without nanofillers lost approximately 92% of their elastic modulus after exposure to 600 ºC, while mortars with nanofillers faced static modulus losses ranging between 65% and 87%. This experimental data is also in accordance with the previously mentioned microstructural observations.

Results of dynamic modulus of elasticity of all series are illustrated in Figure 43.

Figure 43 – Dynamic modulus of elasticity and relative residual dynamic modulus factor of plain mortars and mortars with a) MWCNT or b) CBN exposed to high temperatures

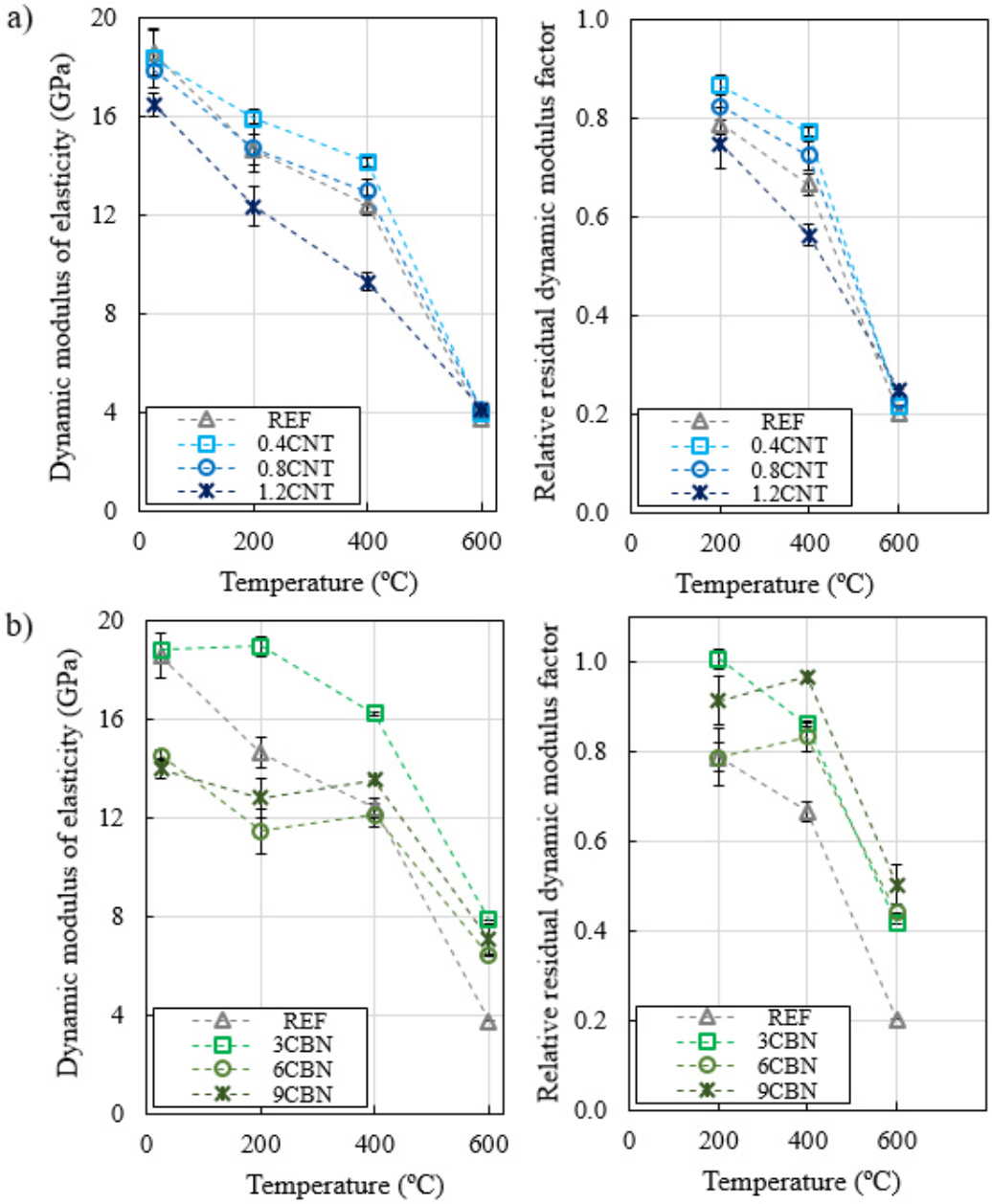

Source: Author (2020)

The dynamic modulus of elasticity of mortars with CBN was not expressively affected by temperature increases up to 200 ºC. A different trend was verified in plain mortars and mortars with MWCNT, which faced decreases of dynamic modulus of elasticity between 70% and 90% due to the increase of temperature from 25 ºC to 200 ºC. The addition of concentrations of 0.4% and 0.8% of MWCNT or 3% of CBN to plain mortars provided higher dynamic modulus at room temperature and after exposure to any temperature level.

Again, the benefits of carbon nanofillers on the stiffness of cement mortars were more pronounced in composites with a concentration of 3% of CBN. Higher decreases of dynamic modulus of elasticity were observed in specimens exposed to 600 ºC. Cement-based composites with CBN presented the highest values of residual dynamic modulus at this temperature (6.4 - 7.9 GPa), followed by composites with MWCNT (4.0 - 4.1 GPa) and plain mortars (3.75 GPa).

The residual mechanical properties of cement-based materials exposed to elevated temperatures are strongly related to their moisture loss and dehydration effects [5, 6, 20]. Since all specimens had been oven dried at 100 ºC before the thermal treatments presented in Section 3.2.3, the free pore water and the water adsorbed in aggregates and nanofillers had already been lost. Despite this, all specimens lost mass due to the exposure to high temperatures, as shown in Figure 44.

Figure 44 – Mass loss of plain mortars and mortars with a) MWCNT or b) CBN exposed to high temperatures

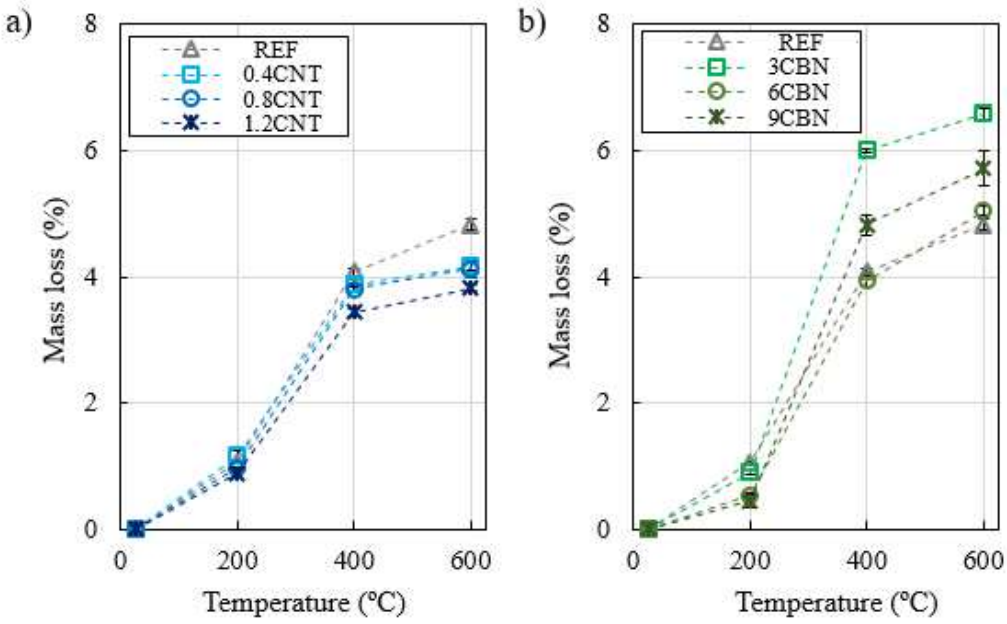

Source: Author (2020)

In the range of 25 ºC to 600 ºC, the mass loss of mortars containing MWCNT was always lower than that of control specimens, which suggests that nanofillers increased the stiffness of CSH gel and the density of the composite microstructure, which hinders the escape of chemically bonded water related to the hydration products. It is in accordance with mass loss results of concrete and mortars with MWCNT reported by Baloch et al. [5] and Sedaghatdoost et al. [20].

Mortars with CBN also presented lower mass losses than plain mortars for exposed temperatures up to 200 ºC. In contrast, the mass loss of mortars with 3% of CBN was higher than that of plain mortars in the range of 200 ºC to 600 ºC. The preliminary study of this research indicated that a lower CBN content increased the development of hydration products of cementitious matrices and caused a greater compressive strength. Then, the high mass loss of mortars with 3% of CBN can be related to the dehydration of portlandite.

3.4. CONCLUSION

An experimental investigation of the effects of MWCNT and CBN on the mechanical properties of mortars exposed to high temperatures was developed in this work. The following conclusions can be drawn:

(1) The addition of lower contents of carbon nanofillers (3% of CBN and 0.4% of MWCNT) improved the residual compressive strength, static and dynamic modulus of elasticity of mortars exposed to 200 ºC, 400 ºC and 600 ºC.

(2) After exposure to 400 ºC, mortars with high contents of carbon nanofillers (9% of CBN and 1.2% of MWCNT) presented values of compressive strength, static and dynamic moduli of elasticity up to 57%, 24% and 25% lower than those of mortars without nanofillers, respectively. In fact, SEM images of specimens exposed to temperatures up to 400 ºC revealed that stable hydrates are less noticeable in cementitious matrices with high nanofiller concentration, in comparison with those without nanofillers.

(3) The residual compressive strength, static and dynamic moduli of elasticity of plain mortars exposed to 600 ºC was lower than that of mortars with any content of nanofillers in the same condition. SEM images of mortars without nanofillers exposed to 600 ºC revealed that these specimens presented the highest formation of voids, micro-cracks and disrupted CSH crystals.

(4) The incorporation of lower concentrations of MWCNT (0.4% or 0.8%) improved the static and dynamic moduli of elasticity of cement mortars in pre-fire and post-fire conditions.

(5) Among all concentrations and types of carbon nanofillers, 3% of CBN provided the best improvements of compressive strength, static and dynamic moduli of elasticity of cement mortars in pre-fire and post-fire conditions.

(6) An evaluation of moisture losses due to temperature increases indicated that improvements of strength and stiffness of mortars can be attributed to the increase of the stiffness of the CSH gel and density of the composite microstructure provided by MWCNT or to the improvement of the hydration process provided by lower concentrations of CBN.

REFERENCES

[1] C. POON, S. AZHAR, M. ANSON and Y. WONG, "Strength and durability recovery of fire-damaged concrete after post-fire-curing," *Cement and Concrete Research,* vol. 31, pp. 1307-1318, 2001.

[2] B. FERNANDES, A. M. GIL, F. L. BOLINA and B. F. TUTIKIAN, "Microstructure of concrete subjected to elevated temperatures: physico-chemical changes and analysis techniques," *IBRACON Structures and Materials Journal,* vol. 10, pp. 838-863, 2017.

[3] J. OLIVEIRA, J. RIBEIRO, L. PEDROTI, C. FARIA, G. NALON and A. OLIVEIRA JÚNIOR, "Durability of Concrete After Fire Through Accelerated Carbonation Tests," *Materials Research,* vol. 22, p. e20190049, 2019.

[4] S. MEMON, S. SHAH, R. KHUSHNOOD and W. BALOCH, "Durability of sustainable concrete subjected to elevated temperature – A Review," *Construction and Building Materials,* vol. 199 , p. 435–455, 2019.

[5] W. BALOCH, R. KHUSHNOOD and W. KHALIQ, "Influence of multi-walled carbon nanotubes on the residual performance of concrete exposed to high temperatures," *Construction and Building Materials,* vol. 185, p. 44–56, 2018.

[6] P. SIKORA, M. ELRAHMAN and D. STEPHAN, "The influence of nanomaterials on the thermal resistance of cement-based composites - A review," *Nanomaterials,* vol. 8, p. 465, 2018.

[7] M. HEIKAL, O. AL-DUAIJ and N. IBRAHIM, "Microstructure of composite cements containing blast-furnace slag and silica nano-particles subjected to elevated thermally treatment temperature," *Construction and Building Materials,* vol. 93, p. 1067–1077, 2015.

[8] S. EL-GAMAL, S. ABO-EL-ENEIN, F. EL-HOSINY and M. R. M. AMIN, "Thermal resistance, microstructure and mechanical properties of type I Portland cement pastes

containing low-cost nanoparticles," *Journal of Thermal Analysis and Calorimetry,* vol. 131, p. 949–968, 2018.

[9] S. MAHESWARAN, N. IYER, G. PALANI, R. PANDI, D. DIKAR and S. KALAISELVAM, "Effect of high temperature on the properties of ternary blended cement pastes and mortars," *Research Journal of Recent Sciences,* vol. 122, pp. 775-786, 2013.

[10] S. LIM and P. MONDAL, "Effects of Nanosilica Addition on Increased Thermal Stability of Cement-Based Composite," *ACI Materials Journal,* vol. 112, pp. 305-316, 2015.

[11] R. IBRAHIM and R. HAMID, "Fire resistance of high-volume fly ash mortars with nanosilica addition," *Construction and Building Materials,* vol. 36, pp. 779-786, 2012.

[12] E. HORSZCZARUK, P. SIKORA, K. CENDROWSKI and E. MIJOWSKA, "The effect of elevated temperature on the properties of cement mortars containing nanosilica and heavyweight aggregates," *Construction and Building Materials,* vol. 137, pp. 420-431, 2017.

[13] R. KUMAR, S. SINGH and L. SINGH, "Studies on enhanced thermally stable high strength concrete incorporating silica nanoparticles," *Construction & Building Materials,* vol. 153, pp. 506-513, 2017.

[14] L. YAN, Y. XING, J. LI and J. ZHANG, "Effect of nanosilica on the axial tensile strength of SFRC at high temperature," *Magazine of Concrete Research,* vol. 66, pp. 447-455, 2014.

[15] M. HEIKAL, A. ALI, M. ISMAIL and N. IBRAHIM, "Behavior of composite cement pastes containing silica nano-particles at elevated temperature," *Construction and Building Materials,* vol. 70, pp. 339-350, 2014.

[16] M. BASTAMI, M. BAGHBADRANI and F. ASLANI, "Performance of nano-Silica modified high strength concrete at elevated temperatures," *Construction and Building Materials,* vol. 68, pp. 402-408, 2014.

[17] W. KHALIQ and V. KODUR, "Effectiveness of Polypropylene and Steel Fibers in Enhancing Fire Resistance of High-Strength Concrete Columns," *Journal of Structural Engineering,* vol. 144, pp. 1-12, 2018.

[18] M. AMIN, S. EL-GAMAL and F. HASHEM, "Fire resistance and mechanical properties of carbon nanotubes – clay bricks wastes (Homra) composites cement," *Construction and Building Materials,* vol. 98, p. 237–249, 2015.

[19] P. SIKORA, M. ELRAHMAN, S. CHUNG, K. CENDROWSKI, E. MIJOWSKA and D. STEPHAN, "Mechanical and microstructural properties of cement pastes containing carbon nanotubes and carbon nanotube-silica core-shell structures, exposed to elevated temperature," *Cement and Concrete Composites ,* vol. 95, p. 193–204, 2019.

[20] A. SEDAGHATDOOST and K. BEHFARNIA, "Mechanical properties of Portland cement mortar containing multi-walled carbon nanotubes at elevated temperatures," *Construction and Building Materials,* vol. 176 , p. 482–489, 2018.

[21] L. ZHANG, M. KAI and K. LIEW, "Evaluation of microstructure and mechanical performance of CNT-reinforced cementitious composites at elevated temperatures," *Composites Part A: Applied Science and Manufacturing,* vol. 95, p. 286–293, 2017.

[22] A. MOHAMMED, J. SANJAYAN, A. NAZARI and N. AL-SAADI, "Effects of graphene oxide in enhancing the performance of concrete exposed to high-temperature.," *Australian Journal of Civil Engineering,* vol. 15, pp. 61-71, 2017.

[23] H. CHU, J. JIANG, W. SUN and M. ZHANG, "Mechanical and thermal properties of graphene sulfonate nanosheet reinforced sacrificial concrete at elevated temperatures," *Construction and Building Materials,* vol. 153, p. 682–694, 2017.

[24] T. HAN, H. WANG, X. JIN, J. YANG, Y. LEI, F. Y. X. YANG, Z. TAO, Q. GUO and L. LIU, "Multiscale carbon nanosphere–carbon fiber reinforcement for cement-based composites with enhanced high-temperature resistance," *Journal of Materials Science,* vol. 50, p. 2038–2048, 2014.

[25] A. O. MONTEIRO, P. B. CACHIM and P. J. COSTA, "Self-sensing piezoresistive composite loaded with carbon black particles," *Cement and Concrete Composites,* vol. 81, pp. 59-65, 2017.

[26] H. DEHGHANPOUR, K. YILMAZ and M. IPEK, "Evaluation of recycled nano carbon black and waste erosion wires in electrically conductive concretes," *Construction and Building Materials,* vol. 221, p. 109–121, 2019.

[27] M. REZANIA, M. PANAHANDEH and S. B. F. RAZAVI, "Experimental study of the simultaneous effect of nano-silica and nanocarbon black on permeability and mechanical properties of the concrete," *Theoretical and Applied Fracture Mechanics,* vol. 104, p. 102391, 2019.

[28] W. DONG, W. LI, L. SHEN and D. SHENG, "Piezoresistive behaviours of carbon black cement-based sensors with layer-distributed conductive rubber fibres," *Materials & Design,* vol. 182, pp. 1-12, 2019.

[29] D. YAWEN, S. MINGQING, L. CHENGUO and L. ZHUOQIU, "Electromagnetic wave absorbing characteristics of carbon black cement-based composites," *Cement And Concrete Composites,* vol. 32, pp. 508-513, 2010.

[30] B. HAN, X. YU and J. OU, Self-Sensing Concrete In Smart Structures, Waltham, MA, USA: Elsevier Inc., 2015.

[31] P. COELHO, V. ARMELLINI and A. MORALES, "Assessment of Percolation Threshold Simulation for Individual and Hybrid Nanocomposites of Carbon Nanotubes and Carbon Black," *Materials Research,* vol. 20, pp. 1638-1649, 2017.

[32] B. HAN, K. ZHANG, X. YU, E. KWON and J. OU, "Fabrication of Piezoresistive CNT/CNF Cementitious Composites with Superplasticizer as Dispersant," *Journal of Materials in Civil Engineering,* vol. 24, pp. 658-665, 2012.

[33] ABNT, *NBR 13276: Preparation of mortar for unit masonry and rendering with standard consistence index,* Rio de Janeiro, 2005.

[34] N. GARG, K. WANG and S. MARTIN, "A Raman spectroscopic study of the evolution of sulfates and hydroxides in cement–fly ash pastes," *Cement And Concrete Research,* vol. 53, pp. 91-103, 2013.

[35] M. MOHSEN, A. NASSER, K. RASHID, S. AHMED and A. KHALDOON, "Effect of mixing duration on flexural strength of multi walled carbon nanotubes cementitious composites," *Construction and Building Materials,* vol. 126, pp. 586-598, 2016.

[36] H. KIM, I. PARK and H. LEE, "Improved piezoresistive sensitivity and stability of CNT/cement mortar composites with low water–binder ratio," *Composite Structures,* vol. 116, pp. 713-719, 2014.

[37] ABNT, *NBR 8522: Concrete - Determination of the static elasticity and strain modulus,* Rio de Janeiro, Brazil, 2008.

[38] ABNT, *NBR 15630: Mortar for laying and coating of walls and ceilings - Mortars applied on walls and ceilings - Determination of the elasticity modulus by the ultrasonic wave propagation,* Rio de Janeiro, 2008.

CHAPTER 4: RESIDUAL PIEZORESISTIVE PROPERTIES OF MORTARS CONTAINING CARBON NANOMATERIALS EXPOSED TO HIGH TEMPERATURES

4.1. INTRODUCTION

Fire can cause severe damage in concrete structures. Even after a severe fire, retrofitting of damaged concrete elements can be the most economical solution, instead of demolishing them. However, the definition of the most suitable repairing and strengthening methods for concrete elements exposed to fire depends on a precise and quick diagnosis of their residual structural performance. The primary step for evaluating the post-fire behavior of concrete structures consists of a visual investigation of crack state, spalling, deflections and color of the structural elements. A more detailed analysis can be developed through non-destructive tests, concrete core and steel bar sampling, loading tests, material sample analysis, microstructural evaluations, analytical methods, finite element simulations and other inspection techniques [1-3].

Recently, Nanoscience and Nanotechnology enabled the development of an innovative technology for assessment of damage and structural performance of civil structures: a nanomodified cement-based composite with intrinsic sensing ability. This technology consists of conductive nanofillers added to cement-based materials, in order to develop composites able to work as structural elements, monitor strain and detect damage in concrete elements [4-7]. This kind of technology seems to be promising for the assessment of the residual structural performance of fire-damaged concrete structures and diagnosis of their damage level during and after their exposure to high temperatures.

The influence of temperature on the sensing ability of self-sensing cement-based composites has been investigated by a few number of researchers and most of them focused on temperature levels close to the room temperature. The electrical resistivity of cement-based sensors can be affected by environmental temperature variations because atomic cores of conductive materials move more fiercely and disorderedly at higher temperatures, which improves their electrical conductivity [4]. In addition, temperature variations cause expansion and contraction of the composites, which changes the distance between conductive fillers and causes variations in their electrical resistivity [8].

Azhari [9] observed that the electrical resistivity of carbon fiber (CF) reinforced cement-based composites decreases when the temperature increased from – 15 ºC to 60 ºC and the variations were completely reversible. Chacko et al. [10] exposed carbon fiber reinforced cement-based composites to temperature levels ranging from – 20 ºC to 65 ºC and verified that as the temperature increased, the electrical resistivity decreased. However, compared with strain, the effects of temperature on the composite conductivity was insignificant. Consequently, Chacko et al. [10] concluded that their experimental observations imply a lack of need for temperature correction.

Monteiro et al. [11] determined the electrical resistance, fractional change in resistivity, gauge factor and stress sensitivity of self-sensing mortars with carbon black nanoparticles (CBN) at temperatures of 15 ºC, 25 ºC, 35 ºC and 45 ºC. They observed a clear decrease of the amplitude of fractional changes in resistivity (FCR) with the increase of the temperature, which resulted in lower piezoresistive response. Despite this, good linearity and repeatability were observed in all piezoresistive tests. Han et al. [8] also observed changes in the electrical resistivity of concrete with CF and CBN due to temperature variations between – 30 ºC and 50 ºC. Despite this, a compensation circuit was successfully applied to eliminate the effects of temperature on the output of the sensors.

Dong et al. [12] observed irreversible FCR in composites containing 3% of CBN exposed to – 20 ºC, 60 ºC or 100 ºC. After a temperature calibration of FCR to remove thermal exchange effects, those cement-based sensors presented good synchronicity and repeatability in piezoresistive tests. Demircilioglu et al. [13] evaluated electrical properties of a smart concrete with brass fibers exposed to temperatures up to 200 ºC. They stated that its electrical resistance decreased linearly up to 50 ºC. After 150 ºC, they observed a sharp increase of electrical resistance, which is related to damage resulted from the mismatch strain between fibers, paste and aggregates. Then, they concluded that this kind of smart concrete can be used as a fire alarm sensor and alert residents and technicians to evacuate the structure (building, bridge, tunnel) in case of danger.

There is no previous study dealing with the effects of temperatures levels higher than 100 ºC on the residual electrical resistivity and piezoresistive response of self-sensing cement-based composites. Despite this, it is known that carbon nanomaterials have excellent thermal endurance and strength, unlike other fibers such as polypropylene that decomposes at low temperatures (167 - 170 ºC) [14, 15]. The experimental work described in this chapter aimed to investigate the residual sensing ability of cement-based composites with CBN or multi-walled carbon nanotubes (MWCNT) exposed to temperatures of 200 ºC, 400 ºC and

600 ºC. The objective was the identification of the maximum temperature to which a self-sensing cement-based composite can be exposed, so that it remains viable for monitoring strain of concrete structures in post-fire conditions and contributes for a precise diagnosis of damage and residual structural performance.

4.2. EXPERIMENTAL METHODS

The same materials and mix proportions presented in Section 2.2.2.1 and Section 3.2.1 were used in the present investigation. For each mortar type presented in Table 4, sixteen 4 cm × 4 cm × 7.5 cm mortar prisms were produced, as described in Section 2.2.2.1. In each prism, two high temperature resistant Kanthal KA1 plates of 1.5 cm × 5.0 cm × 0.15 cm were embedded in a straight line at equal distance of about 2.0 cm from each other. The specimens were stored during 28 days in a moisture room at temperature of (23 ± 2) ºC and relative humidity of 95%. In order to decrease the role of ionic conduction, after the curing period the samples were oven dried for (24 ± 2) hours at 100 - 105 ºC and then cooled down to room temperature, as recommended by Mohsen et al. [16] and Kim et al. [17]. Then, they were exposed to the heating and cooling regimes described in Section 3.2.3.

Composites were designated as X/Y-SZ, in which the "X" term refers to the type of carbon nanofiller and its concentration (REF, 0.4CNT, 0.8CNT, 1.2CNT, 3CBN, 6CBN or 9CBN), the "Y" term refers to fire simulation temperature (25 ºC, 200 ºC, 400 ºC or 600 ºC) and the "Z" term is the identification number of the sample (1, 2, 3 or 4).

After the thermal treatments, one of the specimens (S4) of each series was used to estimate the ultimate compressive strength of the material (ABNT NBR 13279 [18]). The other (S1, S2 and S3) were subjected to the electrical and electromechanical tests described in Sections 2.2.2.2 to 2.2.2.4.

After the compression test, an internal fragment of each kind of composite located between the electrodes was subjected to a Raman analyses at the age of 28 days, according to the procedures mentioned in Section 2.4.2.3. The wavenumber range of 1000 - 2000 cm^{-1}, 3 seconds exposure time and one accumulation per spectrum were used.

A DTG-60H thermogravimetric analyzer from Shimadzu was used to develop a thermogravimetric analysis (TGA) of the nanofillers over the temperature range from ambient to 900 ºC, at a heating rate of 10 ºC/min. The initial mass of MWCNT used in the test was about 5 mg, while the mass of CNT was about 10 mg. Tests in two different atmospheres were performed: air and nitrogen at 50 mL/min.

4.3. RESULTS AND DISCUSSION

Results of DC tests are shown in Figure 45, Figure 46, Figure 47 and Figure 48. Regardless the exposure temperature, U_{comp}/i values in the range of 10^5 - 10^6 V/A were observed in specimens without conductive nanofillers. Values with the same magnitude were always verified in samples with concentration of 3% of CBN by mass of cement, which means that this filler content is below the percolation threshold. In addition, all of the composites doped with MWCNT presented U_{comp}/i ratios of the same order of magnitude after being exposed to 600 ºC. The reason for this electrical resistivity increase is discussed later in this section. The general trend observed in all of the other series was the sharp decrease of electrical resistivity and internal capacitance with the increase of CBN or MWCNT concentration.

Figure 45 - U_{comp}/i ratios vs. time curves of DC tests of mortars that were not exposed to high temperatures.

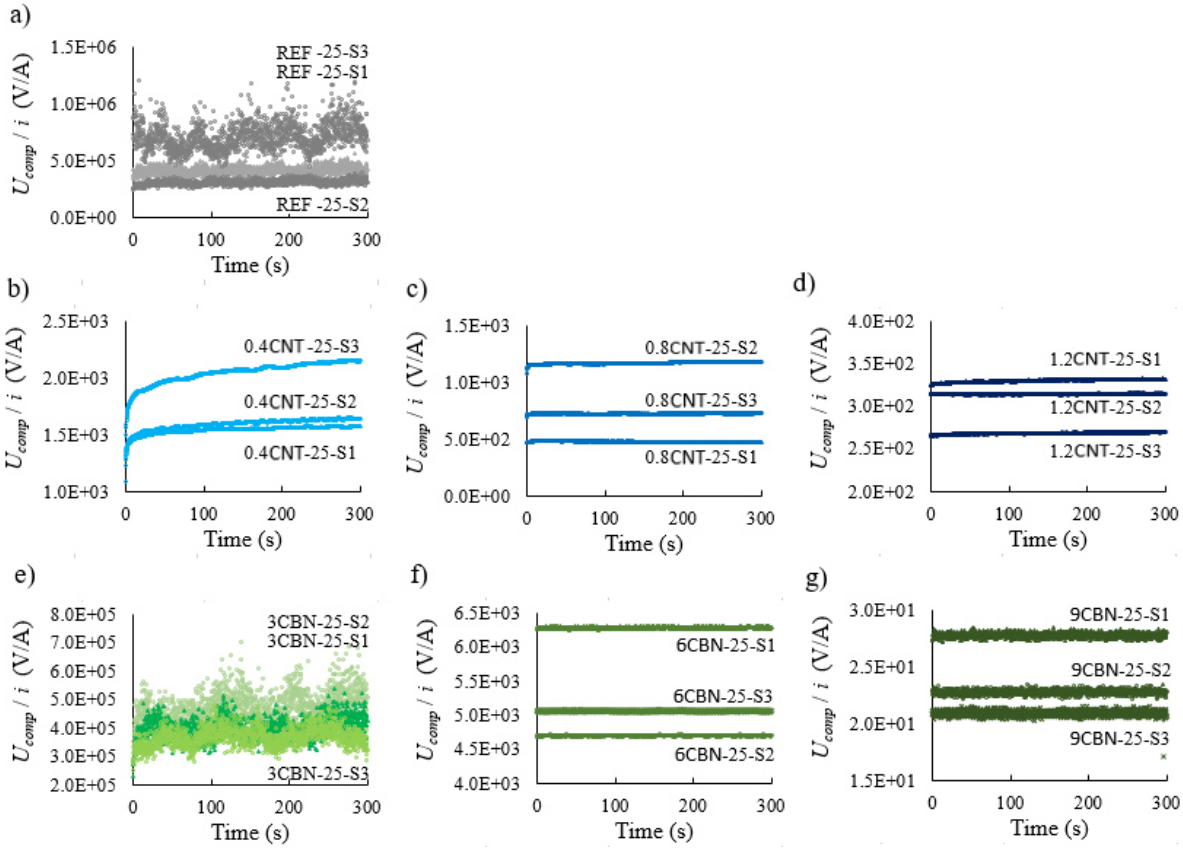

Source: Author (2020)

Figure 46 - U_{comp}/i ratios vs. time curves of DC tests of mortars exposed to 200 ºC

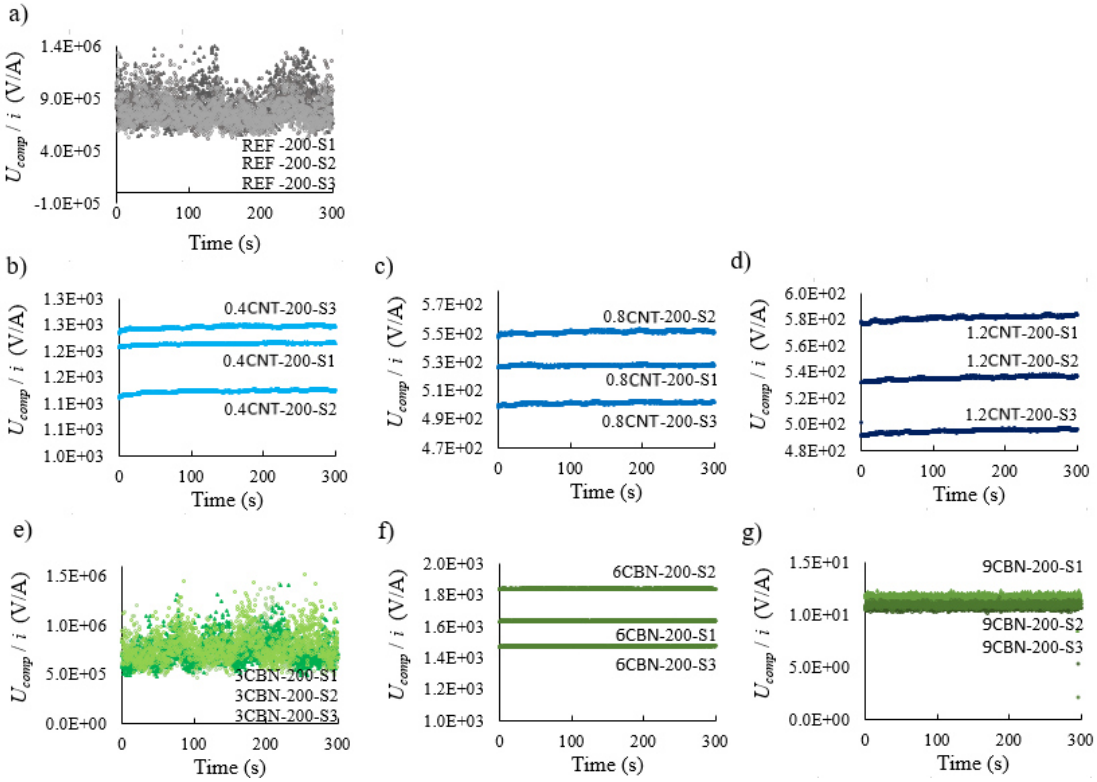

Source: Author (2020)

Figure 47 – U_{comp}/i ratios vs. time curves of DC tests of mortars exposed to 400 ºC

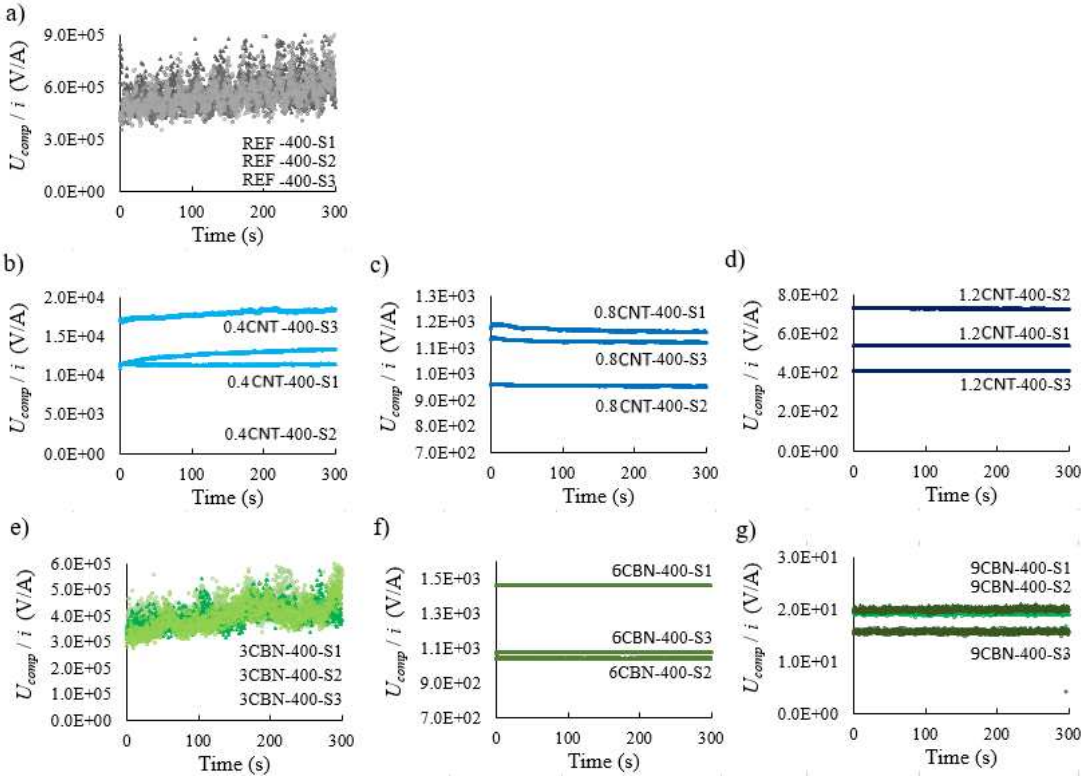

Source: Author (2020)

Figure 48 – U_{comp}/i ratios vs. time curves of DC tests of mortars exposed to 600 ºC

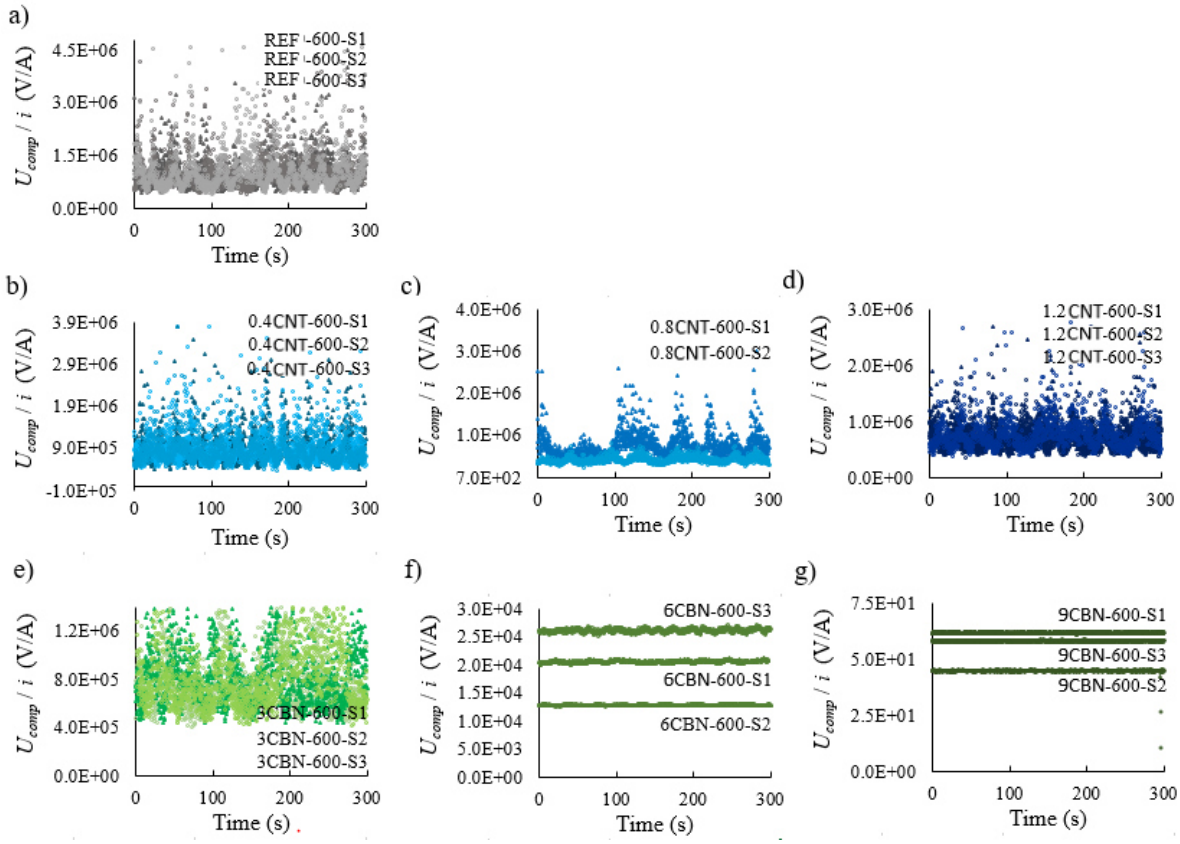

Source: Author (2020)

A significant capacitive behavior was only observed in the series with the lowest concentration of MWCNT. Electrical current vs. time regression models obtained with Eq. 2 and Eq. 3 of Chapter 2 indicated average time constants τ of 57.58 seconds and 2.28 seconds in series 0.4CNT/25 and 0.4CNT/200, respectively. It shows that cement-based composites with lower conductive filler concentration still presented slight internal capacitance, despite having been previously dried at 100 ºC.

The increase of temperature from 25 ºC to 200 ºC decreased the time constant in 96%, which indicates that the internal capacitance of the composite sharply decreased with this thermal treatment. It can be attributed to the decrease of the polarization effect due to the release of CSH interlayer water that takes place in the temperature range from 100 ºC to 200 ºC [19, 20]. These results suggest that a significant decrease of the polarization effect happens when the composite is exposed to temperatures higher than 100 ºC. However, it is only evident when the conductive filler concentration is low and the ionic conduction could not be completely neglected. A polarization effect was not observed in one of the three specimens of series 0.4CNT/400. Despite this, the other two specimens of the same series

presented time constants of 164.69 seconds and 101.11 seconds, which are inconsistent with the previously stated comments on attenuation of the polarization effect. Further studies are recommended to elucidate those distinct behaviors.

Results of DC tests also show that some specimens with concentrations of 0.8% and 1.2% presented a very small internal capacitance. Electrical current vs. time regression models obtained with Eq. 2 and Eq. 3 of Chapter 2 indicated very low time constants in these cases (lower than 3 seconds). Higher filler concentrations (1.2% of MWCNT, 6% and 9% of CBN) provided an elimination of the composite internal capacitance, as previously stated by Ubertini et al. [6], Han et al. [7] and Han et al. [8].

The effects of temperature exposure on the electrical resistivity of mortars (determined through DC and biphasic DC methods) are summarized in Figure 49. A CBN content of 9% and a MWCNT content of 1.2% provided composites with electrical resistivity up to four orders of magnitude lower than that of plain mortars.

Figure 49 – Electrical resistivity of mortars with CBN and MWCNT determined through a) DC and b) biphasic DC methods.

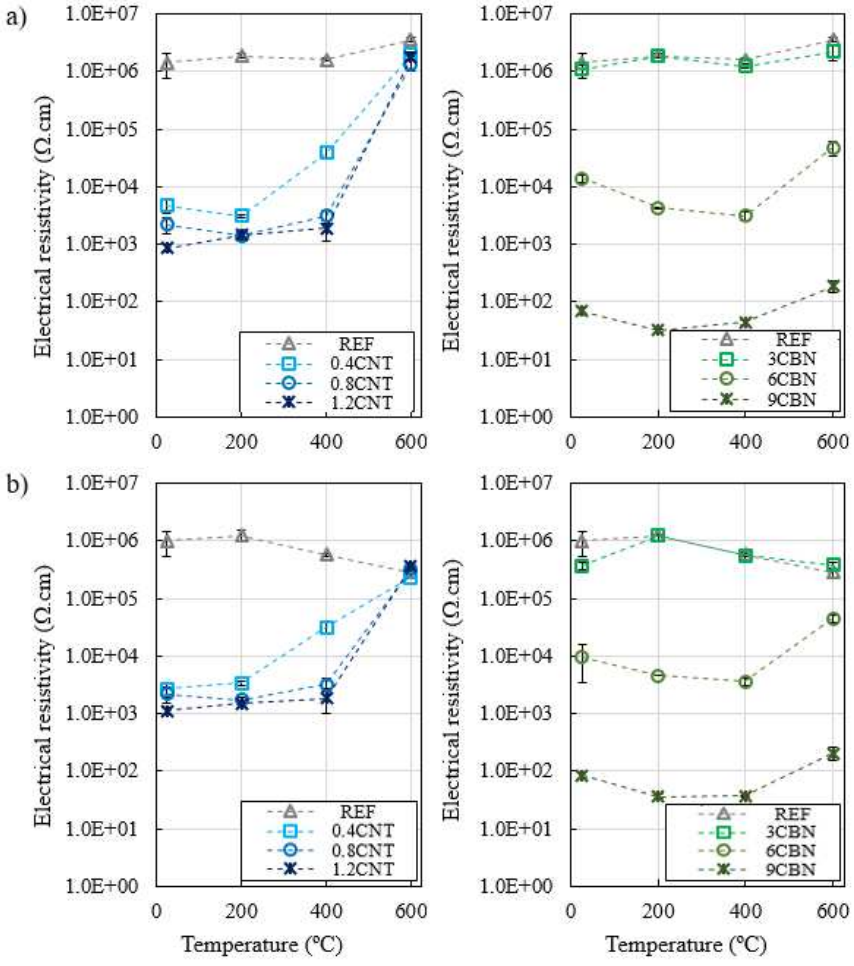

Source: Author (2020)

Analyses of variance and post-hoc Tukey's multiple comparison tests were performed to compare the average biphasic DC electrical resistivity of mortars with 0.8% of MWCNT exposed to different temperatures. A significance level of 5% was considered. After that, the same statistical comparison was performed for the other composites that also presented a reasonable electrical conductivity (0.4% of MWCNT, 1.2% of MWCNT, 6% of CBN and 9% of CBN).

The statistical tests indicated that the increase of the temperature from 25 ºC to 400 ºC did not change the biphasic DC electrical resistivity of mortars with 0.8% of MWCNT, 1.2% of MWCNT, 3% of CBN and 6% of CBN, while their exposure to a temperature of 600 ºC did so. In contrast, a similar statistical analysis performed on data of series with 0.4% of MWCNT indicated that the electrical resistivity of these composites starts to change at the exposure temperature of 400 ºC and this change is accentuated at 600 ºC. Then, it is important to investigate the possible causes for these changes of electrical resistivity.

The main factor affecting the electrical resistivity of the composite is the conductive filler. Then, TGA in air and nitrogen atmosphere was performed in order to determine the temperature range for the oxidation of as-received CBN and MWCNT. The results presented in Figure 50 show that oxidation of both fillers begins at about 500 ºC. It is evident that the availability of oxygen significantly favors mass loss.

Figure 50 – TGA of CBN and MWCNT

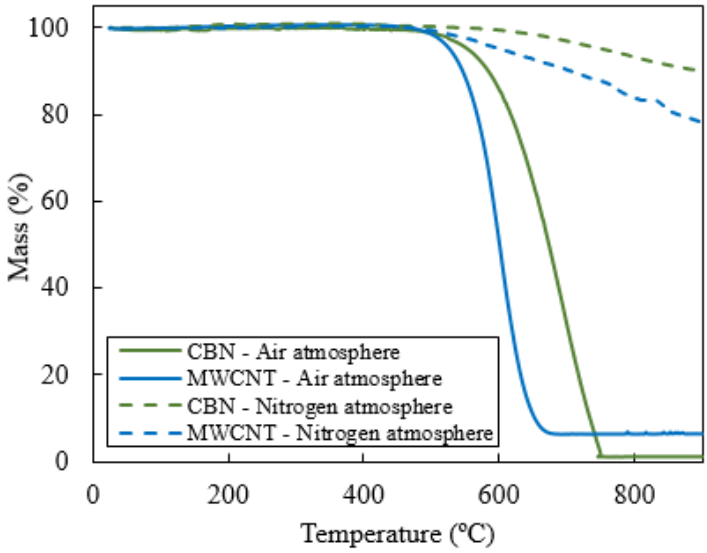

Source: Author (2020)

In air atmosphere, the maximum mass loss rate of MWCNT occurred at 600 ºC and its initial mass was reduced by about 94%. At 685 ºC, all MWCNT had been oxidized and

the remaining residue results from cobalt inclusions. CNT presented a better thermal stability, since their maximum mass loss rate happened at about 680 ºC. At 760 ºC, approximately 100% of the initial mass of CBN had been oxidized. On the other hand, the oxidation rate of the nanomaterials is significantly small in nitrogen atmosphere. In this case, only 22% and 10% of the initial mass of MWCNT and CBN were oxidized at the temperature of 900 ºC, respectively. Quantifying the availability of oxygen for oxidation of all of the nanomaterials inside the composites is challenging. Then, another strategy was used to estimate possible oxidation of the nanoparticles: the Raman spectroscopy analysis.

Two characteristic bands can be observed in both MWCNT and CBN: the tangential stretching G mode at about 1550 - 1650 cm^{-1} and the D mode at about 1350 cm^{-1} [21, 22, 23]. Raman maps of each composite were elaborated, by analyzing the spectra at 81 locations distributed in an internal fragment of the composite. Maps were constructed according to the methodology proposed by Liu and Sun [24], in which a specific color (gray) was assigned to points where the bands of the studied compound appeared. If no band was detected, the point was deemed not to contain the compound and a white color was assigned. At the end, the area fractions of nanofillers were calculated from Raman maps for each different composite and exposure temperature, as shown in Figure 51. Raman maps obtained from the different types of specimens are shown in Figure 52. Typical Raman spectra (after baseline correction) in measurement locations with high concentration of CBN and MWCNT are exemplified in Figure 53a and Figure 53b, respectively.

Figure 51 – Area fraction for MWCNT and CBN peaks in the Raman maps

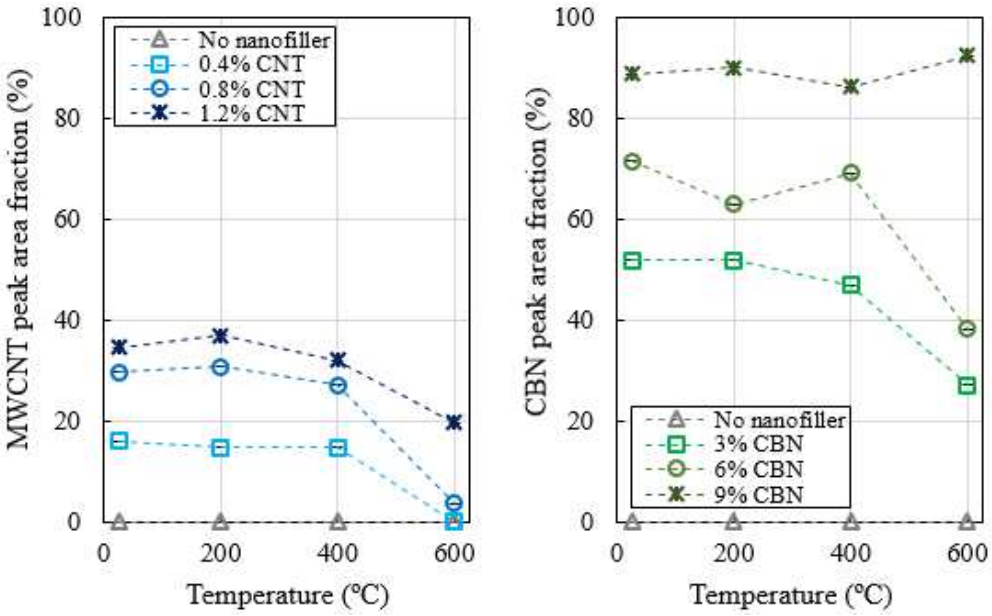

Source: Author (2020)

Figure 52 – Raman maps for MWCNT and CBN monitoring in the specimens

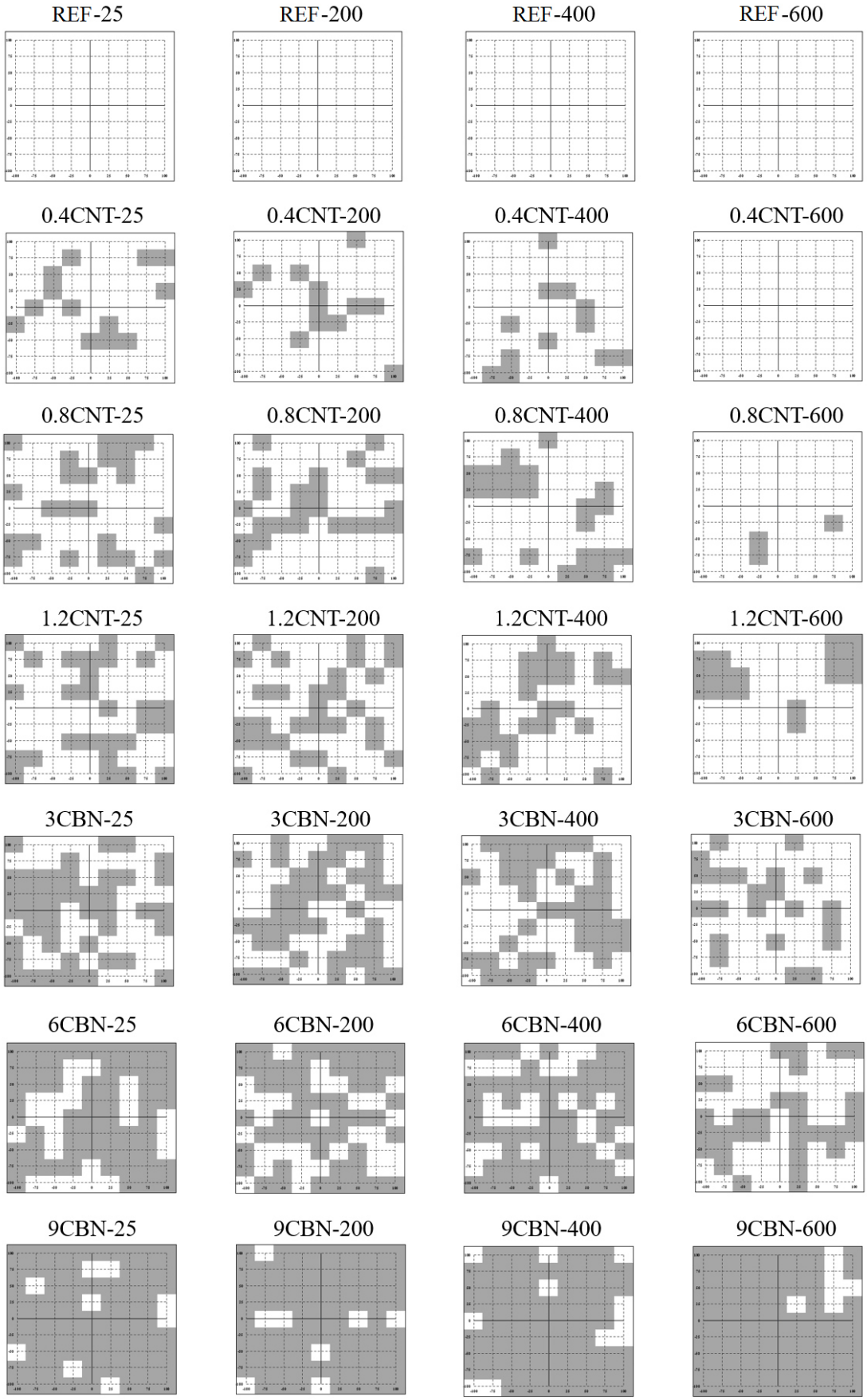

Source: Author (2020)

Figure 53 – Typical Raman spectrum collected in measurement locations with high concentration of a) CBN or b) MWCNT.

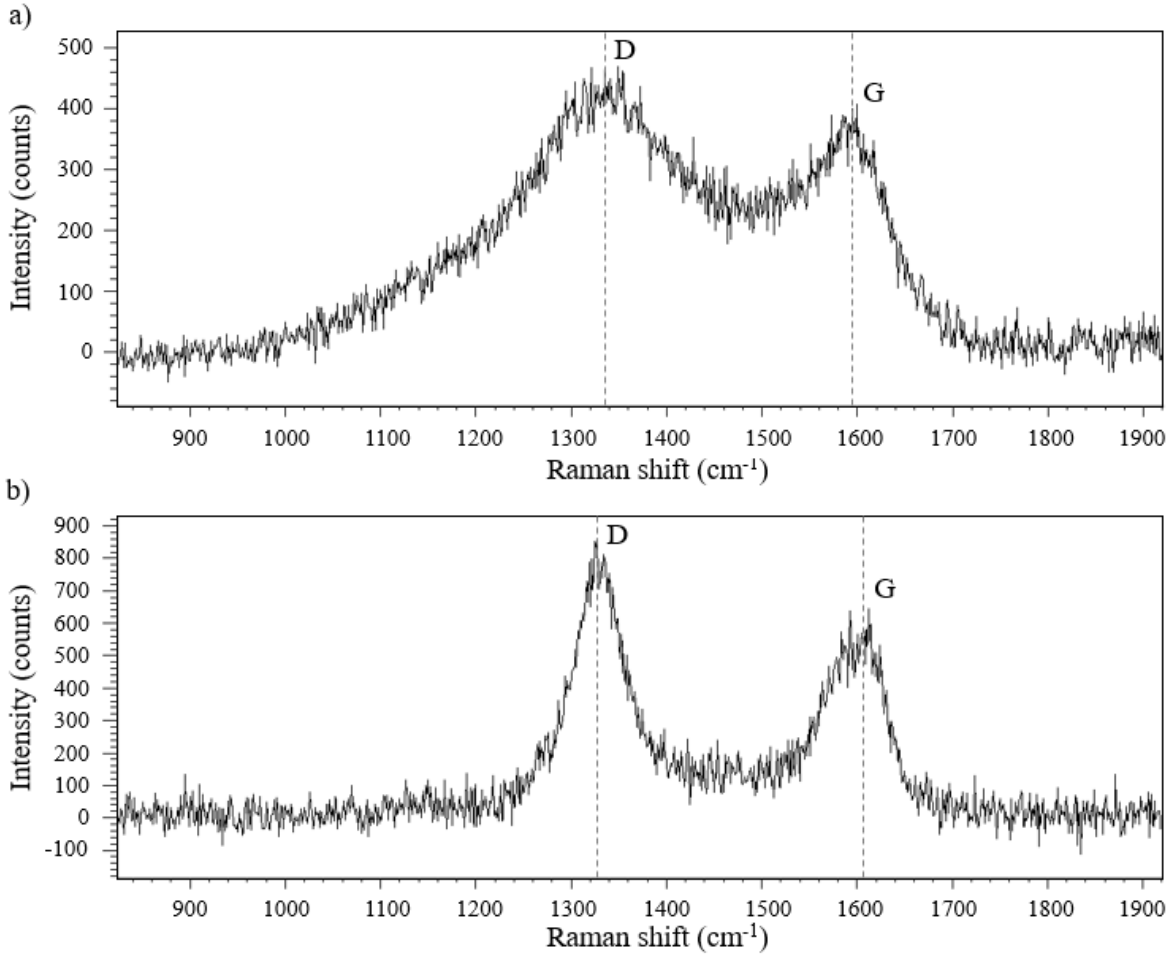

Source: Author (2020)

A mutual analysis of Raman maps and TGA curves suggests that nanoparticles oxidation begins at around 500 ºC. The MWCNT peak area fraction of the series 1.2CNT, 0.8CNT and 0.4CNT decreased in 37.5%, 85.2% and 100% from 400 ºC to 600 ºC, which proves that the amount of MWCNT inside the composites significantly decreased, which is the cause of the sharp increase in the electrical resistivity in this range indicated in Figure 49.

The CBN peak area fraction of the series 3CBN and 6CBN also decreased in 42.55% and 44.93%, which also indicates oxidation of a significant amount of CBN in this series. Consequently, the electrical resistivity of specimens with 3% of CBN remained very high and the electrical resistivity of specimens with 6% of CBN presented an increase of 11.46%.

Only specimens with a concentration of 9% of CBN kept the same amount of nanofillers after exposure to 600 ºC, which suggests that the oxygen available inside the pores of the composite oxidized a negligible amount of functional fillers. Then, it is possible to suspect that the variation in the electrical resistivity of this composite is mostly related to the

internal damage of the cementitious matrix. Previous studies [7-9, 25-27] have already reported that cracks due to high intensity loading cause interruptions in the conductive pathways of smart cement-based composites, increasing their electrical resistivity. High temperatures increase porosity and average pore diameter of cementitious materials and cause micro-cracks due to thermal stresses, decomposition of hydration products, high pore vapor pressure, shrinkage of cement matrix and expansion of aggregates [28, 29]. Then, the increase in the electrical resistivity of composites with 9% of CBN is probably due to the increases in porosity and cracking.

Curiously, the curve of temperature versus dynamic elastic modulus of mortars with 9% of CBN shown in Chapter 3 demonstrated a very similar behavior. Both electrical resistivity and dynamic modulus were not affected by the increase of temperature from 25 ºC to 400 ºC. A sharp increase in the electrical resistivity happened together with a sharp decrease of dynamic modulus of elasticity. Then, specimens of the 9%CBN series seem to have a kind of damage detection ability. The changes in the electrical resistivity of these composites due to the exposure to high temperatures can be used in the future for assessment of fire damage in structural elements.

The piezoresistive response and FCR vs. strain curves of the specimens are shown in APPENDIX A. Only specimens without nanofillers and with 3% of CBN (concentration below the percolation threshold) did not present a piezoresistive behavior at the temperatures of 25 ºC, 200 ºC and 400 ºC. The other specimens presented an adequate piezoresistive response before exposure to 600 ºC, which is directly related to the improvement of electrical conductivity indicated in Figure 49. Mortars with 6% or 9% of CBN also exhibited a piezoresistive behavior after being exposed to 600 ºC because the oxygen available in the pores was not enough to decompose a significant amount of nanofillers.

Linear regression analyses with zero intercept were performed to determine the models that provide the best fit to FCR vs. strain curves. The gauge factor of the composites was determined based on the angular coefficient of these regression equations. Their coefficients of determination R^2 were also determined. Specimens with MWCNT exposed to 400 ºC presented two regions with distinct gauge factors. Then, two different regression equations were developed in order to properly describe the relationship between strain and FCR along the entire elastic regime.

The values obtained for the residual gauge factor, coefficient of determination and stress sensibility of each series of composites are summarized in Figure 54.

Figure 54 – Residual gauge factor (a), coefficient of determination (b) and stress sensitivity (c) of the composites

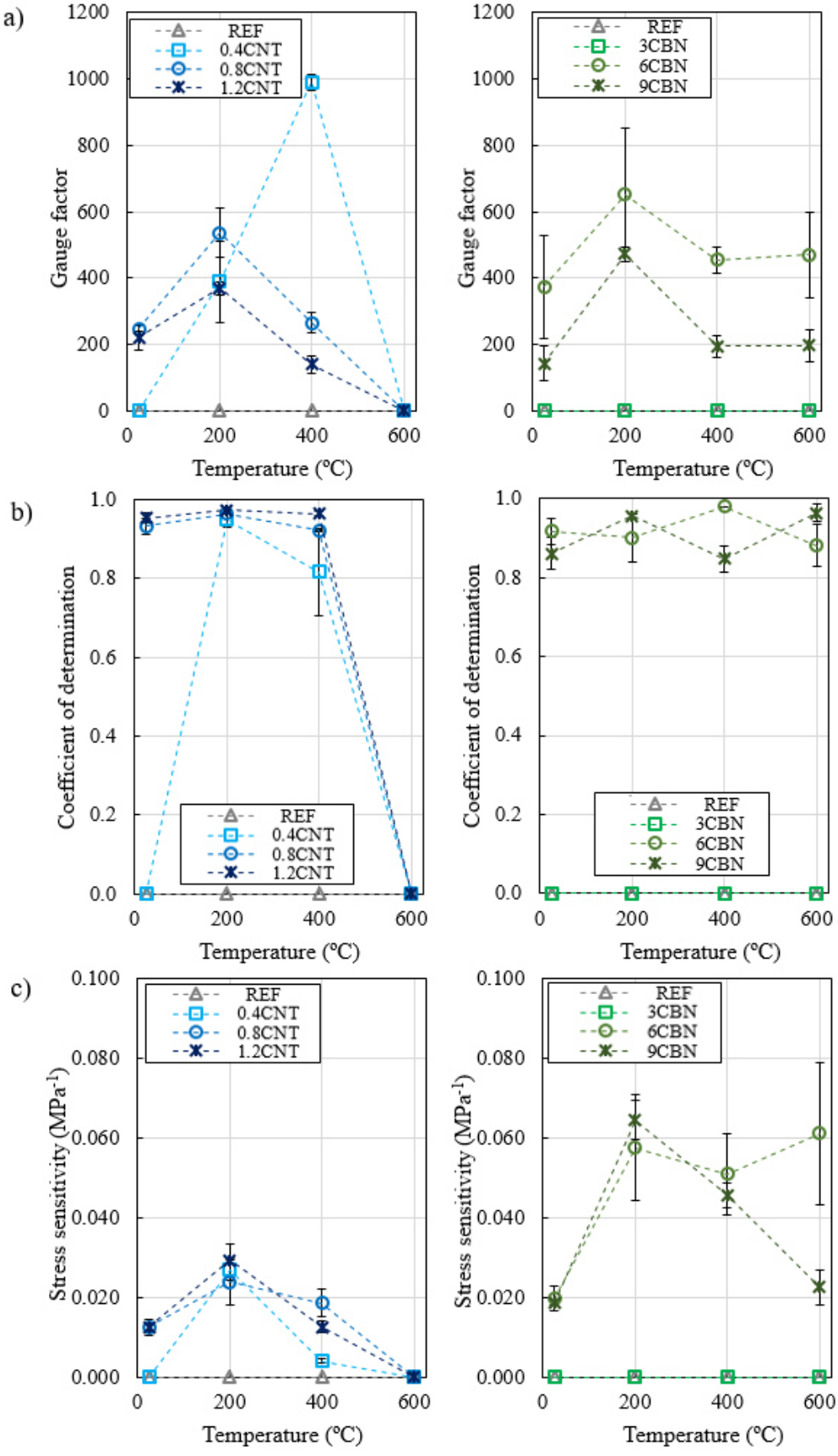

Source: Author (2020)

The residual gauge factor and stress sensitivity seem to be dependent on the maximum exposure temperature, since it causes different changes in the conductive pathways. Series produced with the 0.8CNT, 1.2CNT, 6CBN and 9CBN mortars improved their sensing ability in the range of 25 ºC to 200 ºC. At higher temperatures, their sensing ability decreased. Analyses of variance and post-hoc Tukey's multiple comparison tests at the 5% significance level indicate that the gauge factor of mortars with 9% of CBN did not change after being exposed to temperature of 400 ºC and 600 ºC. High coefficients of determination were obtained for series produced with the 0.8CNT, 1.2CNT, 6CBN and 9CBN mortars in the range between 25 ºC and 400 ºC, which suggests that these composites can be used to estimate the post-fire structural performance if they did not reach temperatures higher than 400 ºC. For 600 ºC, only mortars with 6% of CBN or 9% of CBN presented a piezoresistive response.

4.4. CONCLUSIONS

This work derived the following conclusions:

(1) The influence of the temperature levels of 200 ºC, 400 ºC and 600 ºC on the internal capacitance, residual electrical resistivity and piezoresistive response of composite sensors with CBN and MWCNT were firstly presented and discussed in this work.

(2) Oxidation of carbon nanofillers in cement-based composites due to exposure to high temperatures was investigated through TGA and Raman spectroscopy. These tests revealed that the decomposition of nanofillers inside the composite was significant in series with 0.4%, 0.8% or 1.2% of MWCNT and 3% or 6% of CBN, at temperatures higher than 500 ºC. On the other hand, decomposition of nanofillers was not observed in composites with 9% of CBN, which suggests that the oxygen available inside the pores of the composite decomposed a negligible amount of functional fillers.

(3) Increases of residual electrical resistivity of composites with 9% of CBN exposed to temperatures up to 600 ºC were attributed to increases in porosity and cracking, which suggests that they exhibited an ability of self-detection of damage due to fire exposure.

(4) Cement-based composites with 0.8% of MWCNT, 1.2% of MWCNT or 6% of CBN exhibited a residual self-sensing ability for monitoring deformation in locations of concrete structures exposed to temperatures up to 400 ºC. Cement-based composites with 9% of CBN presented an adequate residual self-sensing ability for structural healthy monitoring of concrete elements exposed to temperatures up to 600 ºC.

REFERENCES

[1] H. CHO, D. LEE, H. JU, H. PARK, H. KIM and K. KIM, "Fire Damage Assessment of Reinforced Concrete Structures Using Fuzzy Theory," *Applied Sciences,* vol. 7, p. 518, 2017.

[2] A. ASEEM, W. BALOCH, R. KHUSHNOOD and A. MUSHTAQ, "Structural health assessment of fire damaged building using non-destructive testing and micro-graphical forensic analysis: A case study," *Case Studies in Construction Materials,* vol. 11, 2019.

[3] T. HA, J. KO, S. LEE, S. KIM, J. JUNG and D. KIM, "A Case Study on the Rehabilitation of a Fire-Damaged Structure," *Applied Sciences,* vol. 6, 2016.

[4] W. DONG, W. LI, Z. TAO and K. WANG, "Piezoresistive properties of cement-based sensors: Review and perspective," *Construction and Building Materials,* vol. 203, p. 146–163, 2019.

[5] S. DING, S. DONG, A. ASHOUR and B. HAN, "Development of sensing concrete: principles, properties and its applications," *Journal of Applied Physics,* p. 126, 2019.

[6] F. UBERTINI, S. LAFLAMME and A. D'ALESSANDRO, "Smart cement paste with carbon nanotubes," in *Innovative Developments of Advanced Multifunctional Nanocomposites in Civil and Structural Engineering*, 2016, pp. 97-120.

[7] B. HAN, S. DING and X. YU, "Intrinsic self-sensing concrete and structures: A review," *Measurement,* vol. 59, pp. 110-128, 2015.

[8] B. HAN, X. YU and J. OU, Self-Sensing Concrete In Smart Structures, Waltham, MA, USA: Elsevier Inc., 2015.

[9] F. AZHARI, Cement-based sensors for structural healthy monitoring, Vancouver, 2008.

[10] R. CHACKO, N. BANTHIA and A. MUFTI, "Carbon-fiber-reinforced cement-based sensors," *Canadian Journal of Civil Engineering,* vol. 34, pp. 284-290, 2007.

[11] A. MONTEIRO, A. LOREDO, P. COSTA and M. C. P. OESER, "A pressure-sensitive carbon black cement composite for traffic monitoring," *Construction and Building Materials,* vol. 154, pp. 1079-1086, 2017.

[12] W. DONG, W. LI, N. LU, F. QU, K. VESSALAS and D. SHENG, "Piezoresistive behaviours of cement-based sensor with carbon black subjected to various temperature and water content," *Composites Part B,* vol. 178, p. 107488, 2019.

[13] E. DEMIRCILIOGLU, E. TEOMETE, E. SCHLANGEN and J. BAEZA, "Temperature and moisture effects on electrical resistance and strain sensitivity of smart concrete," *Construction and Building Materials,* vol. 224, p. 420–427, 2019.

[14] W. BALOCH, R. KHUSHNOOD and W. KHALIQ, "Influence of multi-walled carbon nanotubes on the residual performance of concrete exposed to high temperatures," *Construction and Building Materials,* vol. 185, pp. 44-56, 2018.

[15] W. KHALIQ and V. KODUR, "Effectiveness of Polypropylene and Steel Fibers in Enhancing Fire Resistance of High-Strength Concrete Columns," *Journal of Structural Engineering,* vol. 144, pp. 1-12, 2018.

[16] M. MOHSEN, A. NASSER, K. RASHID, S. AHMED and A. KHALDOON, "Effect of mixing duration on flexural strength of multi walled carbon nanotubes cementitious composites," *Construction and Building Materials,* vol. 126, pp. 586-598, 2016.

[17] H. KIM, I. PARK and H. LEE, "Improved piezoresistive sensitivity and stability of CNT/cement mortar composites with low water–binder ratio," *Composite Structures,* vol. 116, pp. 713-719, 2014.

[18] ABNT, *NBR 13279: Mortars applied on walls and ceilings - Determination of the flexural and the compressive strength in the hardened stage,* Rio de Janeiro, Brazil, 2005.

[19] P. SIKORA, M. ELRAHMAN and D. STEPHAN, "The influence of nanomaterials on the thermal resistance of cement-based composites - A review," *Nanomaterials,* vol. 8, p. 465, 2018.

[20] B. FERNANDES, A. M. GIL, F. L. BOLINA and B. F. TUTIKIAN, "Microstructure of concrete subjected to elevated temperatures: physico-chemical changes and analysis techniques," *IBRACON Structures and Materials Journal,* vol. 10, pp. 838-863, 2017.

[21] S. OSSWALD, M. HAVEL and GOGOTSI, "Monitoring oxidation of multiwalled carbon nanotubes," *Journal of Raman Spectroscopy,* vol. 38, p. 728–736, 2007.

[22] M. PAWLYTA, J. ROUZAUD and S. DUBER, "Raman microspectroscopy characterization of carbon blacks: Spectral analysis and structural information," *Carbon,* vol. 84, pp. 479-490, 2015.

[23] T. AWHARI, A. ROID and J. CASADO, "Raman spectroscopic characterization of some commercially available carbon black materials," *Carbon ,* vol. 33, pp. 1561-1565, 1995.

[24] F. LIU and Z. SUN, "Chemical mapping of cement pastes by using confocal Raman spectroscopy," *Frontiers of Structural and Civil Engineering,* pp. 1-6, 2015.

[25] S. WEN and D. CHUNG, "Electrical-resistance-based damage self-sensing in carbon fiber reinforced cement," *Carbon,* vol. 45, pp. 710-716, 2007.

[26] A. DOWNEY, E. GARCIA-MACIAS, A. D'ALESANDRO, S. LAFLAMME, R. CASTRO-TRIGUERO and F. UBERTINI, "Continuous and embedded solutions for SHM of concrete structures using changing electrical potential in self-sensing cement-based composites," *Nondestructive Characterization and Monitoring of Advanced Materials, Aerospace, and Civil Infrastructure,* vol. 10169, pp. 1-13, 2017.

[27] F. AZHARI and N. BANTHIA, "Cement-based sensors with carbon fibers and carbon nanotubes for piezoresistive sensing," *Cement and Concrete Composites,* vol. 34, pp. 866-873, 2012.

[28] Q. MA, R. GUO, Z. ZHAO, Z. LIN and K. HE, "Mechanical properties of concrete at high temperature - A review," *Construction and Building Materials,* vol. 93, p. 371–383, 2015.

[29] G. WANG, C. ZHANG, B. ZHANG, Q. LI and Z. SHUI, "Study on the high-temperature behavior and rehydration characteristics of hardened cement paste," *Fire and Materials,* vol. 39, p. 741–750, 2014.

CHAPTER 5: EFFECTS OF REHYDRATION ON THE MECHANICAL PROPERTIES OF MORTARS CONTAINING CARBON NANOMATERIALS EXPOSED TO FIRE CONDITIONS

5.1. INTRODUCTION

Cementitious materials undergo a series of transformations in their chemical composition and physical structure when exposed to fire, such as the decomposition of the hydrated cement paste [1-3]. Consequently, high temperatures can cause serious damages to the mechanical properties and durability of concrete structures [1, 4, 5]. From an ecological and economic perspective, repair and rehabilitation of fire-damaged concrete structures may be a good solution, instead of demolishing them [6, 7]. However, many previous studies indicate that cementitious materials exposed to high temperatures can recovery strength and durability without the need of special repairs, if they are properly recured in water or in a moist environment [1, 3, 8-16].

In the rehydration process, dehydrated phases of the fire-damaged material react with water and form new CSH gel and calcium hydroxide [9]. Rehydration increases the degree of silicate polymerization of CSH and improves the reaction between decomposed CaO and silicates, which results in new CSH [13]. In addition, fire opens up the capillaries previously blocked off in the hydrated paste [8]. Then, rehydration of decomposed CSH gel and hydration of unhydrated cement grains provide recovery of mechanical properties [10].

Poon et al. [1] observed significant strength and durability recovery of fire-damaged concrete recured with different methods: while water-recuring provided high rate of rehydration during the first seven days and then slowed down, air-recuring provided a slow and gradual rehydration rate. In addition, concrete exposed to 600 ºC presented higher strength and durability recovery than concrete exposed to 800 ºC, since significant decomposition of the CSH gel only starts at about 550 ºC. Matesová [11] also observed that the recuring of concrete exposed to 600 ºC in a humid environment (relative humidity of 90% ± 10%) during ten months increased its residual compressive strength in about 100%.

Very high strength recovery was also observed in firebrick/slag concrete specimens tested by Sarshar and Khoury [16]. After being exposed to 500 ºC and recured in water and humid environment (relative humidity of 100%) by 90 days, these specimens recovered 90% to 100% of their original strength before heating. Cement pastes previously exposed to

temperatures from 300 ºC to 900 ºC were left by Shui et al. [9] in an environment with relative humidity close to 100%. After a recuring period of 28 days, high rehydration degrees were observed in specimens exposed to temperatures up to 800 ºC. Teixeira [12] evaluated the rehydration of fire-damaged concrete through a combination between a water-recuring process of 24 hours and an air-recuring process of 14 days. He observed significant recovery of compressive strength and modulus of elasticity in specimens exposed to temperatures between 400 ºC and 800 ºC. Suh et al. [13] also highlighted significant mechanical strength recovery of cement pastes exposed to temperature levels between 200 ºC and 500 ºC due to different rehydration conditions, such as air-recuring at relative humidity of 60% and water-recuring after fast or slow cooling. On the other hand, they observed no mechanical recovery after rehydration of cement pastes exposed to temperatures between 800 ºC and 1000 ºC, due to the complete decomposition of CSH.

The addition of different nanomaterials in cementitious matrices has been recently investigated, in order to improve mechanical properties, ductility and durability after fire exposure. Nanoinclusions can provide the refinement of the composite's pore structure, the amplification of the hydration process and the prevention of crack development [4, 17, 18].

Many studies have investigated the rehydration process in ordinary cement pastes, mortars and concretes. However, there is no previous research focused on the evaluation of the effects of rehydration on the mechanical properties of cement-based materials containing carbon nanomaterials exposed to high temperatures. Rehydration effects reported in the literature cannot be generalized for nanomodified cementitious materials, due to their different composition and properties. Therefore, the study reported in this chapter aimed to investigate the influence of rehydration on the microstructure, compressive strength, elastic and dynamic modulus of mortars containing different contents of carbon black nanoparticles (CBN) and multi-walled carbon nanotubes (MWCNT) exposed to high temperatures.

5.2. EXPERIMENTAL METHODS

Materials and mix proportions presented in Section 2.2.2.1 and Section 3.2.1 were used in this study. Mortar cylindrical specimens were produced with the procedures described in Section 3.2.2 and exposed to the heating and cooling regimes defined in Section 3.2.3. After that, fire-damaged mortars were soaked in water for 24 hours and then subjected to air-recuring at temperature of (25 ± 2) ºC and relative humidity of (90 ± 10) % during 27 days. Finally, the specimens were subjected to the experimental test methods listed in Section 3.2.4.

5.3. RESULTS AND DISCUSSION

The values of compressive strength and relative residual strength factors obtained from the experimental tests of this study are shown in Figure 55. These results can be compared to those of Chapter 3 in order to evaluate the compressive strength recovery due to the rehydration process. However, specimens of Chapter 3 were tested at the age of 28 days, while the specimens of the present work were tested at the age of 56 days, due to the 28-days rehydration period described in the previous section.

Figure 55 – Compressive strength and relative residual strength factors of plain mortars and mortars containing a) MWCNT or b) CBN, before and after rehydration

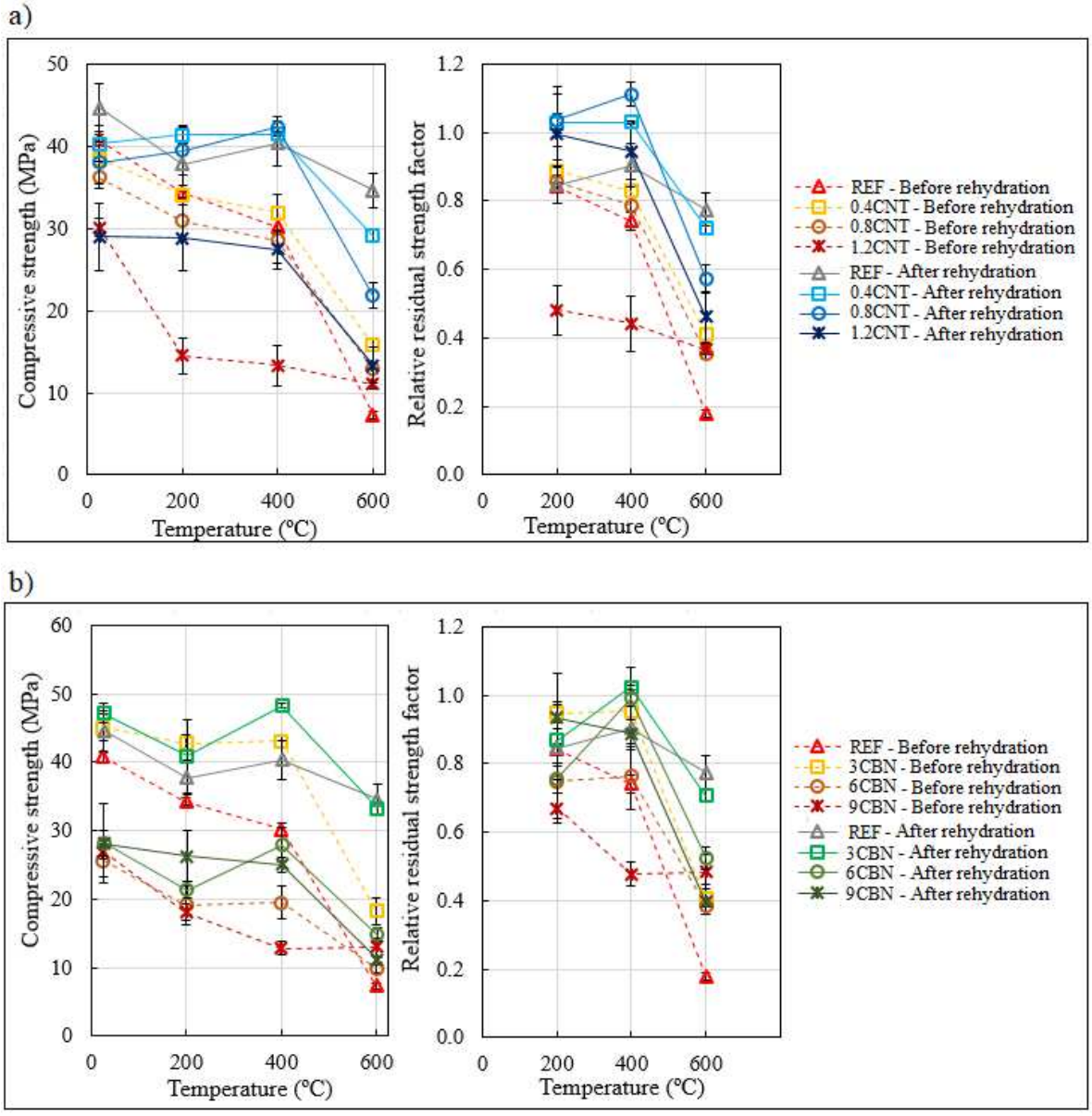

Source: Author (2020)

Before evaluating the effects of rehydration on these parameters, a statistical method was applied to verify the influence of age on the average compressive strength of the mortars that were not exposed to high temperatures. For each kind of mortar, an analysis of variance at the 5% significance level was developed in order to check if the obtained 28-days average strengths are statistically equal to the 56-days average strengths (Table 5). P-values higher than 5% were observed in all these comparisons, which confirms the null hypothesis that the compared averages are statistically equal. Then, it is possible to conclude that the compressive strength of all mortar types did not change significantly after a curing period of 28 days and, consequently, any strength recovery reported in this section can be attributed to the rehydration itself.

Table 5 – P-values obtained from the analyses of variance

Mortar type	Comparison between 28-days and 56-days compressive strength	Comparison between 28-days and 56-days elastic modulus	Comparison between 28-days and 56-days dynamic modulus
0	0.249	0.031	0.904
0.4CNT	0.312	0.269	0.144
0.8CNT	0.410	0.215	0.141
1.2CNT	0.813	0.745	0.224
3CBN	0.294	0.727	0.041
6CBN	0.292	0.076	0.158
9CBN	0.783	0.321	0.873

A regain of strength due to the rehydration process was observed in all specimens. All of the non-rehydrated mortars exposed to 200 ºC presented strength reductions lower than 40% except for mortars with 1.2% of MWCNT, which have a 50% reduction. On the other hand, mortars exposed to 200 ºC and subjected to rehydration presented strength values between 75% and 100% of their original compressive strength. Mortars exposed to 400 ºC lost up to 60% of their original strength. After rehydration, they presented compressive strength values higher than 80% of their initial strength, which proves the efficiency of rehydration for strength recovery. The relative residual strength factors of rehydrated mortars exposed to 400 ºC and containing any kind of nanofiller were greater than that of mortars exposed to 400 ºC without nanofillers. Mortars exposed to 600 ºC presented compressive strength values from 15% to 50% of their original strengths. Rehydration provided strength values between 50% and 80% of the initial ones.

Strength recovery can be attributed to the development of rehydration products shown in SEM images of plain and nanomodified mortars (Figure 41). A densification of the pore

system due to rehydration is observed in all images. As previously observed by Xuan and Shui [3] and Shui et al. [9], the rehydrated structures consist of a rough microstructure morphology resulted from the disordered formation of rehydration products in voids and micro-cracks of the fire-damaged specimens.

Figure 56 – SEM images of plain and nanomodified cementitious matrices exposed to different temperature levels, before and after rehydration

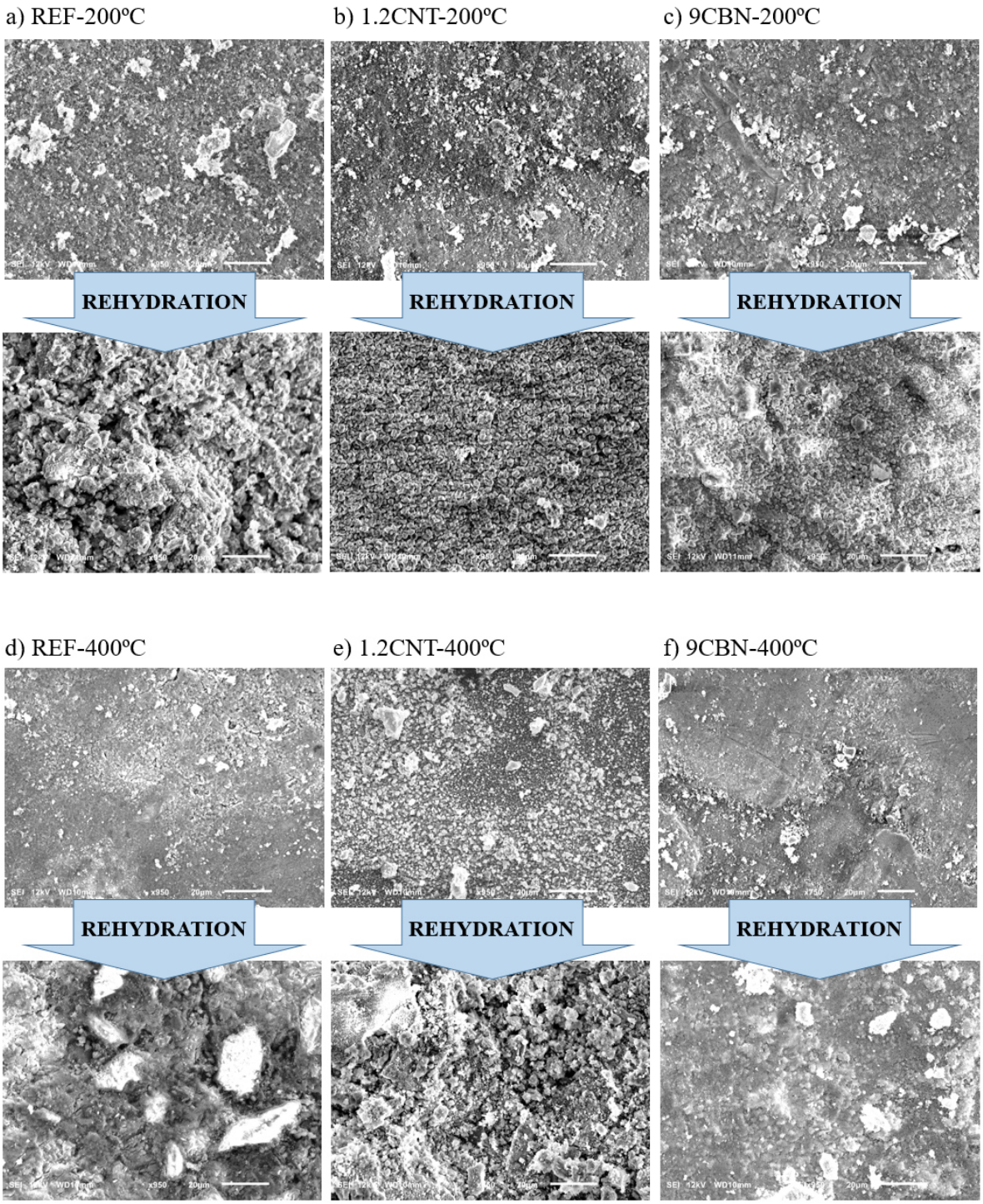

(to be continued)

Figure 57 – SEM images of plain and nanomodified cementitious matrices exposed to different temperature levels, before and after rehydration (continued)

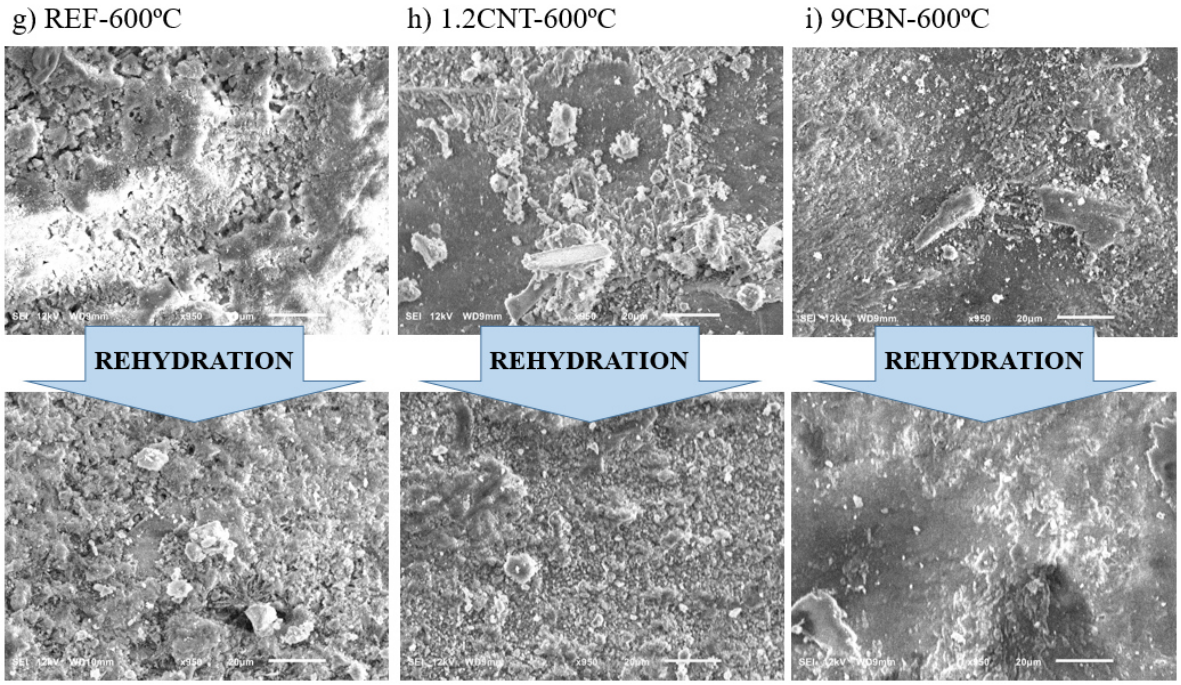

Source: Author (2020)

For exposure temperatures up to 400 ºC, nanomodified mortars presented a strength recovery higher than that observed in mortars without nanofillers (Figure 55). While mortars without nanofillers presented relative residual strength factors of 0.85 - 0.90, mortars with MWCNT and mortars with 3% of CBN presented relative residual strength factors very close to 1.00. It indicates that small contents of nanofillers improved the rehydration process, being responsible for a complete recovery of compressive strength of composites exposed to temperatures up to 400 ºC.

In the technical literature, Zhang et al. [19] and Han et al. [20] observed that water molecules are adsorbed by CBN and MWCNT added to cement-based materials, respectively. The experimental results of this study suggest that the small fraction of water adsorbed by the carbon nanofillers during the 24-hours water-recuring step may have been used later to provide a greater rehydration and strength recovery.

On the other hand, specimens exposed to a temperature of 600 ºC presented relative residual strength factors lower than 0.80, which indicates that most of the CSH decomposition products at about 550 ºC [1] could not be rehydrated by the recuring process proposed in this research. The small fraction of water adsorbed by the carbon nanofillers was not enough to provide a significant improvement of the rehydration of higher amount of CSH decomposition products. In fact, analyses of variance suggested that the residual strength

factors of rehydrated mortars with 0.4% of MWCNT or 3% of CBN previously exposed to 600 ºC are statistically equal to the residual strength factor of mortars without nanofillers exposed to the same conditions (the P-values were 0.213 and 0.130, respectively).

Higher nanofiller concentrations provided residual strength factors even lower in mortars exposed to 600 ºC and then rehydrated. Their residual strength factors are about 50% - 88% of the residual strength factor of mortars without nanofillers exposed to the same conditions. Then, results suggest that high concentrations of nanofillers can make more difficult for water to reach decomposed CSH gel or unhydrated cement grains. Figure 41 shows that rehydration after exposure to 600 ºC provided a more evident pore filling effect in mortars without nanofillers than in mortars with high amount of nanofillers (1.2% of MWCNT and 9% of CBN). SEM images suggest that voids and micro-cracks of mortars without carbon nanofillers were filled by the rehydration products, which resulted in high strength recovery. However, rehydration provided a strength recovery in all mortars exposed to 600 ºC. While their residual strength values were between 18% and 48% of the original ones, rehydration provided strengths between 40% and 78% of the original values.

The influence of temperature and rehydration process on the static and dynamic moduli of elasticity of mortars was also analyzed (Figure 42 and Figure 43, respectively). Analyses of variance at the 5% significance level were run on experimental data of mortars that were not exposed to high temperatures (Table 5), in order to compare their 28-days average modulus of elasticity (shown in Chapter 3) with their 56-days average moduli of elasticity presented in Figure 42 and Figure 43. P-values higher than 5% were observed in most of the comparisons (Table 5), which suggests that significant changes in modulus of elasticity were not statistically observed after a curing period of 28 days. Then, it is possible to assume that any modulus of elasticity recovery reported in this section can be mainly attributed to the rehydration itself. It is important to highlight that the comparison between static moduli of mortars without nanoinclusions and the comparison between dynamic moduli of mortars with 3% of CBN demonstrated a statistical difference between these parameters at the ages of 28 and 56 days (P-values of 0.031 and 0.041, respectively). For instance, mortars with 3% of CBN presented a slight difference between the 28-days and 56-days average dynamic moduli of about 1.4 GPa. However, this difference is about 8 times lower than the maximum reduction of dynamic modulus due to high temperatures and about 6 times lower than its maximum dynamic modulus recovery.

Figure 58 – Static modulus of elasticity and relative residual static modulus factor of rehydrated plain mortars and mortars containing a) MWCNT or b) CBN, before and after rehydration

a)

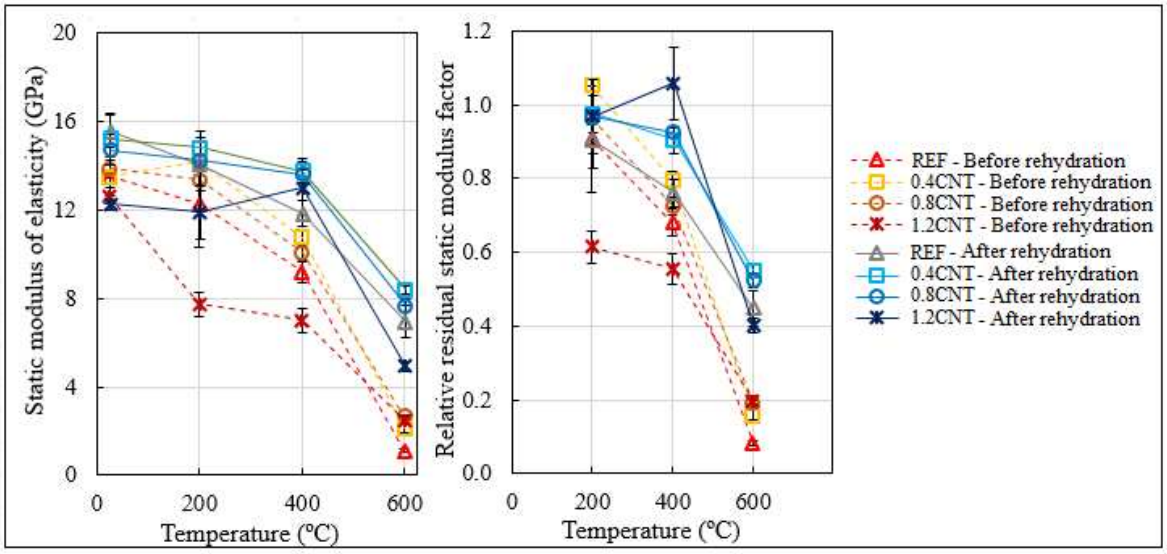

b)

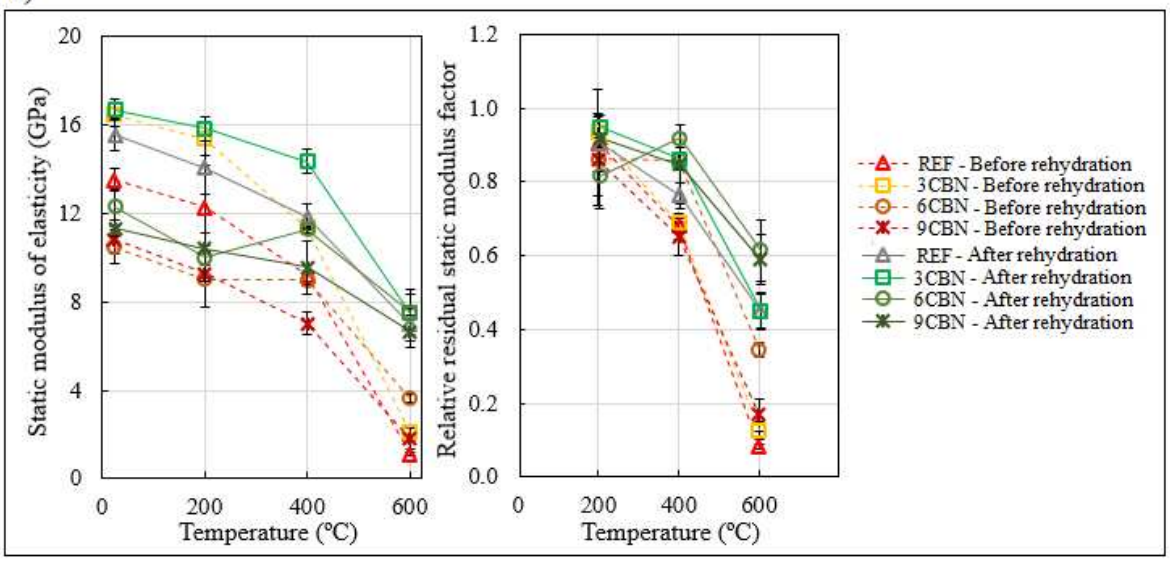

Source: Author (2020)

Figure 59 – Dynamic modulus of elasticity and relative residual dynamic modulus factor of rehydrated plain mortars and mortars containing a) MWCNT or b) CBN, before and after rehydration

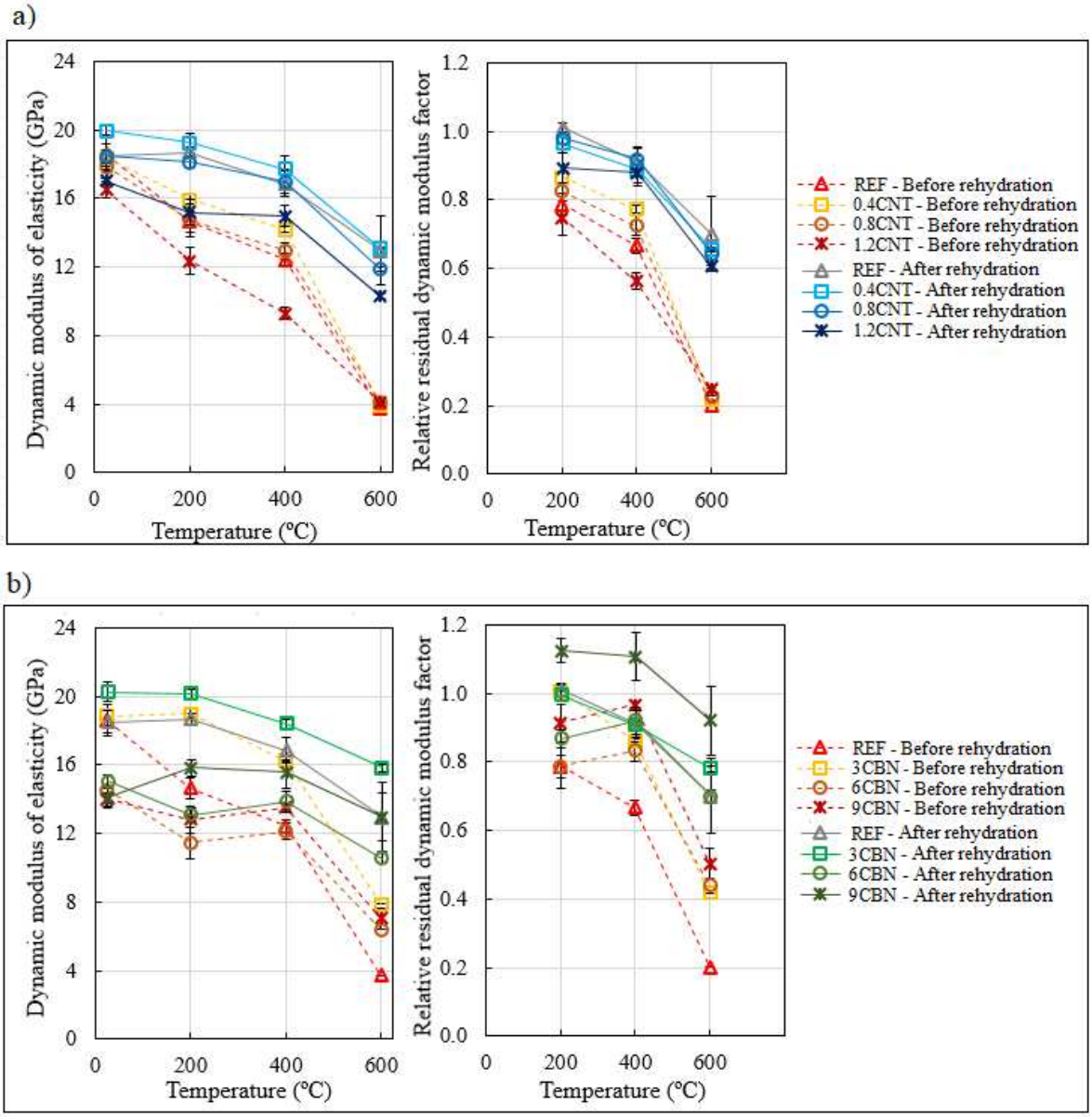

Source: Author (2020)

After exposure to any temperature level and rehydration, mortars with lower concentrations of carbon nanofillers (0.4% of MWCNT or 3% of CBN) presented values of elastic and dynamic moduli up to 15% higher than those of mortars without nanofillers. Despite this, the densification of the pore structure due to rehydration observed in Figure 41 resulted in significant stiffness improvements of any type of fire-damaged mortar.

According to Chapter 3, all mortars exposed to 200 ºC presented static modulus reductions lower than 15% except for mortars with 1.2% of MWCNT, which presented a

reduction of 40%. Reductions of dynamic modulus due to exposure to 200 ºC were lower than 25%. Experimental data presented in Figure 42 indicate that all mortars exposed to 200 ºC presented values of static and dynamic moduli between 90% and 100% of their original static modulus after the rehydration process, which indicates its efficiency for stiffness recovery. Mortars exposed to 400 ºC lost up to 44% of their original stiffness. After rehydration, plain and nanomodified mortars presented modulus of elasticity values greater than 76% and 85% of their original modulus, respectively. Mortars exposed to 600 ºC presented dynamic modulus values between 20% and 50% of their pre-fire dynamic modulus. Rehydration provided dynamic modulus values between 60% and 92% of the original values. An exposure temperature of 600 ºC caused a more severe damage in the static moduli of the mortars, since they assumed values between 8% and 35% of the original ones. After rehydration, they increased for values between 40% and 60% of the original ones.

5.4. CONCLUSION

The results of this research indicated that the structural behavior of nanomodified mortars rehydrated after exposure to high temperatures is different from that of mortars without carbon nanofillers in similar conditions. The main conclusions of this study can be summarized as follows:

(1) A regain of strength, static and dynamic moduli due to the rehydration process was verified in mortars with MWCNT, CBN and without nanofillers. A densification of the pore system due to rehydration was observed in SEM images of all mortars.

(2) The proposed re-curing methodology was able to provide a complete recovery of strength or modulus of elasticity in some composites previously exposed to temperatures up to 400 ºC.

(3) Small fraction of water adsorbed by the carbon nanofillers during the water-recuring process was used later to provide a greater rehydration and strength recovery of mortars exposed to temperatures up to 400 ºC. On the other hand, higher concentrations of carbon nanofillers can make more difficult for water to reach the greater amount of CSH gel decomposed up to 600 ºC.

(4) The best strength and stiffness recovery was observed in mortars with small contents of MWCNT (0.4% by weight of cement) and CBN (3% by weight of cement). In these composites, the rehydration process provided values of compressive strength, static and dynamic moduli higher than 85% of their original ones. After exposure to any

temperature level and rehydration, mortars with lower concentrations of carbon nanofillers presented values of elastic and dynamic moduli up to 15% higher than the values observed in mortars without nanofillers.

REFERENCES

[1] C. POON, S. AZHAR, M. ANSON and Y. WONG, "Strength and durability recovery of fire-damaged concrete after post-fire-curing," *Cement and Concrete Research,* vol. 31, pp. 1307-1318, 2001.

[2] B. FERNANDES, A. M. GIL, F. L. BOLINA and B. F. TUTIKIAN, "Microstructure of concrete subjected to elevated temperatures: physico-chemical changes and analysis techniques," *IBRACON Structures and Materials Journal,* vol. 10, pp. 838-863, 2017.

[3] D. XUAN and Z. SHUI, "Rehydration activity of hydrated cement paste exposed to high temperature," *Fire and materials,* vol. 35, pp. 481-490, 2011.

[4] S. MEMON, S. SHAH, R. KHUSHNOOD and W. BALOCH, "Durability of sustainable concrete subjected to elevated temperature – A Review," *Construction and Building Materials,* vol. 199 , p. 435–455, 2019.

[5] J. OLIVEIRA, J. RIBEIRO, L. PEDROTI, C. FARIA, G. NALON and A. OLIVEIRA JÚNIOR, "Durability of Concrete After Fire Through Accelerated Carbonation Tests," *Materials Research,* vol. 22, p. e20190049, 2019.

[6] H. CHO, D. LEE, H. JU, H. PARK, H. KIM and K. KIM, "Fire Damage Assessment of Reinforced Concrete Structures Using Fuzzy Theory," *Applied Sciences,* vol. 7, p. 518, 2017.

[7] T. HA, J. KO, S. LEE, S. KIM, J. JUNG and D. KIM, "A Case Study on the Rehabilitation of a Fire-Damaged Structure," *Applied Sciences,* vol. 6, 2016.

[8] D. CROOK and M. MURRAY, "Regain of strength after firing of concrete," *Magazine of Concrete Research,* vol. 22, p. 149–154, 1970.

[9] Z. SHUI, D. XUAN, W. CHEN, R. YU and R. ZHANG, "Cementitious characteristics of hydrated cement paste subjected to various dehydration temperatures," *Construction and Building Materials,* vol. 23, pp. 531-537, 2009.

[10] G. KHOURY, "Compressive strength of concrete at high temperatures: a reassessment," *Magazine of Concrete Research,* vol. 44, pp. 291-309, 1992.

[11] D. MATESOVÁ, "Effect of exposure time after heating and w/c ratio on residual strength concrete: pilot studies," in *XI International Conference on Ecology and New Building Materials and Products*, Czech Republic, 2007.

[12] G. TEIXEIRA, Análise experimental da resistência e do módulo de elasticidade pós incêndio de concretos com agregados da região de Viçosa-MG, Viçosa: M.S. Thesis, Department of Civil Engineering, Federal University of Viçosa, 2018.

[13] H. SUH, H. JEE, J. KIM, R. KITAGAKI, S. OHKI and S. WOOE, "Influences of rehydration conditions on the mechanical and atomic structural recovery characteristics of Portland cement paste exposed to elevated temperatures," *Construction and Building Materials,* vol. 235, p. 117453, 2020.

[14] G. WANG, C. ZHANG, B. ZHANG, Q. LI and Z. SHUI, "Study on the high-temperature behavior and rehydration characteristics of hardened cement paste," *Fire and Materials,* vol. 39, p. 741–750, 2014.

[15] M. FARAGE, J. SERCOMBE and C. GALLÉ, "Rehydration and microstructure of cement paste after heating at temperatures up to 300 °C," *Cement and Concrete Research,* vol. 33, p. 1047–1056, 2003.

[16] R. SARSHAR and G. KHOURY, "Material and environmental factors influencing the compressive strength of unsealed cement paste and concrete at high temperatures," *Magazine of Concrete Research,* vol. 45, p. 51–61, 1993.

[17] W. BALOCH, R. KHUSHNOOD and W. KHALIQ, "Influence of multi-walled carbon nanotubes on the residual performance of concrete exposed to high temperatures," *Construction and Building Materials,* vol. 185, no. Waqas Latif Baloch, Rao Arsalan Khushnood, Wasim Khaliq, p. 44–56, 2018.

[18] P. SIKORA, M. ELRAHMAN and D. STEPHAN, "The influence of nanomaterials on the thermal resistance of cement-based composites - A review," *Nanomaterials,* vol. 8, p. 465, 2018.

[19] L. ZHANG, M. KAI and K. LIEW, "Evaluation of microstructure and mechanical performance of CNT-reinforced cementitious composites at elevated temperatures," *Composites Part A: Applied Science and Manufacturing,* vol. 95, p. 286–293, 2017.

[20] B. HAN, X. YU and J. OU, "Effect of water content on the piezoresistivity of MWNT/cement," *Journal of Materials Science,* vol. 45, p. 3714–3719, 2010.

CHAPTER 6: EFFECTS OF REHYDRATION ON THE PIEZORESISTIVE PROPERTIES OF MORTARS CONTAINING CARBON NANOMATERIALS EXPOSED TO FIRE CONDITIONS

6.1. INTRODUCTION

High temperatures cause changes in the chemical composition and physical structure of cement paste and aggregates that lead to a deterioration of the mechanical properties of the material [1-4]. Cracking, porosity and average pore diameter of cementitious materials increase with temperature exposure [5]. Cracking at high temperatures is related to different factors, such as spalling due to high pore vapor pressure or thermal gradient, decomposition of hydration products, shrinkage of cement matrix and expansion of aggregates [6].

Rehydration has been proposed by different studies as an efficient alternative for regain of strength, stiffness and durability of fire-damaged cementitious materials [1, 5, 7-15]. Even in the case of a severe fire, water and air-recuring methods promise significant recovery of mechanical properties and extension of the service life of concrete structures. Rehydration of decomposed CSH gel and hydration of unhydrated cement grains are the main responsible for this recovery [10]. Then, instead of being demolished, fire-damaged concrete elements can be rehydrated.

The reuse of fire-damaged buildings requires a precise diagnosis of the performance of their rehydrated structural elements. The diagnosis of residual structural performance can be investigated through visual inspections, non-destructive tests, material sample analyses and microstructural evaluations [16-18]. Traditional SHM devices can also be used to this proposal, but they have some drawbacks, such as limited durability and robustness, low sensitivity, low anti-electromagnetic interference, high error for long-term measuring, high cost, among others [19-21]. In addition, the compact morphology of cement-based materials prevents the monitoring of the crack sealing process in some susceptible-to-cracking areas [22].

The incorporation of conductive nanofillers in cementitious matrices allowed the creation of cement-based materials with intrinsic abilities of strain monitoring and damage detection [23-26]. Chapter 4 presented the development of innovative smart cement-based composites for assessment of damage and residual structural performance after exposure to high temperatures. In this chapter, another experimental program was elaborated in order to

create a smart mortar able to evaluate the rehydration activity in key locations of fire-damaged concrete elements. Then, this study aimed to evaluate the self-sensing ability of mortars with carbon black nanoparticles (CBN) or multi-walled carbon nanotubes (MWCNT) exposed to temperatures of 200 ºC, 400 ºC and 600 ºC and subjected to a rehydration process. It presents some initial findings that can be used for a future application of these smart materials to monitor the effectiveness of a rehydration process for damage recovery, cracking sealing and stiffness regain of fire-damaged concrete elements.

6.2. EXPERIMENTAL METHODS

Materials and mix proportions presented in Section 2.2.2.1 and Section 3.2.1 were used in this experimental program. Prismatic mortar specimens were produced according to the steps of Section 4.2 and exposed to the heating and cooling regimes presented in Section 3.2.3.

After that, all fire-damaged specimens were soaked in water for 24 hours and then subjected to air-recuring at temperature of (25 ± 2) ºC and relative humidity of (90 ± 10) % during a period of 27 days. Finally, they were subjected to the experimental tests listed in Section 4.2.

6.3. RESULTS AND DISCUSSION

The values of U_{comp}/i measured during DC tests are exposed in Figure 60, Figure 61, Figure 62 and Figure 63. Very high values (10^5 - 10^6 V/A) were observed in rehydrated mortars without carbon nanomaterials and with 3% of CBN. This behavior is typically observed in the insulation zone, in which the filler concentration is much lower than the percolation threshold [26, 27]. High U_{comp}/i values were also observed in all rehydrated mortars subjected to a temperature level of 600 ºC, except those with 6% and 9% of CBN.

As previously discussed in Chapter 4, a mutual analysis of Raman maps of samples of fire-damaged mortars and TGA curves of the nanomaterials suggested that the oxygen available in the pores of the composites was enough to cause oxidation of lower concentrations of nanoinclusions at about 500 ºC. Consequently, only rehydrated specimens with higher contents of carbon nanofillers (6% and 9% of CBN) exhibited electronic conduction and lower U_{comp}/i values after exposure to 600 ºC.

Figure 60 – U_{comp}/i ratios vs. time curves of DC tests of mortars that were not exposed to high temperatures

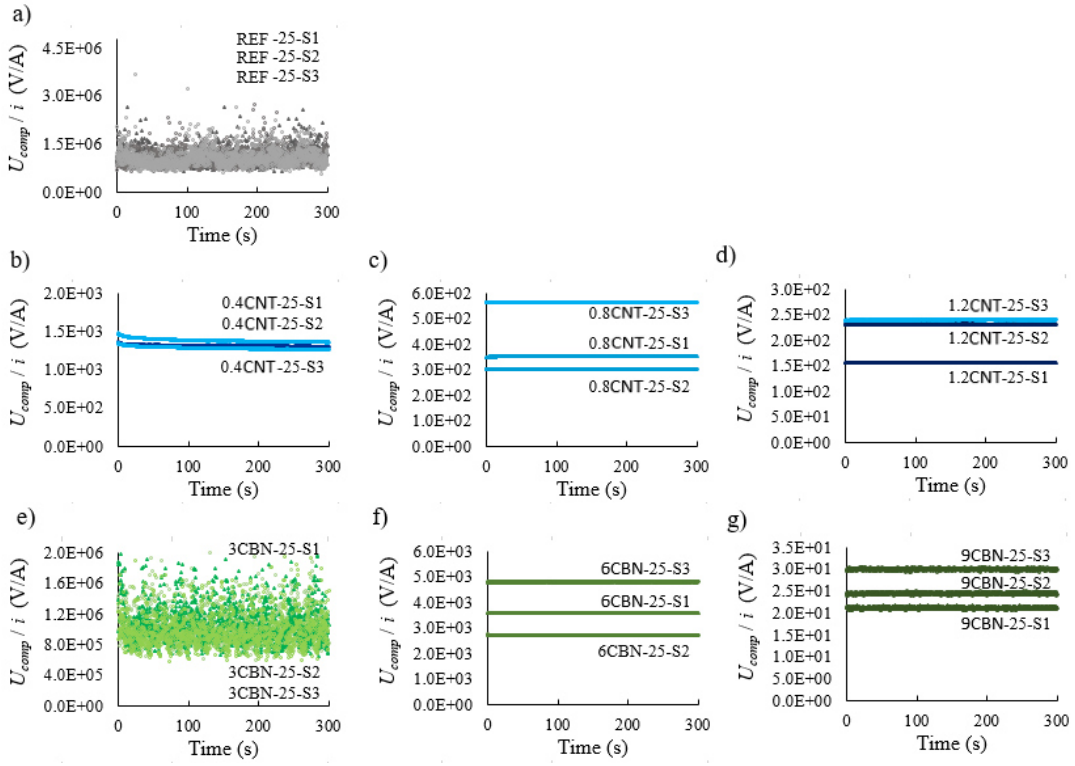

Source: Author (2020)

Figure 61 – U_{comp}/i ratios vs. time curves of DC tests of mortars exposed to 200 ºC

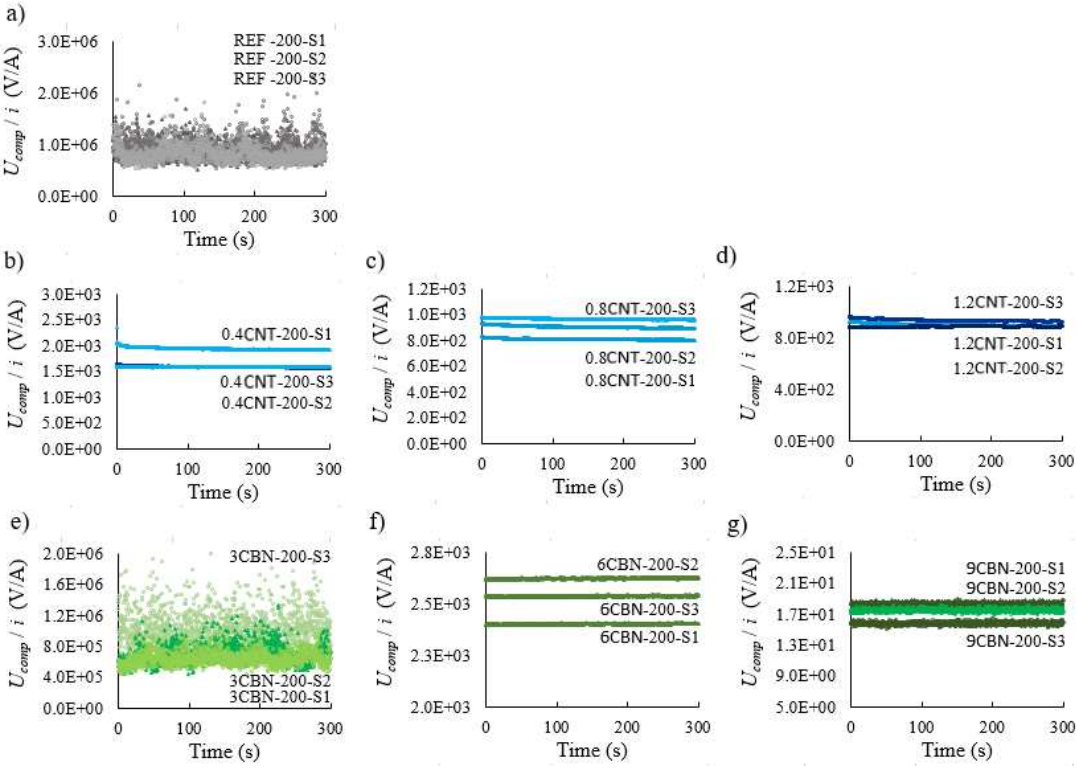

Source: Author (2020)

Figure 62 – U_{comp}/i ratios vs. time curves of DC tests of mortars exposed to 400 ºC

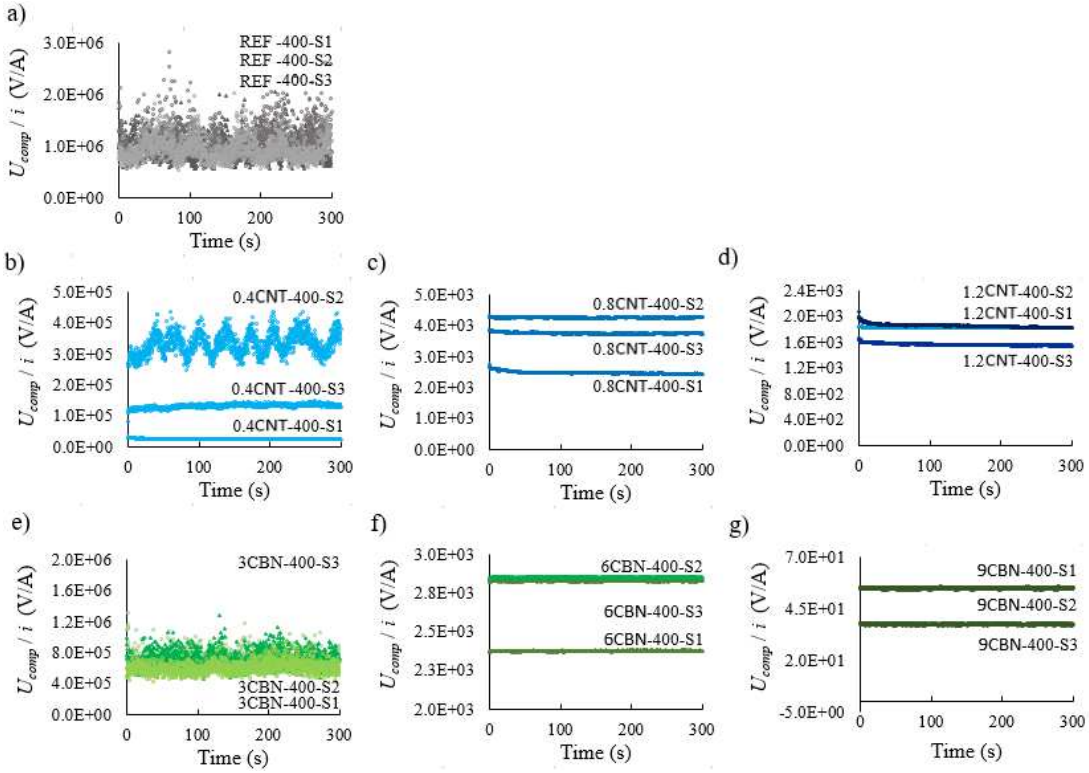

Source: Author (2020)

Figure 63 – U_{comp}/i ratios vs. time curves of DC tests of mortars exposed to 600 ºC

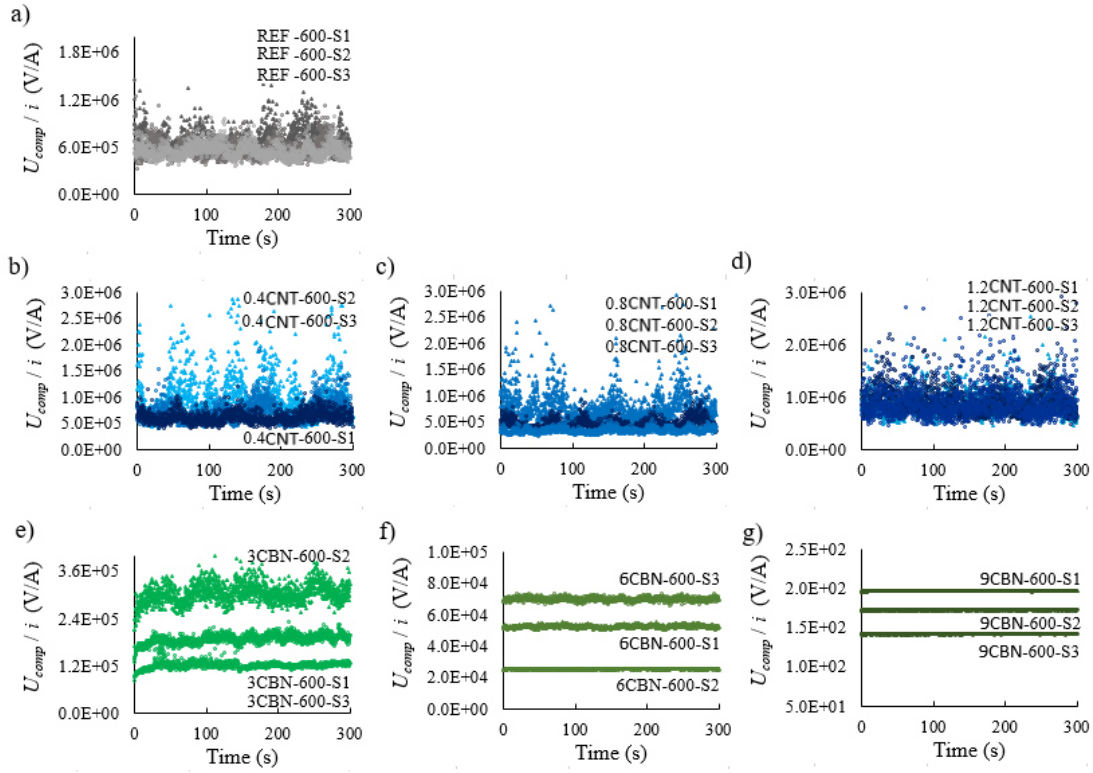

Source: Author (2020)

Composites with 0.4% of MWCNT that were not exposed to high temperatures exhibited changes in electrical current over time in DC tests, which are related to a slight capacitive behavior. Results of Chapter 4 indicated that temperatures higher than 200 ºC were able to eliminate this slight internal capacitance due to loss of CSH interlayer water. After rehydration, all fire-damaged composites presented a reasonable constant U_{comp}/i value in DC tests. It suggests that water molecules that filled mortar pores during the recuring process did not reach the interlayer space within the CSH structure that remained after heating.

The electrical resistivity determined through DC and biphasic DC methods is shown in Figure 64. The incorporation of higher concentrations of carbon nanofillers (9% of CBN or 1.2% of MWCNT) provided a sharp decrease in the mortars' electrical resistivity.

Figure 64 – Electrical resistivity of rehydrated mortars with CBN and MWCNT determined through a) DC and b) biphasic DC methods.

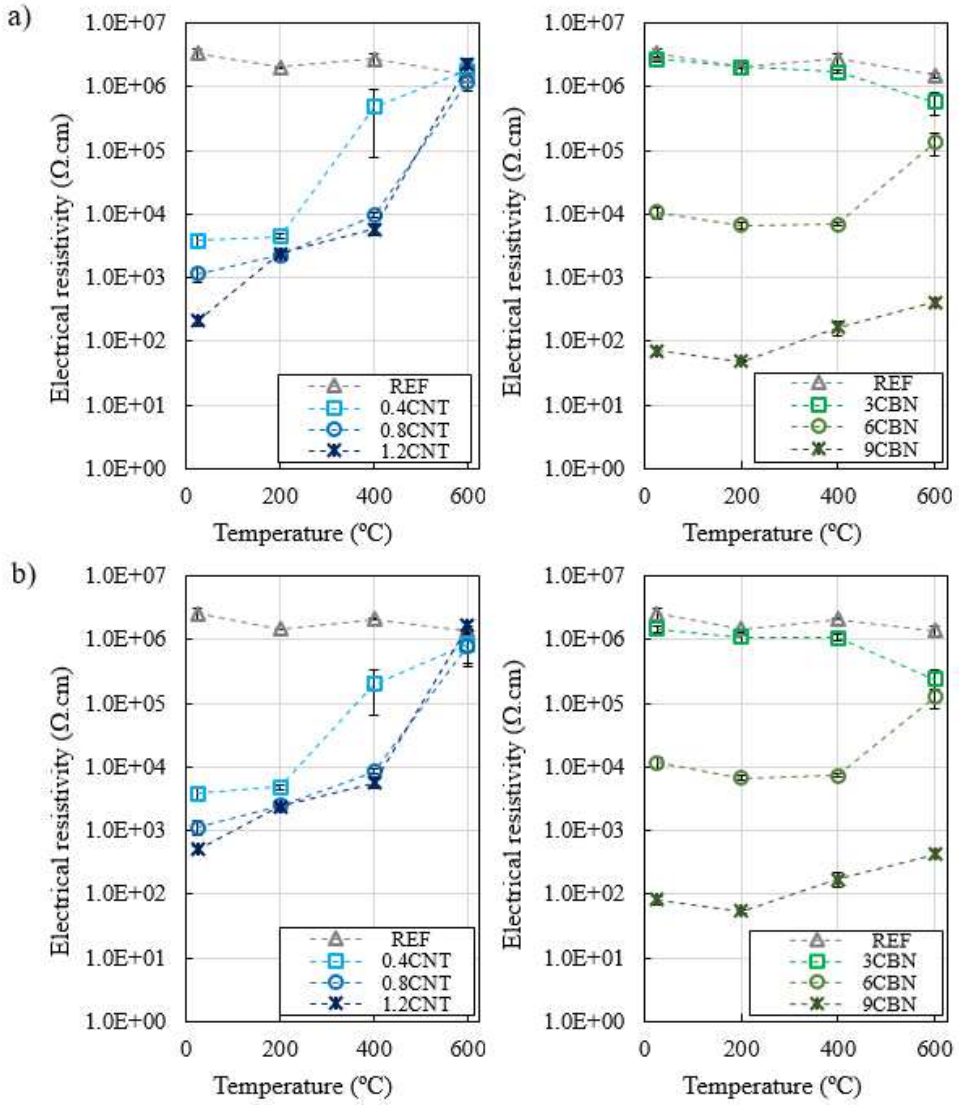

Source: Author (2020)

Analyses of variance and post-hoc Tukey's multiple comparison tests (at 5% of significance level) indicated that the increase of the temperature from 25 ºC to 400 ºC did not change the biphasic DC electrical resistivity of rehydrated mortars with 0.8% of MWCNT, 1.2% of MWCNT, 6% of CBN and 9% of CBN, while their exposure to 600 ºC did. On the other hand, a similar statistical analysis indicated that the electrical resistivity of mortars with 0.4% of MWCNT starts to change at the exposure temperature of 400 ºC and this change is amplified at 600 ºC. A similar behavior was described in Chapter 4, which indicates that rehydrated and non-rehydrated specimens exhibited exactly the same behavior pattern.

When the temperature increased from 400 ºC to 600 ºC, significant increases of electrical resistivity was verified in rehydrated mortars with 0.4% of MWCNT, 0.8% of MWCNT, 1.2% of MWCNT or 6% of CBN. Raman maps of samples of fire-damaged mortars and TGA curves of the nanomaterials presented in Chapter 4 suggested that this increase is related to the oxidation of the lower contents of carbon nanofillers at about 500 ºC. In contrast, Raman maps suggested that mortars with 9% of CBN kept the same amount of nanofillers after exposure to 600 ºC, since the oxygen available inside the pores oxidized a negligible amount of nanoparticles.

There are some differences between the biphasic DC electrical resistivity of fire-damaged conductive composites tested in this research (after rehydration) and those obtained in Chapter 4 (before rehydration), which are presented in Figure 65. Raman maps suggest that these variations are mostly related to a damage recovery in mortars with 0.4% of MWCNT, 0.8% of MWCNT, 1.2% of MWCNT or 6% of CBN exposed to temperatures from 25 ºC to 400 ºC, and in mortars with 9% of CBN exposed to temperatures from 25 ºC to 600 ºC.

The general trend observed in Figure 65 was an increase of electrical resistivity of fire-damaged mortars due to the rehydration process. In Chapter 4, increases of electrical resistivity of smart cementitious composites due to the increase of the exposure temperature were reported. The increases were attributed to interruptions of conductive pathways due to the increase of average pore diameter and cracking at high temperatures. Results reported in Chapter 5 indicated that the recuring of fire-damaged composites provided a rehydration of decomposed CSH gel and hydration of unhydrated cement grains. Therefore, the rehydration process filled pores and sealed cracks with new non-conductive crystalline hydration products. The densification of the pore system with non-conductive rehydration products caused the increases in electrical resistivity presented in Figure 65.

Figure 65 – Effects of rehydration on the biphasic DC electrical resistivity of conductive composites containing a) 9% of CBN, b) 6% of CBN, c) 1.2% of MWCNT, d) 0.8% of MWCNT and e) 0.4% of MWCNT.

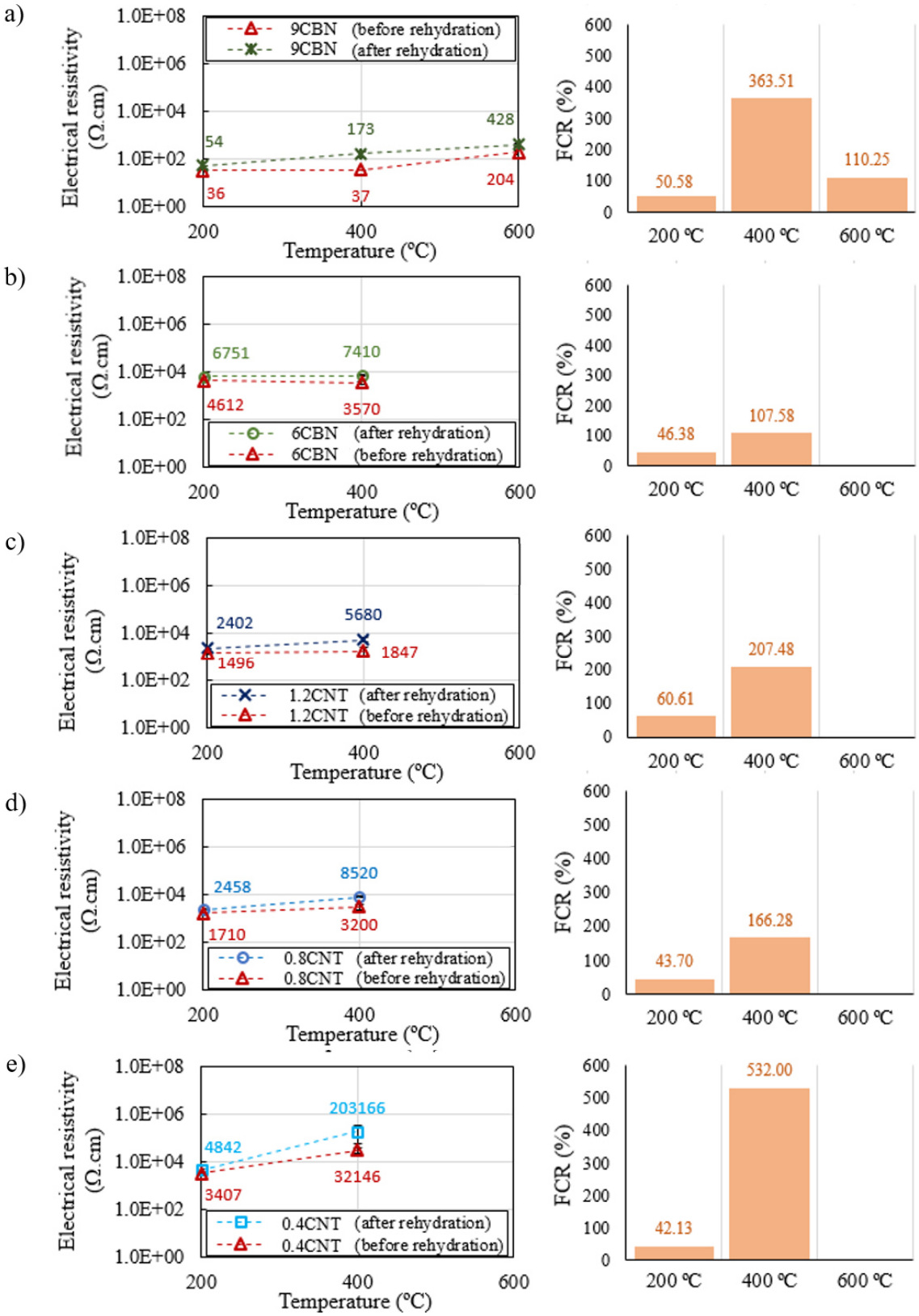

Source: Author (2020)

Mortars with 9% of CBN exposed to 400 ºC (Figure 65a) presented a fractional change in electrical resistivity (FCR) after rehydration (363.51 %) higher than that observed in rehydrated mortars with 9% of CBN exposed to 200 ºC (50.58 %) or 600 ºC (110.25 %). It suggests that the rehydration activity was greater in composites exposed to 400 ºC. In fact, results of Chapters 3 and 5 indicated that the highest strength recovery of mortars with 9% of CBN was observed in specimens exposed to 400 ºC (compressive strength of rehydrated mortars with 9% of CBN exposed to 400 ºC was 94.4% higher than that of non-rehydrated mortars exposed to the same temperature). Lower fractional change of electrical resistivity due to rehydration was observed in mortars with 9% of CBN exposed to 600 ºC (110.25 %). It is in accordance with the low relative residual strength factors obtained in Chapter 5 for composites exposed to 600 ºC, which suggested that most of the products of the CSH decomposition at about 550 ºC [1] could not be rehydrated by the recuring process.

In mortars with 0.4% of MWCNT, 0.8% of MWCNT, 1.2% of MWCNT or 6% of CBN, the fractional change of electrical resistivity due to rehydration was also higher in composites exposed to 400 ºC than in composites exposed to 200 ºC. It also agrees with results reported in Chapters 3 and 5, which show that rehydration provided a higher percentage increase of compressive strength in composites exposed to 400 ºC than in composites exposed to 200 ºC. Then, it is possible to infer that these smart composites were able to detect damage recovery.

The piezoresistive response and FCR vs. strain curves of the rehydrated mortars are presented in APPENDIX B. As expected, no piezoresistive response was observed in plain mortars and mortars with 3% of CBN. In addition, piezoresistivity was not verified in mortars with MWCNT exposed to 600 ºC. It happened because the remaining amount of carbon nanofillers in their cementitious matrix was below the percolation threshold.

In contrast, all the other rehydrated composites presented some piezoresistive response, no matter the temperature exposure. For these composites, linear equations that determine a relationship between FCR and strain were created through regression analyses with zero intercept. Their coefficients of determination R^2 were also calculated. The angular coefficients of these equations were taken as the gauge factors of the specimens. Two distinct regions with different gauge factors were observed in mortars exposed to 400 ºC. Consequently, two distinct models were necessary to define a good relationship between FCR and strain in these cases. The gauge factor, coefficient of determination and stress sensitivity of these series of rehydrated mortars are shown in Figure 66.

Figure 66 – a) Gauge factor, b) coefficient of determination and c) stress sensitivity of rehydrated mortars

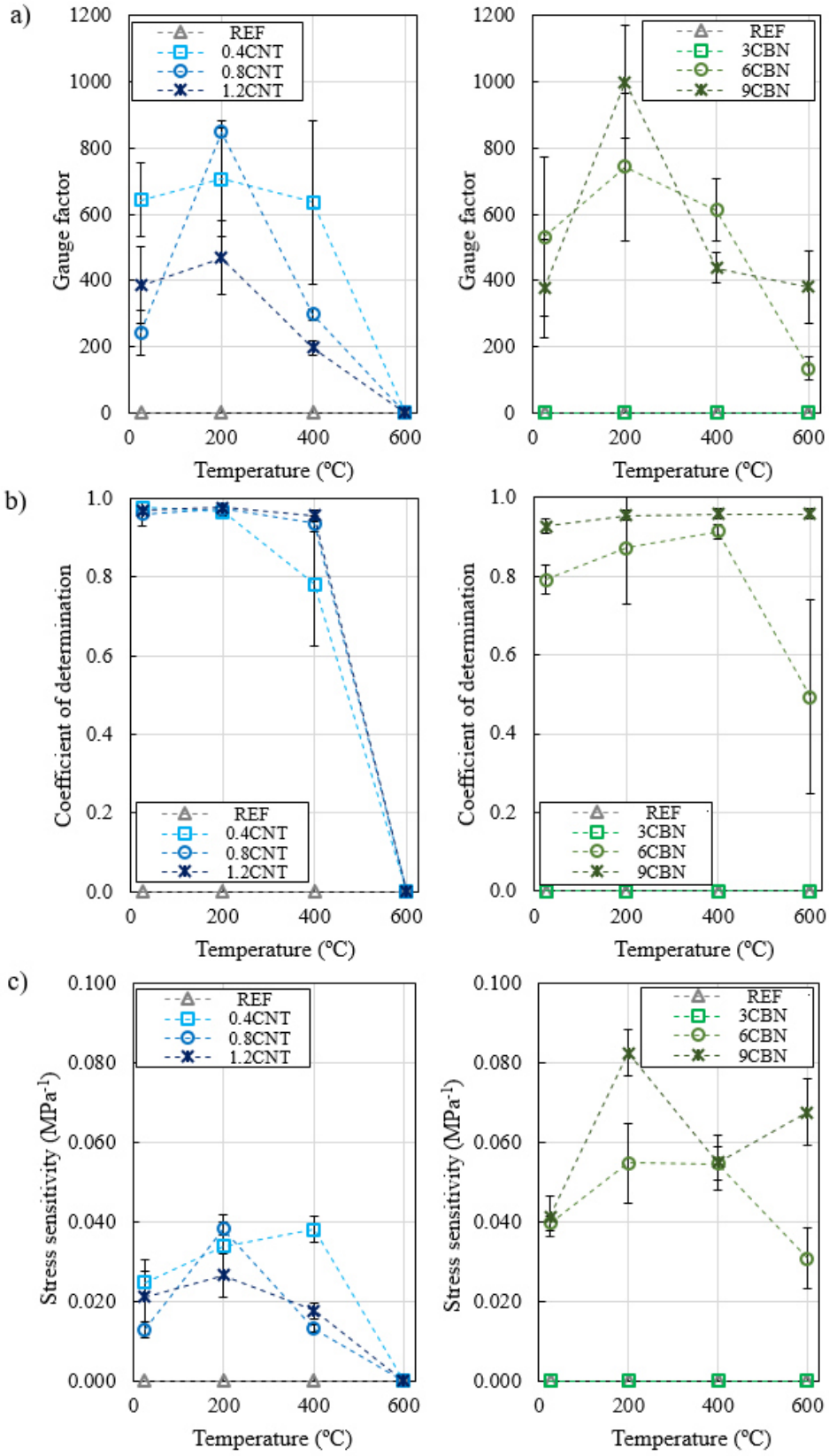

Source: Author (2020)

As previously observed in Chapter 4, the residual gauge factor and stress sensitivity change with maximum exposure temperature. Again, series with 6% of CBN, 9% of CBN, 0.8% of MWCNT and 1.2% of MWCNT presented a maximum gauge factor and stress sensitivity after exposure to 200 ºC.

At higher temperatures, the sensing ability of most of the specimens decreased. However, analyses of variance and post-hoc Tukey's multiple comparison tests at the 5% of significance level suggest that the gauge factors of rehydrated mortars with 9% of CBN exposed to 400 ºC and 600 ºC are the same. All composites exposed to temperatures from 25 ºC to 400 ºC presented high coefficients of determination R^2. Then, they can be successfully used to estimate the post-fire structural performance of sections of concrete elements that did not reach temperatures higher than 400 ºC.

The rehydration process also caused changes in the sensing properties of the composites. The general trend was an increase of gauge factor and stress sensibility with the rehydration process. It happens because the non-conductive crystalline products filled pores, sealed cracks and obstructed some stretches of the conductive network inside the composite. It increased the amount of tunneling gaps and enhanced tunneling or field-emission effect conduction instead of contacting conduction. Consequently, the electrical resistivity of rehydrated composites is easier to be changed by compressive loading.

6.4. CONCLUSIONS

The following conclusions can be drawn from the results presented in this research:

(1) Effects of temperature exposures of 200 ºC, 400 ºC and 600 ºC and rehydration process on the internal capacitance, electrical resistivity and piezoresistive behavior of cement-based sensors with CBN or MWCNT were firstly reported and analyzed.

(2) Increases in electrical resistivity were caused by the rehydration process of fire-damaged composites, since it filled pores and sealed cracks with new non-conductive crystalline hydration products, providing a densification of the pore system.

(3) After being exposed to temperatures up to 600 ºC and subjected to rehydration during 28 days, cement-based composites with 9% of CBN demonstrated an interesting ability of self-detection of damage recovery. Cement-based composites with 0.4%, 0.8% or 1.2% of MWCNT or 6% of CBN exposed to temperatures up to 400 ºC and subjected to rehydration exhibited the same ability.

(4) Rehydrated mortars with 0.8% or 1.2% of MWCNT presented a residual self-sensing ability for monitoring deformation in structures exposed to temperatures up to 400 ºC, while rehydrated mortars with 9% of CBN exhibited an adequate residual self-sensing ability for monitoring deformation in structures exposed to temperatures up to 600 ºC.

(5) An increase of gauge factor and stress sensitivity due to the rehydration process was observed in mortars with higher contents of CBN or MWCNT exposed to high temperatures. Non-conductive crystalline rehydration products filled pores, sealed cracks and obstructed some stretches of the conductive network inside the composite, which suggests improvements of tunneling or field-emission effect conduction instead of contacting conduction. Consequently, the electrical resistivity of rehydrated composites is easier to be changed by compressive loading.

REFERENCES

[1] C. POON, S. AZHAR, M. ANSON and Y. WONG, "Strength and durability recovery of fire-damaged concrete after post-fire-curing," *Cement and Concrete Research,* vol. 31, pp. 1307-1318, 2001.

[2] B. FERNANDES, A. M. GIL, F. L. BOLINA and B. F. TUTIKIAN, "Microstructure of concrete subjected to elevated temperatures: physico-chemical changes and analysis techniques," *IBRACON Structures and Materials Journal,* vol. 10, pp. 838-863, 2017.

[3] D. XUAN and Z. SHUI, "Rehydration activity of hydrated cement paste exposed to high temperature," *Fire and materials,* vol. 35, pp. 481-490, 2011.

[4] S. MEMON, S. SHAH, R. KHUSHNOOD and W. BALOCH, "Durability of sustainable concrete subjected to elevated temperature – A Review," *Construction and Building Materials,* vol. 199 , p. 435–455, 2019.

[5] J. OLIVEIRA, J. RIBEIRO, L. PEDROTI, C. FARIA, G. NALON and A. OLIVEIRA JÚNIOR, "Durability of Concrete After Fire Through Accelerated Carbonation Tests," *Materials Research,* vol. 22, p. e20190049, 2019.

[6] H. CHO, D. LEE, H. JU, H. PARK, H. KIM and K. KIM, "Fire Damage Assessment of Reinforced Concrete Structures Using Fuzzy Theory," *Applied Sciences,* vol. 7, p. 518, 2017.

[7] T. HA, J. KO, S. LEE, S. KIM, J. JUNG and D. KIM, "A Case Study on the Rehabilitation of a Fire-Damaged Structure," *Applied Sciences,* vol. 6, 2016.

[8] D. CROOK and M. MURRAY, "Regain of strength after firing of concrete," *Magazine of Concrete Research,* vol. 22, p. 149–154, 1970.

[9] Z. SHUI, D. XUAN, W. CHEN, R. YU and R. ZHANG, "Cementitious characteristics of hydrated cement paste subjected to various dehydration temperatures," *Construction and Building Materials,* vol. 23, pp. 531-537, 2009.

[10] G. KHOURY, "Compressive strength of concrete at high temperatures: a reassessment," *Magazine of Concrete Research,* vol. 44, pp. 291-309, 1992.

[11] D. MATESOVÁ, "Effect of exposure time after heating and w/c ratio on residual strength concrete: pilot studies," in *XI International Conference on Ecology and New Building Materials and Products*, Czech Republic, 2007.

[12] G. TEIXEIRA, Análise experimental da resistência e do módulo de elasticidade pós incêndio de concretos com agregados da região de Viçosa-MG, Viçosa: M.S. Thesis, Department of Civil Engineering, Federal University of Viçosa, 2018.

[13] H. SUH, H. JEE, J. KIM, R. KITAGAKI, S. OHKI and S. WOOE, "Influences of rehydration conditions on the mechanical and atomic structural recovery characteristics of Portland cement paste exposed to elevated temperatures," *Construction and Building Materials,* vol. 235, p. 117453, 2020.

[14] G. WANG, C. ZHANG, B. ZHANG, Q. LI and Z. SHUI, "Study on the high-temperature behavior and rehydration characteristics of hardened cement paste," *Fire and Materials,* vol. 39, p. 741–750, 2014.

[15] M. FARAGE, J. SERCOMBE and C. GALLÉ, "Rehydration and microstructure of cement paste after heating at temperatures up to 300 °C," *Cement and Concrete Research,* vol. 33, p. 1047–1056, 2003.

[16] R. SARSHAR and G. KHOURY, "Material and environmental factors influencing the compressive strength of unsealed cement paste and concrete at high temperatures," *Magazine of Concrete Research,* vol. 45, p. 51–61, 1993.

[17] W. BALOCH, R. KHUSHNOOD and W. KHALIQ, "Influence of multi-walled carbon nanotubes on the residual performance of concrete exposed to high temperatures," *Construction and Building Materials,* vol. 185, no. Waqas Latif Baloch, Rao Arsalan Khushnood, Wasim Khaliq, p. 44–56, 2018.

[18] P. SIKORA, M. ELRAHMAN and D. STEPHAN, "The influence of nanomaterials on the thermal resistance of cement-based composites - A review," *Nanomaterials,* vol. 8, p. 465, 2018.

[19] L. ZHANG, M. KAI and K. LIEW, "Evaluation of microstructure and mechanical performance of CNT-reinforced cementitious composites at elevated temperatures," *Composites Part A: Applied Science and Manufacturing,* vol. 95, p. 286–293, 2017.

[20] B. HAN, X. YU and J. OU, "Effect of water content on the piezoresistivity of MWNT/cement," *Journal of Materials Science,* vol. 45, p. 3714–3719, 2010.

CHAPTER 7: GENERAL CONCLUSIONS

7.1. CONCLUDING REMARKS

The preliminary studies developed in this work elucidated the effects of the structure, electrical resistivity and surface specific area of carbon black nanoparticles on the electrical resistivity, internal capacitance, piezoresistive response, gauge factor, stress sensitivity and compressive strength of mortars. N234 blacks were selected for the main set of experiments of this dissertation because a higher concentration of this kind of nanofiller provided composites with the highest gauge factor and stress sensitivity and good compressive strength.

Moreover, the first smart cement-based composites produced with Brazilian carbon nanofillers and construction materials were reported in the preliminary studies of this dissertation. These studies indicated that the water content significantly affected the internal capacitance, electrical resistivity and sensing ability of composites with filler concentration above and below the percolation threshold. On the other hand, when the concentration of nanofillers was within the percolation zone, the effects of water content on the piezoresistive response and electronic conduction of the composite were considerably minimized, while values of gauge factor and stress sensitivity were optimized. In order to eliminate a piezoresistive response related to ionic conduction, all specimens of the main experimental program of this research were dried before the piezoresistive tests.

The preliminary studies also validated the investigation of mechanical and piezoresistive properties of nanomodified mortars through a microstructural evaluation characterized by a combination of techniques of scanning electron microscopy, X-ray diffraction and Raman spectroscopy.

The main experimental program revealed the residual mechanical properties of composites with different concentrations of MWCNT or CBN exposed to different high temperature levels. In this respect, the most interesting conclusion was that the addition of lower contents of carbon nanofillers (3% of CBN and 0.4% of MWCNT) improved the residual compressive strength, static and dynamic moduli of elasticity of composites exposed to 200 ºC, 400 ºC and 600 ºC. In addition, concentrations of 3% of CBN, 0.4% of MWCNT or 0.8% of MWCNT provided cement-based composites with higher static and dynamic moduli of elasticity in pre-fire and post-fire conditions. Microstructural evaluation and moisture losses values indicated that these improvements are related to the increase of the

stiffness of the CSH gel and density of the composite microstructure provided by MWCNT or to the improvement of the hydration process provided by lower concentrations of CBN.

Another important contribution of the main experimental program of this dissertation was the analysis of internal capacitance, residual electrical resistivity and piezoresistive response of composites with CBN and MWCNT exposed to high temperatures. Cement-based composites with 0.8% of MWCNT, 1.2% of MWCNT or 6% of CBN exhibited a self-sensing ability when exposed to temperatures up to 400 ºC. However, the best results were observed in cement-based composites with 9% of CBN: they presented an intrinsic ability to measure strain and detect damage after exposure to temperatures up to 600 ºC.

A recovery of strength, static and dynamic moduli due to the rehydration process was verified in plain and nanomodified mortars. It is attributed to the densification of the pore system due to rehydration. The best strength and stiffness recovery was observed in composites with 0.4% of MWCNT or 3% of CBN. It indicates that lower concentrations of carbon nanofillers improve the rehydration activity of cementitious composites.

The main experimental program also provided an evaluation of the effects of rehydration on the internal capacitance, electrical resistivity and piezoresistive response of fire-damaged cement-based sensors with CBN or MWCNT. Rehydration filled pores and sealed cracks with new non-conductive crystalline hydration products, which provided a densification of the pore system and decreased the electrical conductivity. The best results were observed in composites with 9% of CBN: they demonstrated an interesting ability of self-detection of damage recovery due to rehydration and exhibited an adequate residual self-sensing ability for monitoring deformation in structures exposed to temperatures up to 600 ºC.

7.2. FUTURE RESEARCH SUGGESTIONS

During the development of the experimental program of this research, some recommendations for future research could be pointed out, such as:

- Placement of the self-sensing cement-based composites in key locations of different kinds of concrete structural elements (e.g. beams, columns, walls) and evaluation of their self-sensing and damage-detection ability after fire simulation.
- Identification of the nanofiller concentration able to optimize the residual mechanical and sensing properties of fire-damaged cement-composites.

- Production of self-sensing cement-based composites with conductive nanofillers with higher thermal stability and evaluation of their residual sensing ability after exposure to temperatures higher than 600 ºC.
- Evaluation of the electrical resistivity changes in the smart composites during the fire simulation, in order to test the viability of using this information for monitoring damage and structural performance of concrete elements during the exposure to high temperatures.
- Evaluation of the efficiency of self-sensing cement-based composites for monitoring damage recovery of fire-damaged elements rehabilitated with different techniques.
- Analysis of the residual mechanical and piezoresistive properties of fire-damaged cement-based composites containing other nanofillers besides CBN and MWCNT.
- Analysis of the effects of rehydration in mechanical and piezoresistive properties of fire-damaged cement-based composites containing other nanofillers besides CBN and MWCNT.

APPENDIX A – PIEZORESISTIVITY OF NON-REHYDRATED SPECIMENS

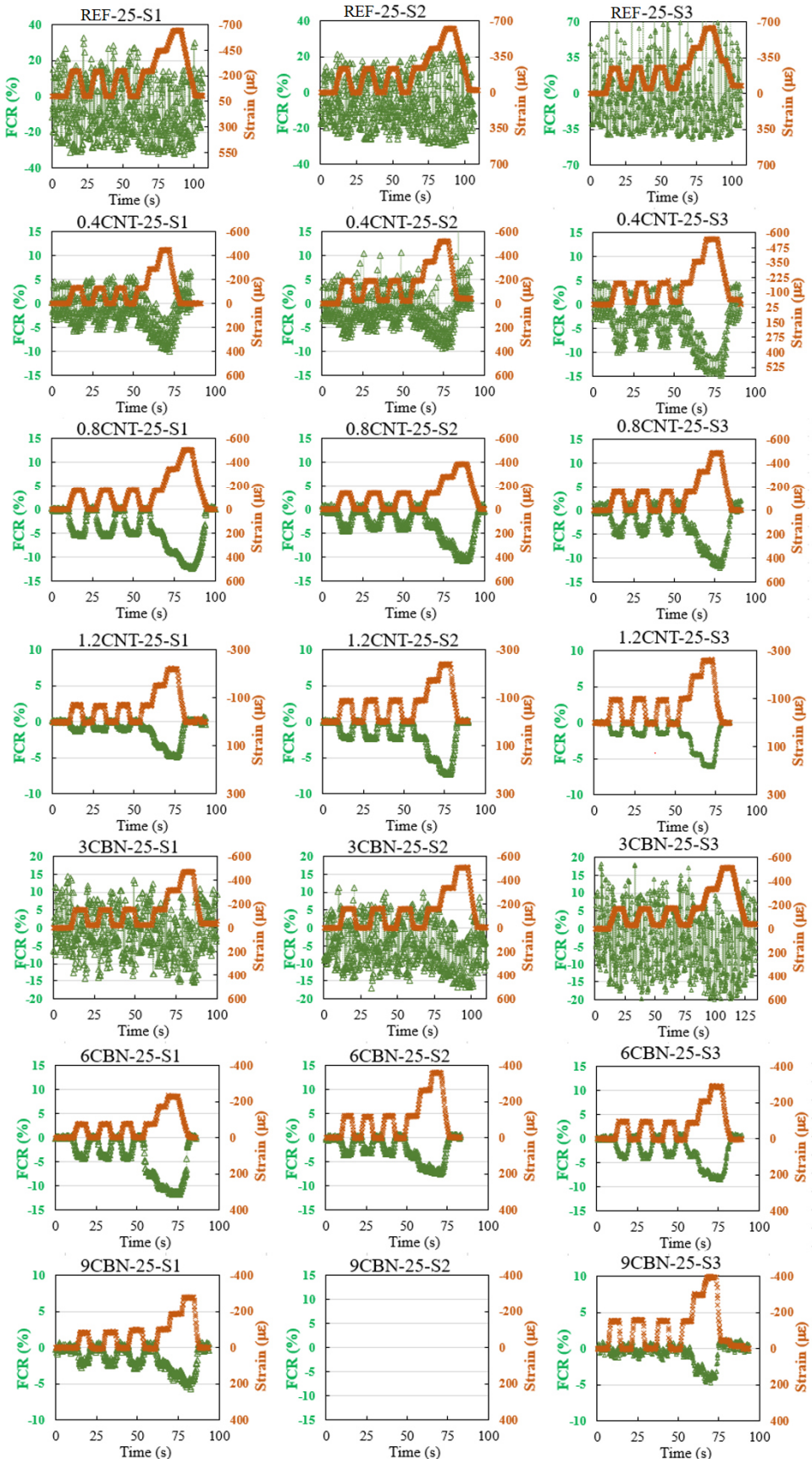

Source: Author (2020)

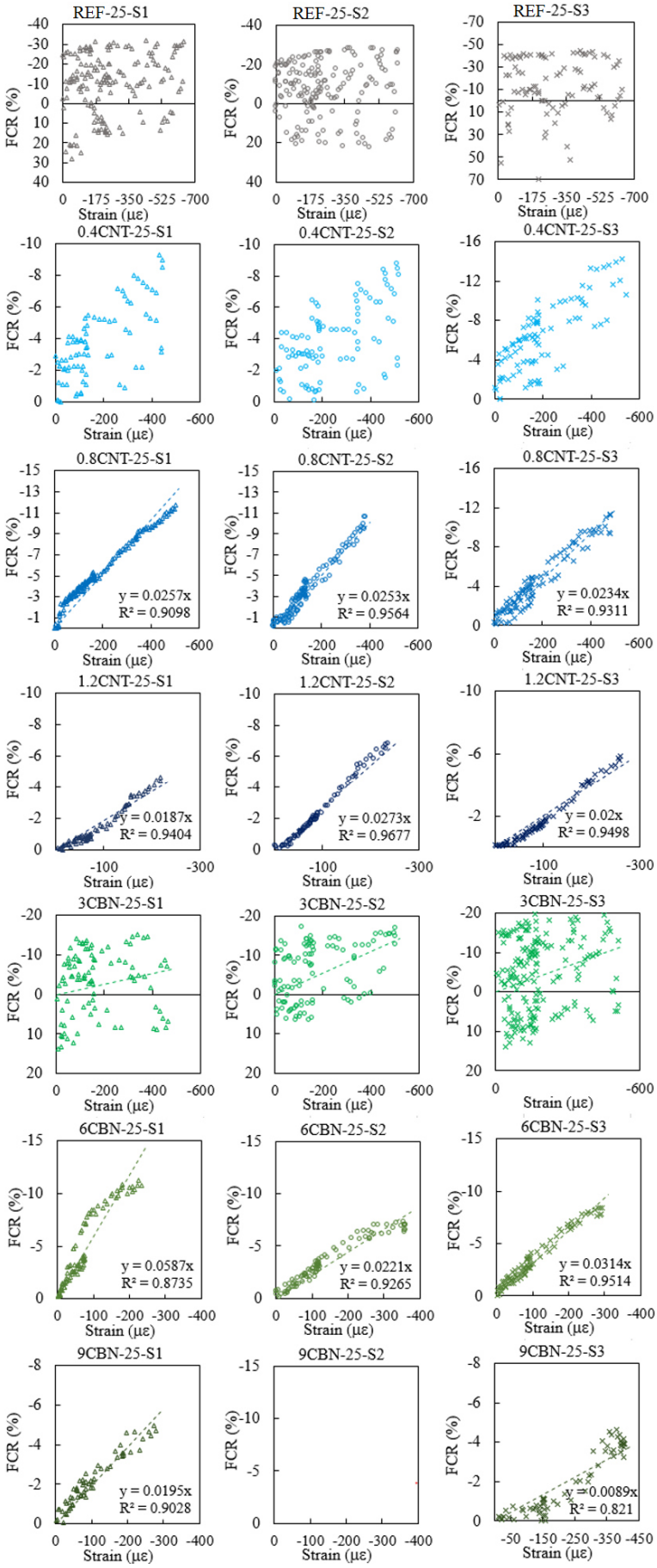

Source: Author (2020)

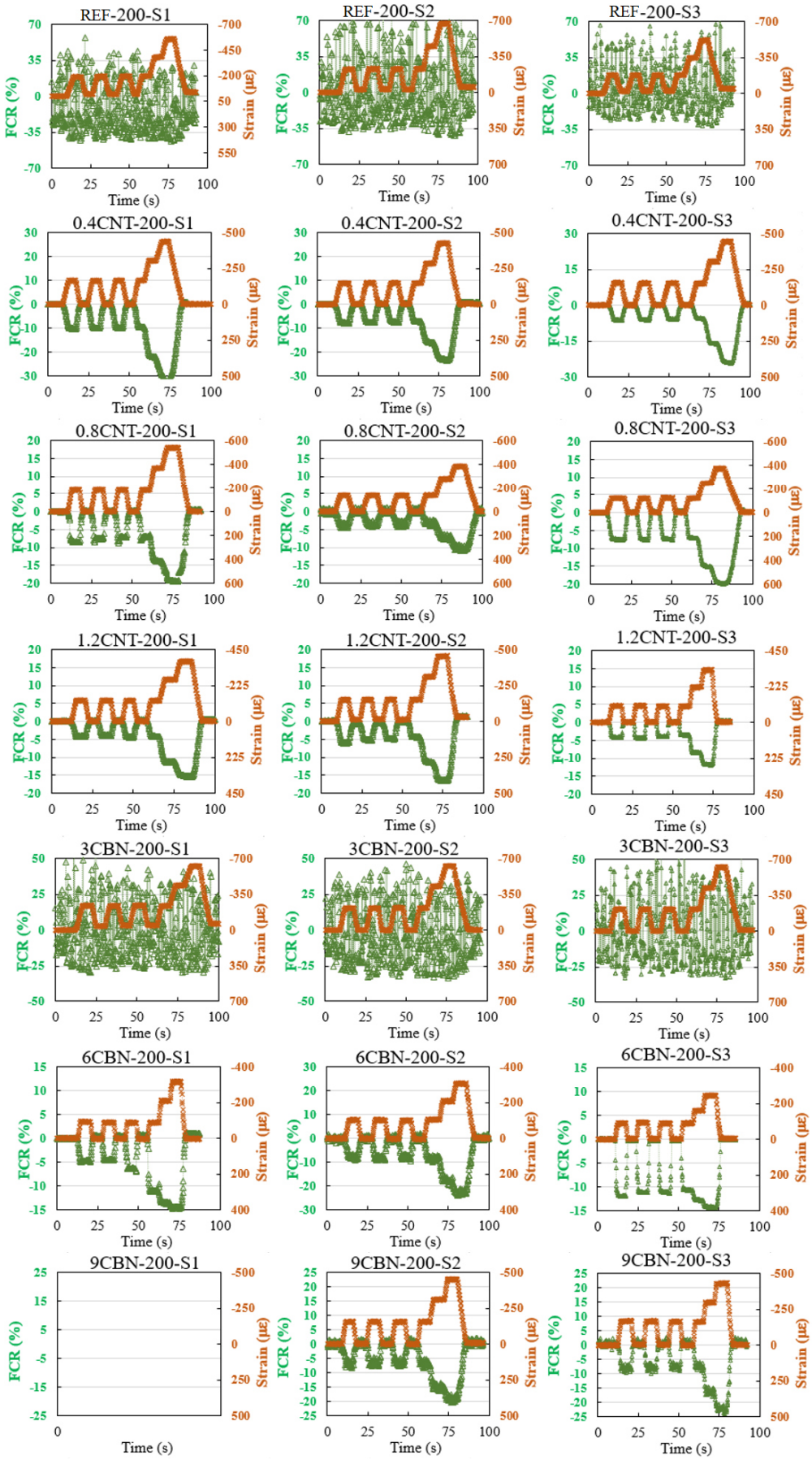

Source: Author (2020)

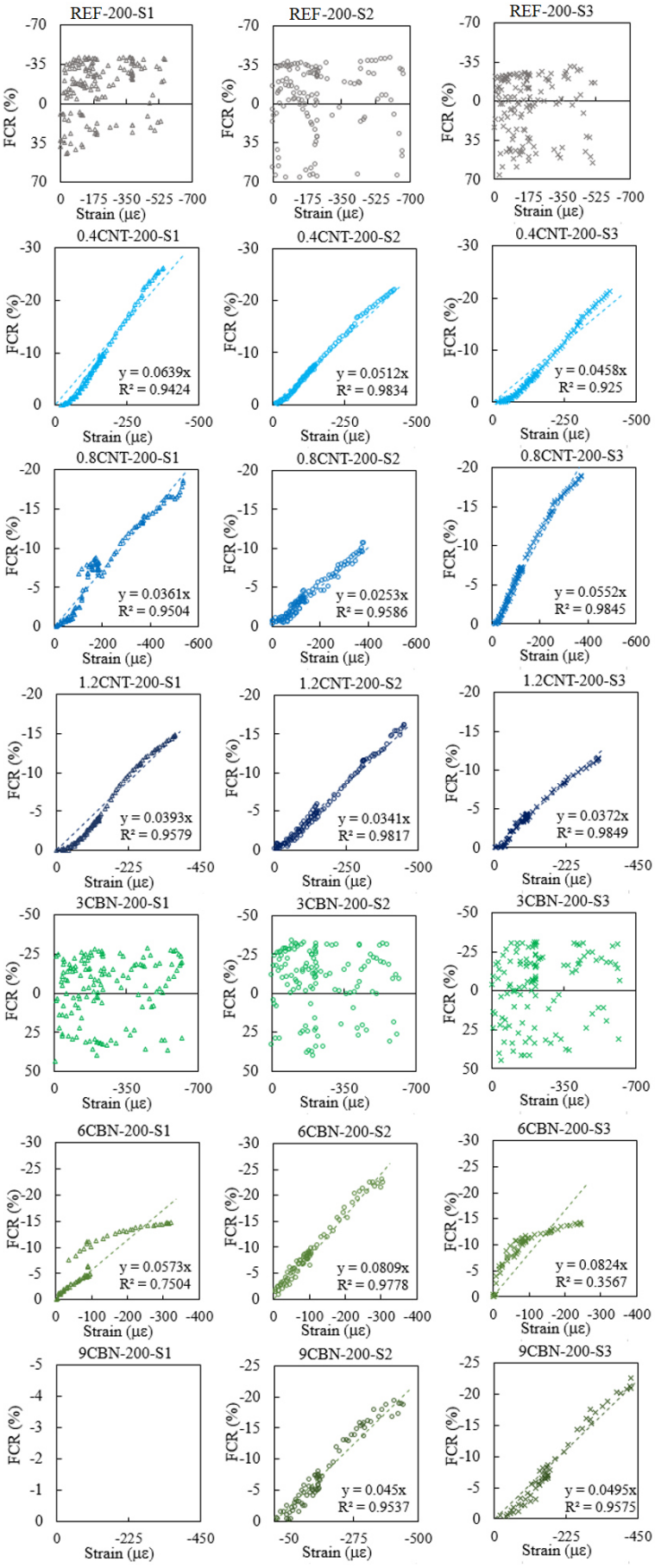

Source: Author (2020)

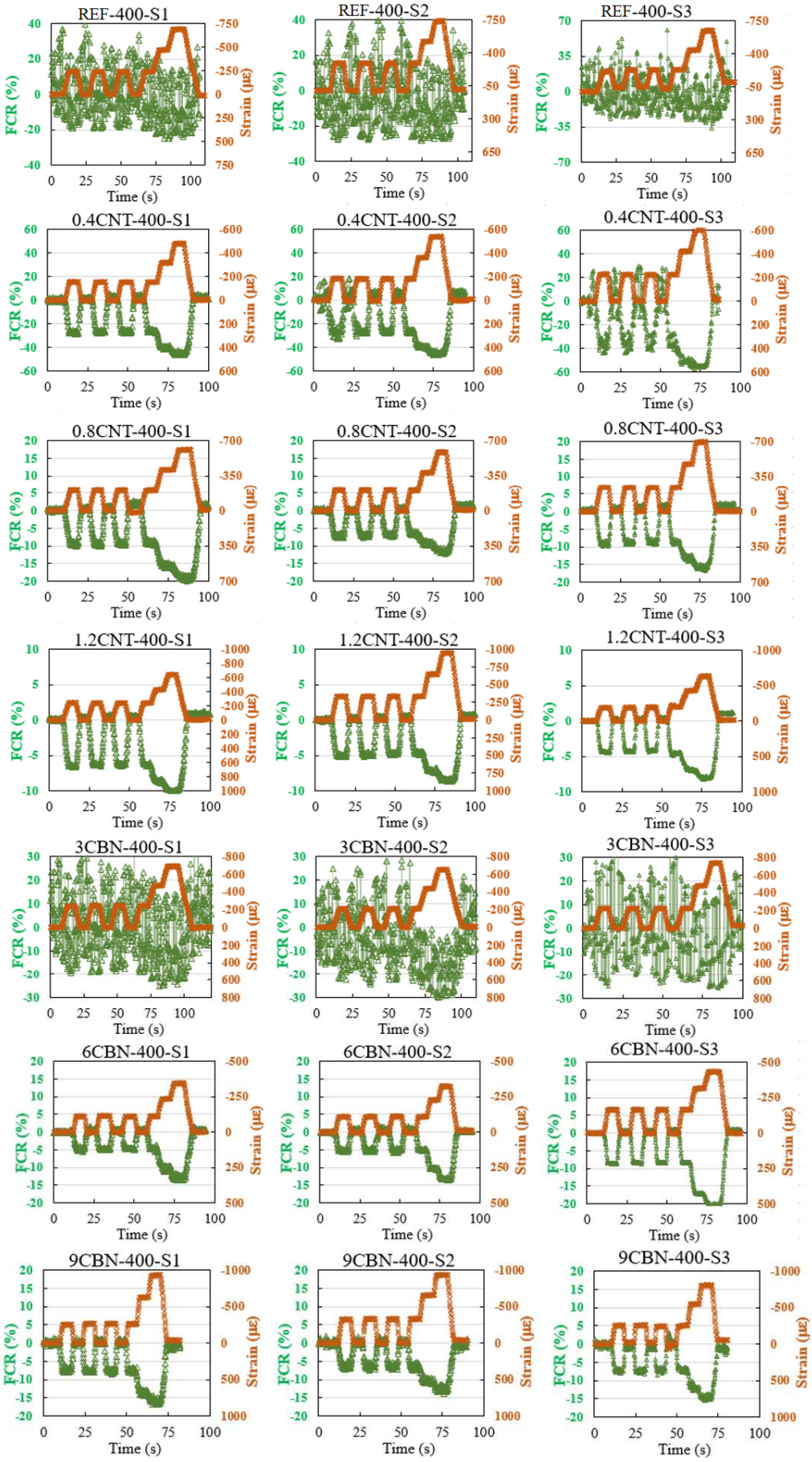

Source: Author (2020)

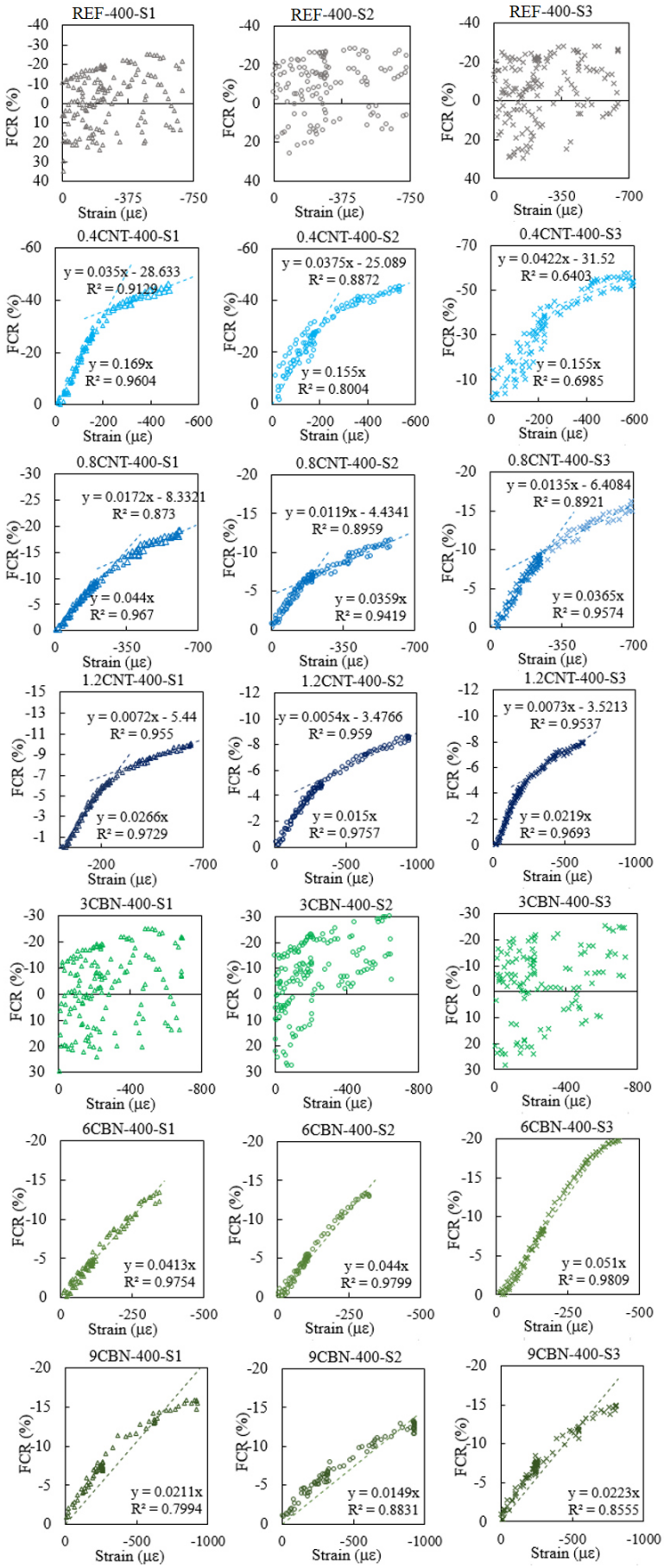

Source: Author (2020)

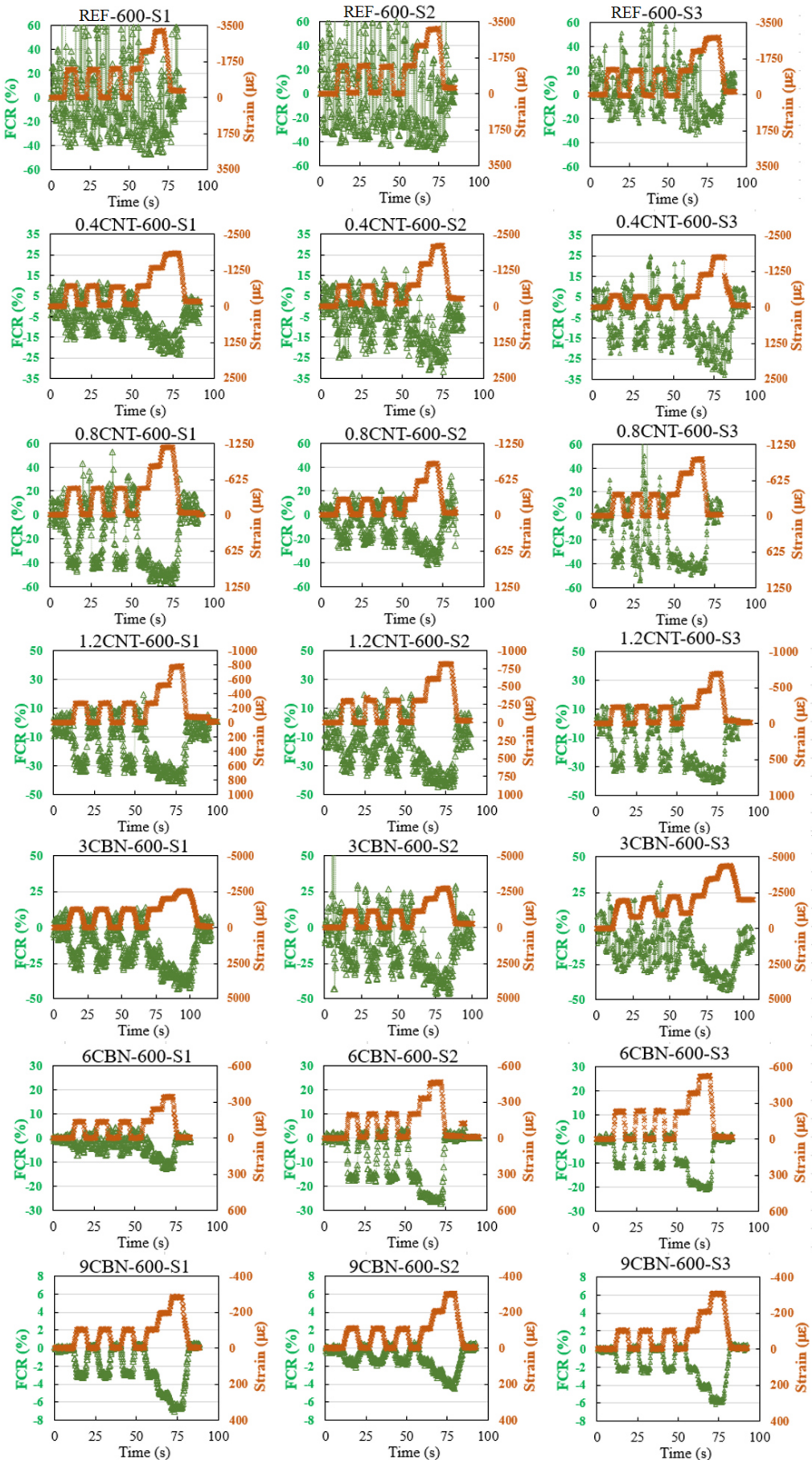

Source: Author (2020)

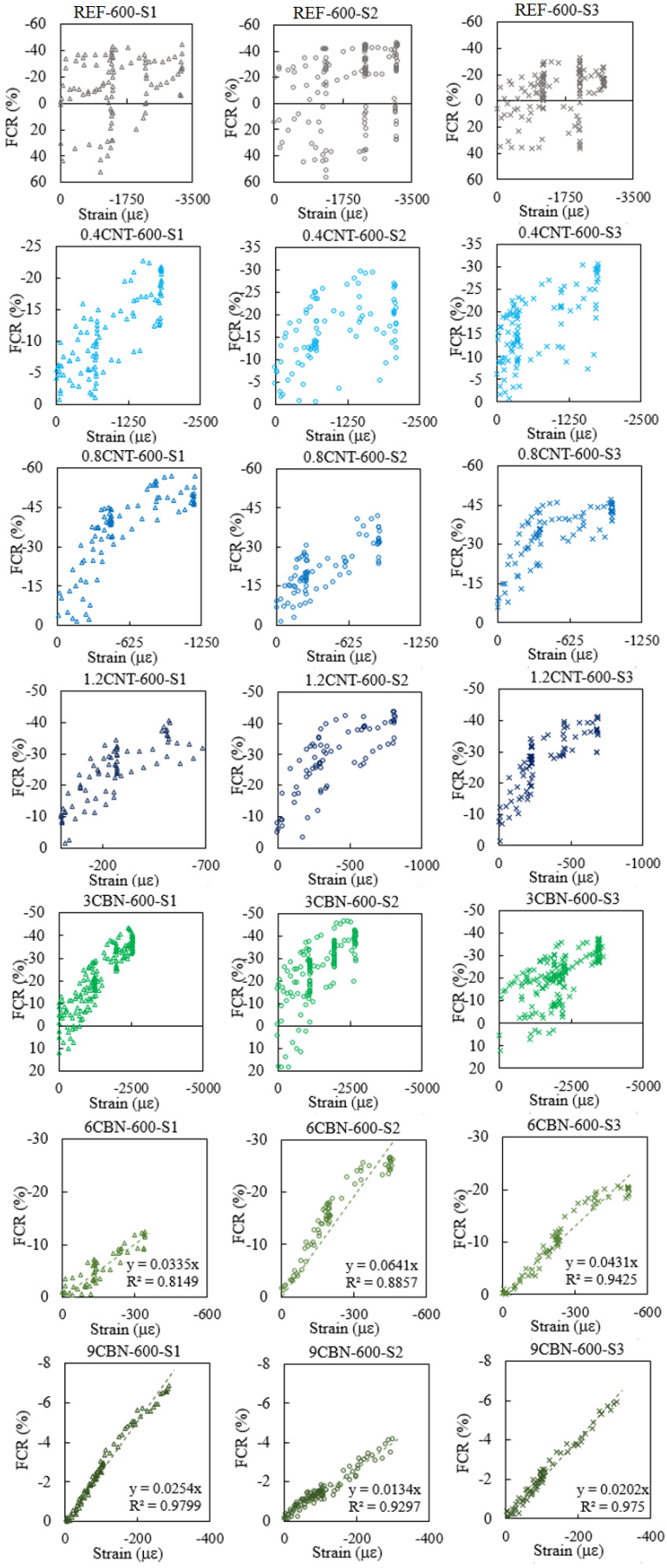

Source: Author (2020)

APPENDIX B – PIEZORESISTIVITY OF REHDRATED SPECIMENS

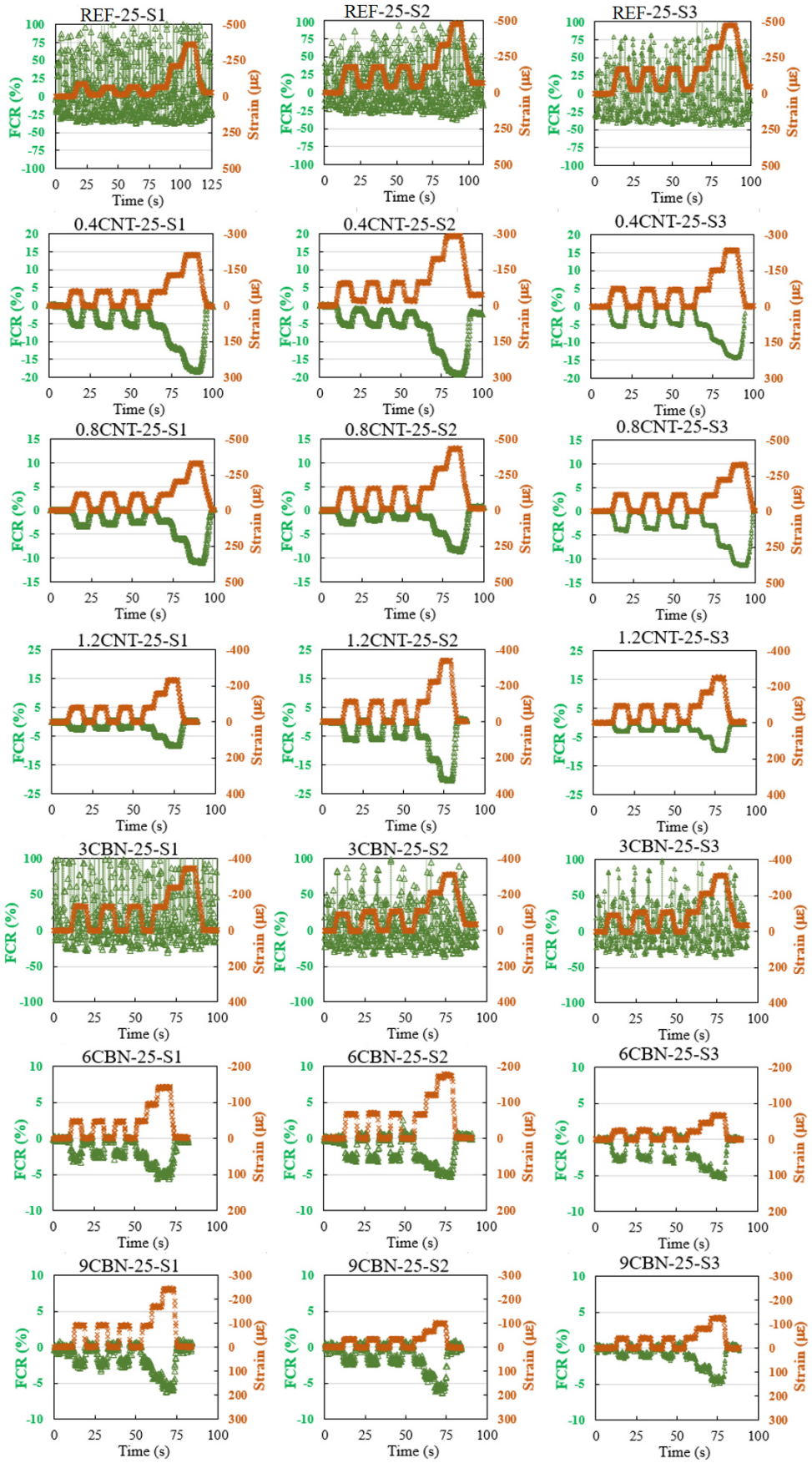

Source: Author (2020)

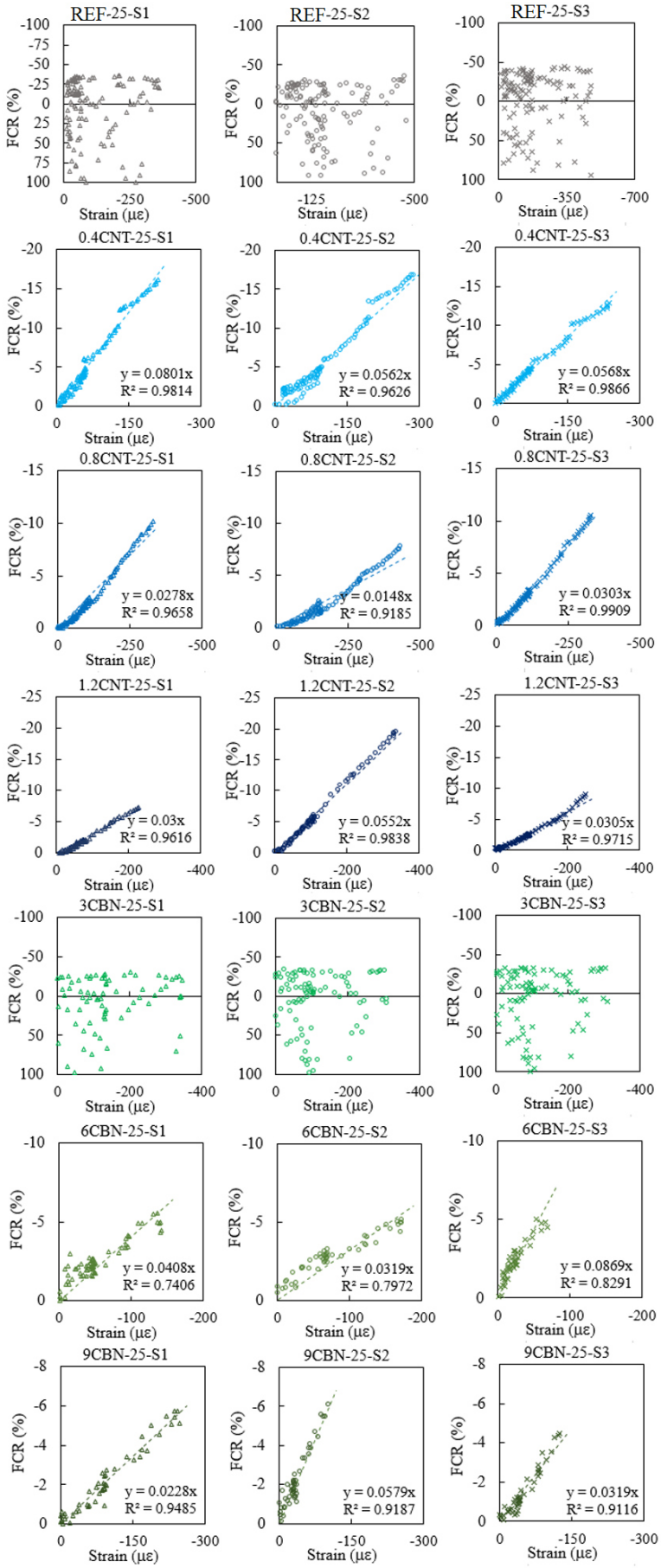

Source: Author (2020)

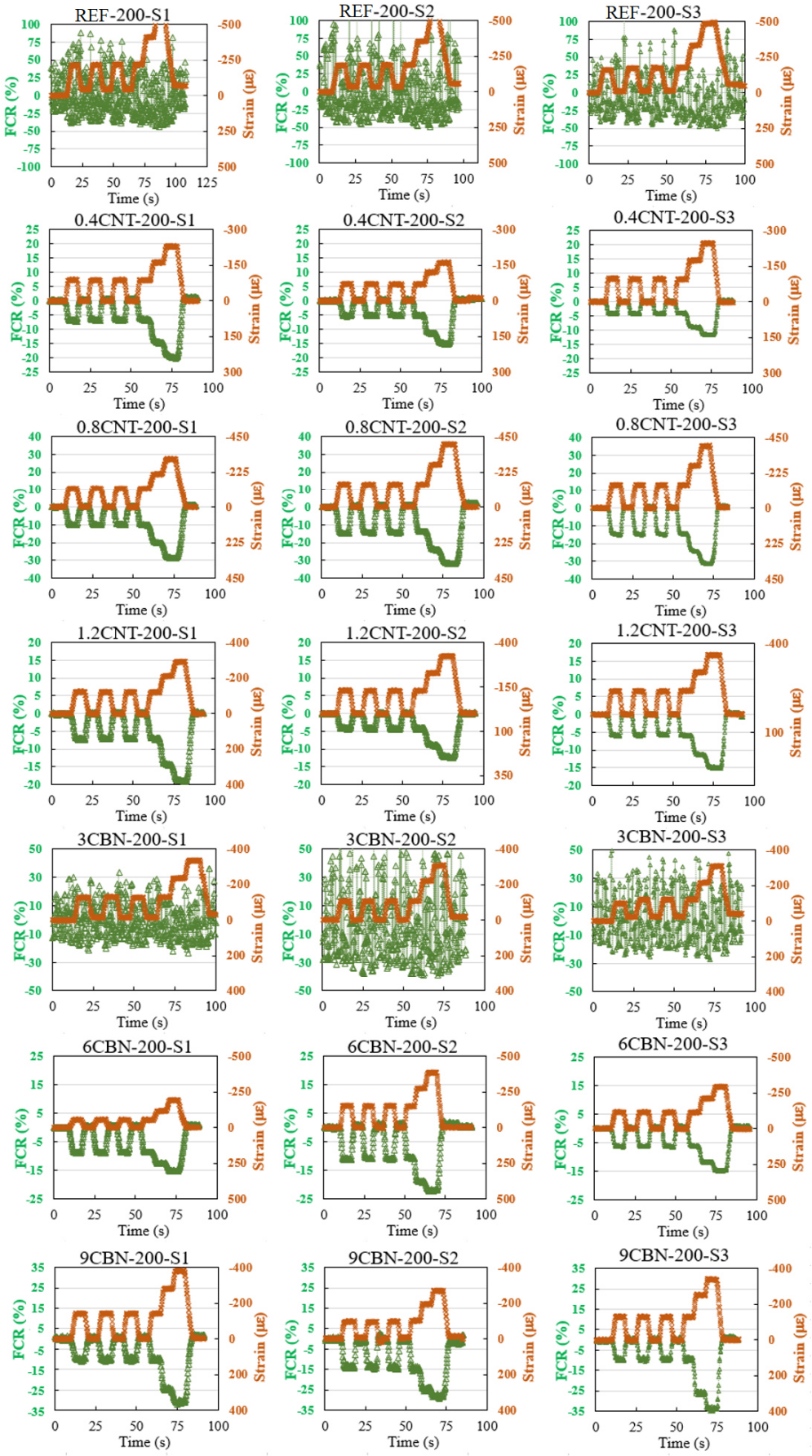

Source: Author (2020)

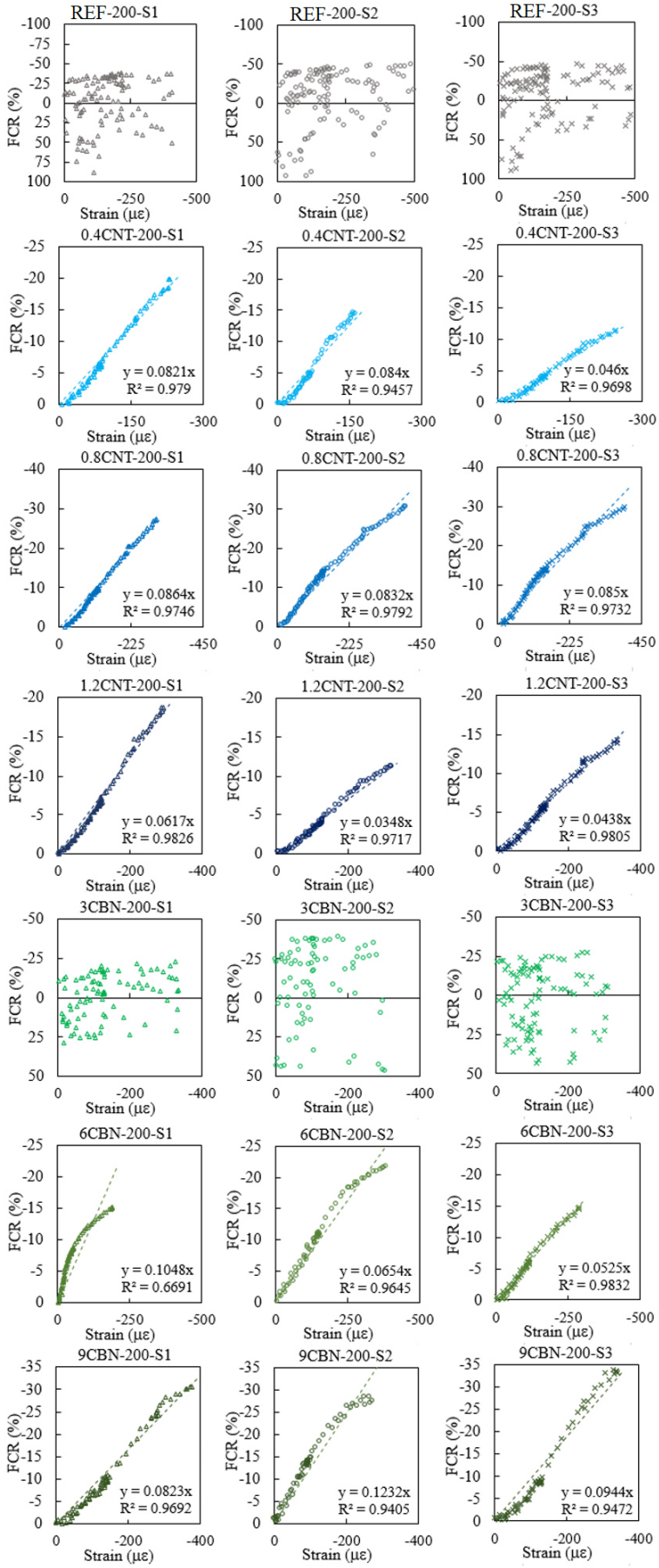

Source: Author (2020)

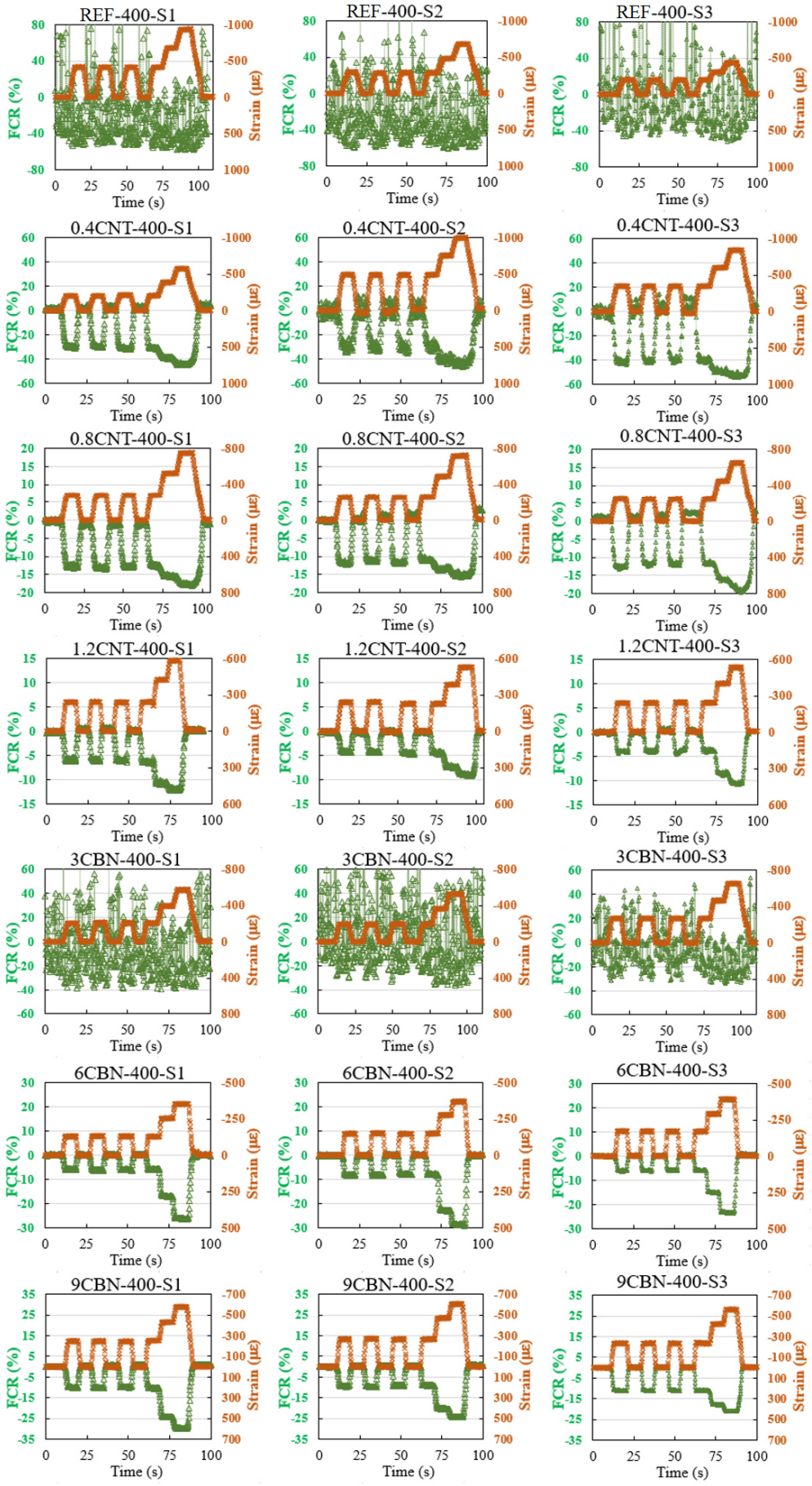

Source: Author (2020)

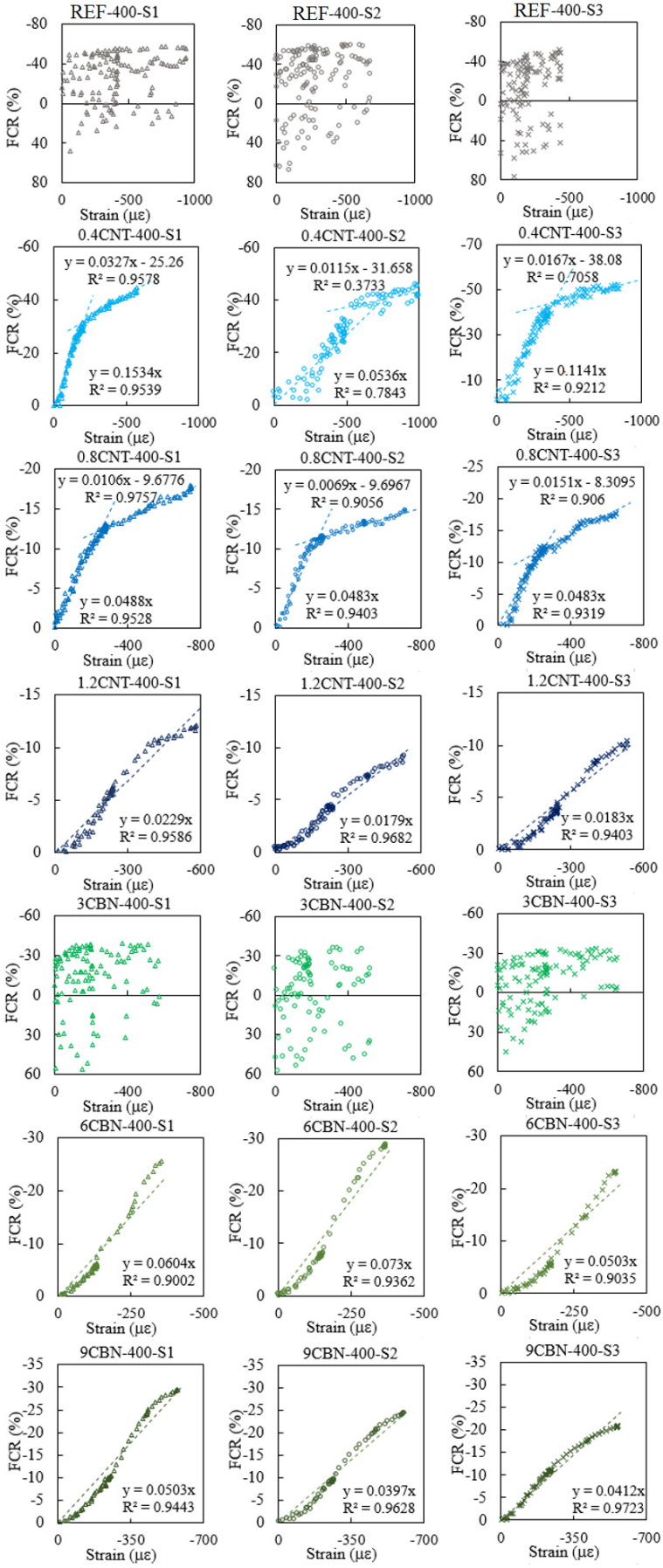

Source: Author (2020)

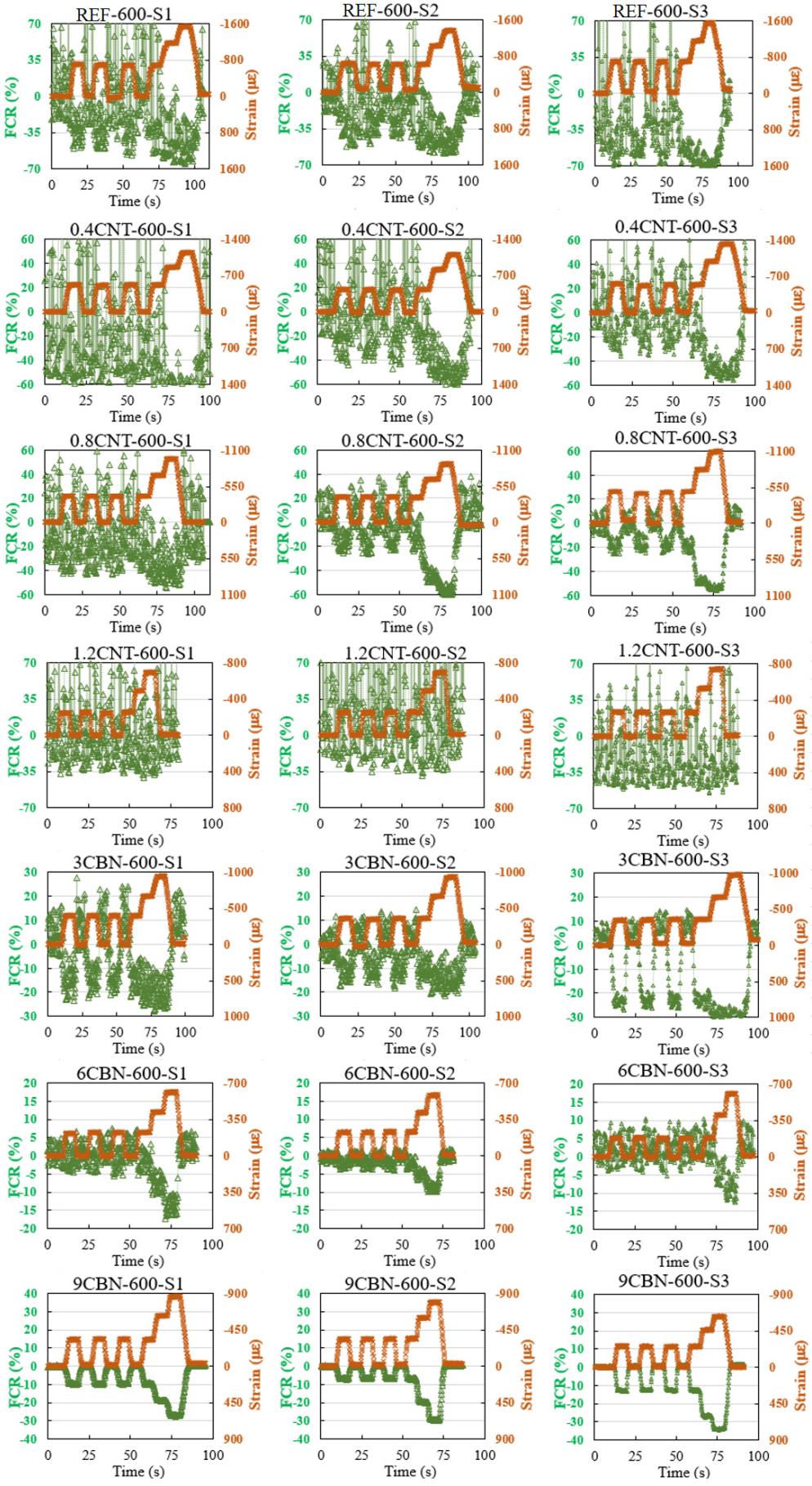

Source: Author (2020)

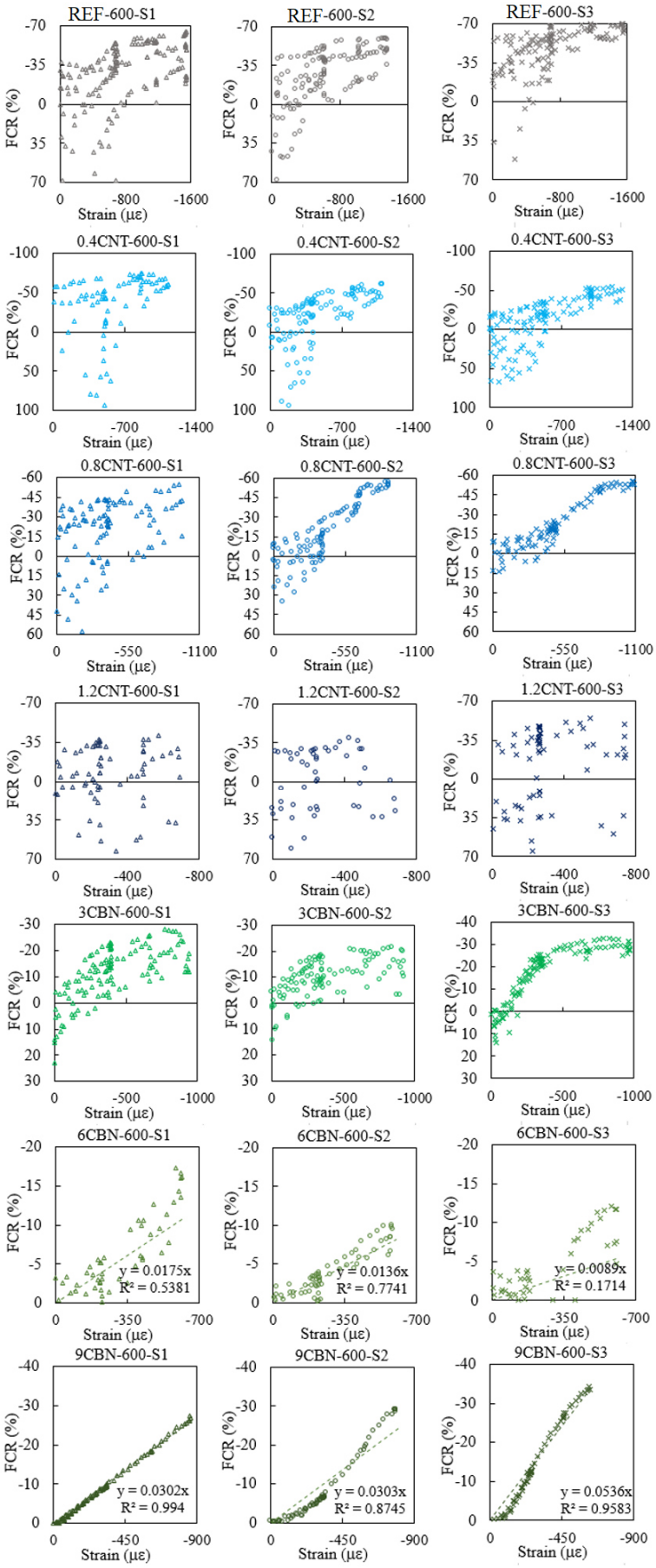

Source: Author (2020)